JYU DISSERTATIONS 157

Pekka Hautasaari

Exercise Effects on Early Cortical Somatosensory and Nociceptive Processing in the Human Brain

UNIVERSITY OF JYVÄSKYLÄ
FACULTY OF SPORT AND
HEALTH SCIENCES

JYU DISSERTATIONS 157

Pekka Hautasaari

Exercise Effects on Early Cortical Somatosensory and Nociceptive Processing in the Human Brain

Esitetään Jyväskylän yliopiston liikuntatieteellisen tiedekunnan suostumuksella
julkisesti tarkastettavaksi yliopiston vanhassa juhlasalissa S212
marraskuun 29. päivänä 2019 kello 12.

Academic dissertation to be publicly discussed, by permission of
the Faculty of Sport and Health Sciences of the University of Jyväskylä,
in building Seminarium, auditorium S212, on November 29, 2019 at 12 o'clock noon.

JYVÄSKYLÄN YLIOPISTO
UNIVERSITY OF JYVÄSKYLÄ

JYVÄSKYLÄ 2019

Editors
Anne Viljanen
Faculty of Sport and Health Sciences, University of Jyväskylä
Päivi Vuorio
Open Science Centre, University of Jyväskylä

Permanent link to this publication: http://urn.fi/URN:ISBN:978-951-39-7949-2

ISBN 978-951-39-7949-2 (PDF)
URN:ISBN:978-951-39-7949-2
ISSN 2489-9003

ABSTRACT

Hautasaari, Pekka
Exercise effects on early cortical somatosensory and nociceptive processing in the human brain
Jyväskylä: University of Jyväskylä, 2019, 70 p.
(JYU Dissertations
ISSN 2489-9003; 157)
ISBN 978-951-39-7949-2 (PDF)
Finnish summary
Diss.

Functional brain imaging methods were utilized to investigate early cortical somatosensory and nociceptive processing and how exercise may affect these processes. *Study I* examined automatic somatosensory change detection system with EEG and exercise effects on this system utilizing data collected from monozygotic twin pairs who were discordant in their long-term exercise status within pair. The results of *Study I* showed that long-term exercise selectively modulates specific early somatosensory electrophysiological brain responses as the inactive co-twins showed stronger somatosensory mismatch response (SMMR) compared to their active co-twins. *Study II* investigated somatosensory automatic change detection system with magnetoencephalography (MEG) using SMMR experiment design with electrical and tactile stimulation. The results of *Study II* demonstrated the feasibility of both tactile and electrical stimulation in reliably detecting SMMR with MEG. Furthermore, these results support previous studies indicating the involvement of the primary and secondary somatosensory cortices in the somatosensory automatic change detection system. *Study III* examined which uni- and bilateral cortical areas are involved in early somatosensory automatic processing with MEG utilizing innocuous and nociceptive electrical stimulations. The results of *Study III* demonstrated spatial and temporal dissociation in brain activations following electrical stimulation to slightly diverging hand areas. *Study IV* investigated the effects of acute exercise on cortical nociceptive processing and excitability in the sensorimotor cortex. The results of *Study IV* revealed modulation in the oscillatory nociceptive processing over sensorimotor cortex after acute exercise. This modulation was observed in the ~20 Hz motor cortex rhythm as the stimulation-induced suppression was stronger followed by a tendency towards weaker rebound. Overall, the findings in this dissertation demonstrate interaction between exercise and cortical somatosensory and nociceptive systems. Further research is necessary for better understanding of the mechanisms underlying this interaction and linking this information to designing optimal rehabilitation paradigms.

Keywords: physical activity, magnetoencephalography, electroencephalography, event-related potentials, event-related fields

Author's address

Pekka Hautasaari, MSc, pt
Faculty of Sport and Health Sciences
University of Jyväskylä
P.O. Box 35
FI-40014 University of Jyväskylä
Jyväskylä, Finland
pekka.t.hautasaari@student.jyu.fi

Supervisors

Adjunct Professor Ina M. Tarkka, PhD
Faculty of Sport and Health Sciences
University of Jyväskylä
Jyväskylä, Finland

Professor Urho M. Kujala, MD, PhD
Faculty of Sport and Health Sciences
University of Jyväskylä
Jyväskylä, Finland

Professor Jarmo A. Hämäläinen, PhD
Department of Psychology
University of Jyväskylä
Jyväskylä, Finland

Reviewers

Sven Braeutigam, Dipl.-Phys., PhD
Magnetoencephalography Physicist at the Wellcome Centre for Integrative Neuroimaging and Senior Researcher, Department of Psychiatry
University of Oxford
Warneford Hospital
Oxford, United Kingdom

Adjunct Professor Erika Kirveskari, MD, PhD
Head of Clinical Neurophysiology
HUS Medical Imaging Center
Clinical Neurosciences
Helsinki University Hospital and University of Helsinki
Helsinki, Finland

Opponent

Professor Massimiliano Valeriani, MD, PhD
Neurology Ward Unit
Ospedale Pediatrico Bambino Gesù
Rome, Italy

TIIVISTELMÄ (FINNISH ABSTRACT)

Hautasaari, Pekka
Liikunnan vaikutukset aivojen automaattiseen somatosensoriseen ja nosiseptiiviseen prosessointiin
Jyväskylä: Jyväskylän yliopisto, 2019, 70 s.
(JYU Dissertations
ISSN 2489-9003; 157)
ISBN 978-951-39-7949-2 (PDF)
Yhteenveto suomeksi
Diss.

Tutkimuksessa käytettiin toiminnallisia aivokuvantamismenetelmiä mittaamalla lyhytlatenttisia somatosensorisia ja nosiseptiivisiä aivoprosesseja sekä selvitettiin, vaikuttaako liikunta näihin prosesseihin. *Tutkimuksessa I* tutkittiin aivojen automaattista somatosensorista muutoksen havaitsemismekanismia elektroenkefalografialla (EEG) ja liikunnan vaikutusta tähän mekanismiin. Aineisto koostui identtisistä kaksospareista, jotka parin sisällä poikkesivat vuosien ajan liikuntatottumuksiltaan. Tuloksissa havaittiin, että liikunta vaikuttaa somatosensorisiin aivovasteisiin siten, että passiivisilla kaksosilla muutoksenhavaitsemisvaste oli voimakkaampi. *Tutkimuksessa II* tarkasteltiin aivojen muutoksenhavaitsemisvastetta magnetoenkefalografialla (MEG) hyödyntäen sähköistä ja taktiilia stimulaatiota. Tuloksien perusteella molemmat stimulaatiotavat ovat luotettavia menetelmiä. Lisäksi tulokset vahvistavat aiempia tutkimuksia osoittaen primaarisen ja sekundaarisen somatosensorisen aivokuoren osallistuvan muutoksen havaitsemissysteemiin. *Tutkimuksessa III* selvitettiin MEG:lla mitkä uni- ja bilateraaliset aivoalueet osallistuvat lyhytlatenttiseen somatosensoriseen ja nosiseptiiviseen prosessointiin. Tässä hyödynnettiin vaimeata ja nosiseptiivistä sähköstimulaatiota. Tulokset osoittivat aktiivisten aivolähteiden sijainnissa ja ajoituksessa eroja käden eri alueille kohdistettujen eri voimakkuuksisten stimulaatioiden jälkeen. *Tutkimuksessa IV* tutkittiin akuutin liikuntasuorituksen vaikutusta nosiseptiiviseen prosessointiin ja sensorimotorisen aivokuoren ärtyvyyteen. Tulokset osoittivat akuutin liikuntasuorituksen vaikuttavan nosiseptiiviseen prosessointiin liittyvään aivorytmiin sensorimotorisella aivokuorella. Primaarisen motorisen aivokuoren ~20 Hz:n aivorytmissä havaittiin voimakkaampi nosiseptiivisen stimulaation tuottama amplitudin lasku vastaten aivokuoren ärtyvyyden kasvua ja viitteitä heikompaan amplitudin palautumiseen vastaten vähentynyttä inhibitiota. Väitöskirjan tulokset osoittavat selkeästi yhteyden liikunnan ja aivokuoren somatosensorisen ja nosiseptiivisen prosessoinnin välillä. Lisätutkimus on tarpeen tämän vuorovaikutuksen mekanismien ymmärtämiseksi sekä tämän tiedon yhdistämiseksi osaksi optimaalisten kuntoutuskäytäntöjen suunnittelua.

Asiasanat: fyysinen aktiivisuus, magnetoenkefalografia, elektroenkefalografia, herätevasteet

ACKNOWLEDGEMENTS

My PhD studies were carried out at the Sports and Exercise Medicine section, Faculty of Sport and Health Sciences, University of Jyväskylä. First and foremost, I want to warmly thank my scientific mentor and principal supervisor Adjunct Professor Ina Tarkka, PhD. Thank you for introducing me to the challenging field of neurophysiology and providing me great learning opportunities. Your committed guidance has been invaluable for my development as a researcher. I am grateful to my supervisors Professor Urho Kujala, MD, PhD, and Professor Jarmo Hämäläinen, PhD, for your guidance and advice. I want to also acknowledge support from Professor Jyrki Mäkelä, MD, PhD, a member of my dissertation committee. I am especially grateful to Urho for providing essential support at the beginning of my dissertation project and giving me plentiful opportunities to gain broader research experience outside the focus of this dissertation.

I wish to thank the reviewers of my dissertation, Adjunct Professor Erika Kirveskari, MD, PhD, and Sven Braeutigam, Dipl.-Phys., PhD, for your time, expertise, valuable comments and encouraging words. I kindly wish to thank Professor Massimiliano Valeriani, MD, PhD, for accepting the role of the opponent in the public examination.

It has been clear to me since the beginning of this dissertation project that research is teamwork. Thus, I want to express my sincere gratitude to all my colleagues and co-authors Professor Jaakko Kaprio, MD, PhD, Katariina Korniloff, PhD, Maija Koskio, MSc, Otto Loberg, PhD, Susanna McLellan, MSc, Eini Niskanen, PhD, Heidi Pesonen, MSc, Harri Saloranta, MSc and Andrej Savić, PhD. None of these studies would have been carried out without the voluntary participants who are gratefully acknowledged. The EEG and MRI data for the *Study I* originated from the Finnish twin study (FITFATTWIN). The EEG data collection was made possible by the EEG laboratory in the Department of Psychology, University of Jyväskylä. All my MEG data for *Studies II-IV* was collected in the MEG laboratory in the Centre for Interdisciplinary Brain Research (CIBR), University of Jyväskylä. EEG and MEG laboratories, led by Professor Paavo Leppänen, PhD, and Tiina Parviainen, PhD, respectively, are gratefully acknowledged.

Life happens also outside of the office. To my friends, I simply thank you for your friendship. I wish to thank my brother for inspiration to take a dive in the world of research and his family for hospitality during my vacation journeys. Finally, I am always grateful to my parents for their unlimited support until now and into the future.

This work was financially supported by personal grants from the Jenny and Antti Wihuri Foundation, Helsinki, Finland and the Yrjö Jahnsson Foundation, Helsinki, Finland. Also, parts of my work have been supported by the Juho Vainio Foundation, Helsinki, Finland and the Ministry of Education and Culture, Helsinki, Finland. I express my sincere gratitude to all these funding agencies.

Jyväskylä, November 2019
Pekka

FIGURES

LIST OF ORIGINAL PUBLICATIONS

This dissertation is based on the following publications, which are referred to in the text by their Roman numerals.

I Hautasaari, P., Savić, A. M., Loberg, O., Niskanen, E., Kaprio, J., Kujala, U. M. & Tarkka, I. M. 2017. Somatosensory brain function and gray matter regional volumes differ according to exercise history: evidence from monozygotic twins. Brain Topography 30 (1), 77-86.

II Hautasaari, P., Kujala, U. M. & Tarkka, I. M. 2019. Detecting differences with magnetoencephalography of somatosensory processing after tactile and electrical stimuli. Journal of Neuroscience Methods 311, 331-337.

III Hautasaari, P., Saloranta, H., Savić, A. M., Korniloff, K., Kujala, U. M. & Tarkka, I. M. 2018. Bilateral activations in operculo-insular area show temporal dissociation after peripheral electrical stimulation in healthy adults. European Journal of Neuroscience (Epub ahead of print).

IV Hautasaari, P., McLellan, S., Koskio, M., Pesonen, H. & Tarkka, I. M. 2019. Acute exercise modulates pain-induced response on sensorimotor cortex ~20 Hz oscillation. Submitted manuscript.

Taking into account the instructions and comments from the co-authors, the author contributed to the original publications listed above as follows. In *Study I,* the author was privileged to use pre-existing data. The author analyzed the EEG data and wrote the manuscript. In *Studies II-IV*, the author contributed to designing the experiments and stimuli, had a significant role in data collection and coordination, analyzed the data and wrote the manuscripts.

ABBREVIATIONS

2D	two dimensional
3D	three dimensional
ACC	anterior cingulate cortex
BDI	Beck depression inventory
BESA	brain electrical source analysis
BMI	body mass index
CO_2	carbon dioxide
CPM	conditioned pain modulation
CSF	cerebrospinal fluid
DARTEL	diffeomorphic anatomical registration using exponentiated Lie algebra
dSPM	dynamic statistical parametric mapping
DXA	dual-energy X-ray absorptiometry
EEG	electroencephalography
EMG	electromyography
EOG	electro-oculography
ERD	event-related desynchronization
ERF	event-related field
ERP	event-related potential
ERS	event-related synchronization
fMRI	functional magnetic resonance imaging
FDR	false discovery rate
FWE	family-wise error rate
GM	gray matter
HPI	head position indicator
ISI	interstimulus interval
LPP	long latency positivity
MEG	magnetoencephalography
MET	metabolic equivalent
MI	primary motor cortex
MMN	mismatch negativity
MNI	Montreal Neurological Institute
MPRAGE	magnetization-prepared rapid acquisition with gradient echo
MRI	magnetic resonance imaging
ms	millisecond
MVC	maximum voluntary contraction
PET	positron emission tomography
RBDI	Raitasalo Beck depression inventory
RMS	root mean square
ROI	region of interest
RPE	rating of perceived exertion
RV	residual variance
SD	source dipole

SEF	somatosensory evoked field
SEP	somatosensory evoked potential
SI	primary somatosensory cortex
SII	secondary somatosensory cortex
SMMR	somatosensory mismatch response
SPM	statistical parametric mapping
SQUID	superconducting quantum interference device
SSP	signal-space projection
TE	echo time
TI	inversion time
TMS	transcranial magnetic stimulation
TR	repetition time
TSE	temporal spectral evolution
VAS	visual analog scale
VBM	voxel-based morphometry
VO_{2max}	maximal oxygen uptake
WM	white matter

CONTENTS

1 INTRODUCTION

Exercise is considered an important part of a healthy lifestyle and it has been shown to induce positive effects as improved physical functioning and favourable effects on risk factors for various chronic diseases (Kujala 2009, Pasanen et al. 2017). In contrast, physical inactivity and sedentary lifestyle affect health by increasing incidence, for example, in coronary heart disease, type 2 diabetes and premature mortality (Lee et al. 2012). Substantial amount of research has been dedicated to study associations between exercise and cardiorespiratory function, which is reflected in the physical activity guidelines by the American College of Sports Medicine (Kraus et al. 2019), however, recently more experimental research has contributed on studying the effects of exercise on the human brain.

The majority of research on exercise effects on brain health has been targeting the cognitive functioning showing beneficial results (Tyndall et al. 2018, Erickson et al. 2019), but far less is known about a possible interaction between exercise and brain function in other systems, such as somatosensory and nociceptive processing. These neurophysiological systems underlie pain experience, which is an important factor contributing to various chronic diseases and, interestingly, studies have reported maladaptive structural plasticity in chronic pain syndromes affecting, for example, primary somatosensory cortex (Flor et al. 1997, Kuner & Flor 2017). However, exercise has been reported to have positive effects on self-reported pain in conditions, such as chronic non-specific low-back pain (van Middelkoop et al. 2010) and osteoarthritis (Pedersen & Saltin 2015). Furthermore, studies have reported that exercise, e.g. aerobic or resistance, has a hypoalgesic effect, reducing the perception of experimentally induced pain (Naugle, Fillingim & Riley 2012), even with short bouts of acute exercise (Koltyn et al. 2014). Additionally, athletes participating in exercise long-term, have been shown to have reduced pain perception (Tesarz et al. 2012). Even though studies show that exercise can have hypoalgesic effects (Naugle, Fillingim & Riley 2012) and exercise is also reported to induce beneficial neuroplastic effects (Hötting & Röder 2013, Rottensteiner et al. 2015), the underlying neurobiological mechanisms of the interaction between exercise, and somatosensory and

nociceptive processing are unclear. Increased understanding of the neurobiology of exercise effects related to somatosensory and nociceptive processing could significantly contribute to designing more optimal exercise therapy interventions in rehabilitation settings.

The aim of this dissertation was to study somatosensory function and nociceptive processing in the human brain and how exercise may influence these processes. These cortical systems were investigated with functional neuroimaging methods using somatosensory and nociceptive experimental stimulations. The exercise effects were measured in an acute exercise task design, and in a monozygotic twin-pair design where the twin-pairs were discordant in their long-term exercise status within pair. The overall objective of the present study was to gain new information on the underlying neurophysiological mechanisms that may interact between exercise, and cortical somatosensory and nociceptive systems.

2 REVIEW OF THE LITERATURE

2.1 Functional brain imaging: magnetoencephalography and electroencephalography

Functional brain imaging methods are used in basic and clinical research for studying brain function in healthy human behaviour and in diseases. Prominent methods include functional magnetic resonance imaging (fMRI), which is based on measuring the hemodynamic response, i.e. changes in blood flow in the brain areas due to neuronal activation (Könönen, Vanninen & Halme 2018) and positron emission tomography (PET), which measures the accumulation of radioactive tracer in target tissue (Joutsa 2018). These functional brain imaging methods have relatively high spatial accuracy. Their spatial resolution is in millimeter scale but they have relatively low temporal resolution, in timescale of seconds. Electrophysiological methods, magneto- and electroencephalography, have lower spatial resolution compared to fMRI and PET, however, these methods provide higher temporal accuracy in millisecond scale and thus they are most suitable for studying early cortical activations close to stimulation onset (Nevalainen 2018, Vanhatalo et al. 2018).

2.1.1 Magnetoencephalography

Magnetoencephalography (MEG) is a functional brain imaging technique, pioneered by Cohen (1968), which measures the weak magnetic fields (Figure 1) produced by bioelectric currents in synchronously active neurons (Hämäläinen et al. 1993, Lopes da Silva 2010, Braeutigam 2013). The primary source of the MEG signal arises from the postsynaptic activity of the pyramidal neurons of the cortex, which have long apical dendrites aligned perpendicularly to cortex, and while synchronously active they behave as a current dipole and this activity can be detected with MEG sensors (Lopes da Silva 2010, Hari & Salmelin 2012). MEG

sensor capabilities of detecting signals depend on factors such as the geometry and electrical properties of the volume conductor and specifically sensor types. For example, radially oriented currents do not produce magnetic fields outside a spherically symmetric volume conductor. However, the human head is not spherically symmetric and thus, the radial source is not necessarily silent in MEG and source depth, rather than orientation, may be a critical factor in detectability of individual dipole source (Ahlfors et al. 2010). Still, MEG is mainly sensitive to currents that are tangential in relation to the scalp surface and due to the folding of the cortex, MEG is sensitive to neural activation in the walls of the sulci (Ahlfors et al. 2010, Puce & Hämäläinen 2017). Also, deep sources are difficult to detect with MEG because of increased distance between the sensors and the sources, however, magnetic fields are largely unaffected by tissues such as skull and scalp between the brain and MEG sensors (Puce & Hämäläinen 2017). Interestingly, emerging research shows potential in measuring also the deep sources with MEG (Samuelsson et al. 2019). Modern MEG device has a helmet-shaped dewar covering the whole scalp and containing over 100 superconducting quantum interference device (SQUID) sensors, which are sensitive enough to capture the magnetic fields originating from neuronal activity (Hari, Parkkonen & Nangini 2010). However, because of the sensitivity of the SQUID sensors and weakness of the measured signals, MEG requires a specialized experimental environment, i.e. a magnetically shielded room, which filters out the Earth's naturally occurring magnetic field and fields generated from other outside sources (Puce & Hämäläinen 2017). Even though MEG is a technically challenging method, it has practical benefits as it is non-invasive, sensors do not require contact to the participant and it functions silently while measuring continuous data during rest or task execution in an experiment (Braeutigam 2013, Proudfoot et al. 2014). In addition to being a powerful method in research, MEG has a relevant role in clinical setting especially in presurgical evaluation of medically intractable epilepsy patients because of its better spatial resolution in source localization compared to EEG (Mäkelä 2010).

2.1.2 Electroencephalography

Electroencephalography (EEG) is a functional brain imaging technique and the pioneering research on human EEG can be attributed to Berger (1929). EEG measures the electric field potentials (Figure 1) arising from the synchronously active neurons similarly to MEG signal described above (Lopes da Silva & Van Rotterdam 2011, Jackson & Bolger 2014). EEG is measured with electrodes set on the participant's scalp with, e.g. a sensor net, which are usually arranged according to the standardized 10-20 system or its extensions (Seeck et al. 2017, Vanhatalo et al. 2018). Current guidelines recommend using minimum of 26 EEG electrodes in basic clinical applications (Seeck et al. 2017), however, high-density electrode nets of 64, 128 and 256 electrodes are more routinely used in research (Puce & Hämäläinen 2017) providing improved accuracy for source localization, which can be also utilized clinically in presurgical evaluation of epilepsy patients (Vanhatalo et al. 2018). EEG can be measured clinically also at bedside and does

not require robust shielding like MEG, although, it is advisable to prepare the test room for the purpose of measuring EEG and minimize sources producing artefacts (Puce & Hämäläinen 2017). EEG is more sensitive to radial sources and the EEG signal is dominated by the activity from the gyral crown. EEG can also detect tangential sources from the activity in sulci (Jackson & Bolger 2014). Compared to MEG, EEG can more readily detect deeper sources, up to 3 to 4 centimeters below cortex. Deeper sources need to be strong enough to provide sufficient signal-to-noise ratio as the cortical activity usually produces much stronger EEG signals than deeper sources. Furthermore, unlike with MEG, the tissues such as skull and scalp distort and attenuate the EEG signal and for this reason, MEG may have better spatial resolution in source estimation (Puce & Hämäläinen 2017). Regarding source localization, both methods search for a solution to the inverse problem. Forward problem involves determining the electric potentials and magnetic fields from current sources with EEG and MEG sensors. The inverse problem involves estimating the location of these sources, however, it is an ill-posed problem and thus there is no unique solution. For solution, source modeling techniques, such as minimum-norm estimates need to be used and additional assumptions have to be made, e.g. approximation of head-tissue conductivities with EEG for accurate head model (Baillet 2010, Michel & He 2011).

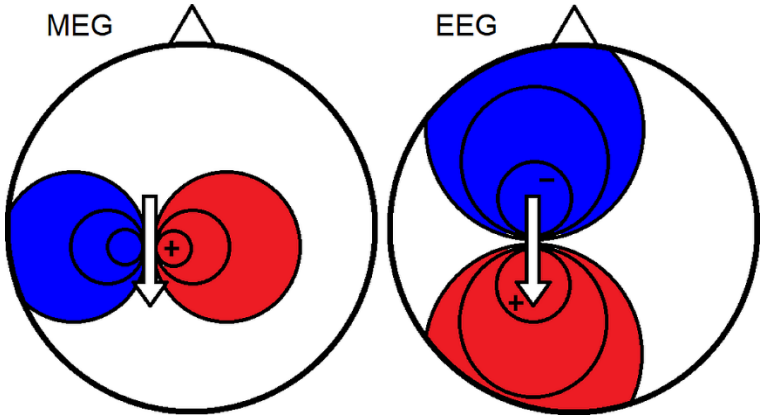

FIGURE 1 Field patterns detected by MEG and EEG. Schematic approximate illustration of field patterns caused by a tangential current dipole (left: MEG and right: EEG). Red areas depict the magnetic flux out of the head (MEG) and positive potential (EEG).

MEG and EEG have different methodological strengths, limitations and sensitivities to cortical activity, however, they are complimentary methods (Hari 2011). Since both these methods have a high temporal accuracy they are suitable for studying brain function close to stimulation event. Thus, common experiment methods used for detecting stimulation-induced neuronal activation are event-related potentials and event-related fields (ERP/ERF) representing activation of a neural population (Lopes da Silva 2011) and event-related desynchronization event-related synchronization (ERD/ERS) representing changes in neuronal oscillatory activity (Pfurtscheller & Lopes da Silva 2011). These experiment

variables are extracted by averaging multiple trials generating a time-locked response for a particular stimulation type, for example, somatosensory stimulation (Kakigi & Forss 2010, Salmelin & Parkkonen 2010).

2.2 Somatosensory system and nociception

2.2.1 Somatosensory processing

Somatosensory system consists of sensory receptors, which react to input from a particular physical property or modality, e.g. touch or temperature, and of tracts and nuclei, which conduct the information from peripheral receptors to the central nervous system (Strominger, Demarest & Laemle 2012; 155-156). The cell bodies of the peripheral sensory nerves are situated in the dorsal root ganglia and the receptor type at the peripheral nerve terminal determines the type of stimulus the neuron detects, e.g. mechanoreceptors that are activated by a mechanical stimulation (Gardner & Johnson 2013). Mechanical stimulation of a tissue activates the receptors causing a depolarization of the receptor neuron and sufficiently strong stimulus produces action potentials, which are transmitted along the axon (Gardner & Johnson 2013). The transmission or conduction velocity depends on the type of nerve fiber. Myelinated, large-diameter axons have faster conduction velocities and mechanoreceptors are primarily Aα and Aβ fibers with conduction velocities of 72-120 meters per second and 36-72 meters per second, respectively (Gardner & Johnson 2013). As electrical stimulation is often used in experiments, it must be noted, that electric stimuli activate nerve fibers starting from the largest ones with lowest electrical resistance and as the intensity is increased the stimuli activates more fibers (Gardner & Johnson 2013). Somatosensory information is conveyed via pathway which consists of three orders of neurons. The first order neurons of the spinal nerves convey somatosensory information from peripheral receptors in the limbs to the spinal cord. The second order neurons, transmitting e.g. tactile information, form an ascending pathway on the ipsilateral side as the dorsal column-medial lemniscal pathway that decussates in the medulla and terminates in the ventral posterior nuclei of the thalamus. Finally, the third order neurons reach the cortex by projecting from the thalamus to the primary and secondary somatosensory areas, which include representations of the body surface in somatotopical order (Figure 2) (Strominger, Demarest & Laemle 2012; 178-182, Gardner & Johnson 2013).

The function of the cortical somatosensory system can be studied with experiments using somatosensory stimulation and measured as somatosensory-evoked field (SEF) with MEG or somatosensory-evoked potential (SEP) with EEG. Brain imaging studies have shown that somatosensory stimulation generate measurable activation in the somatosensory brain areas (Hari & Forss 1999, Kakigi et al. 2000). Electrical stimulation applied on a peripheral nerve, e.g. median nerve at the wrist, is a typical method for evoking SEFs (Kakigi et al. 2000). The stimulation activates mechanoreceptors near the stimulation site

generating action potentials, which propagate through nerve fibers reaching the cortex (Jousmäki 2000). The earliest response in the SI cortex, after median nerve stimulation, typically peaks at 20 milliseconds (ms) and earliest response in the SII cortex is typically measured around 100 ms after stimulation onset (Hari & Forss 1999, Jousmäki 2000).

Another method for studying somatosensory processing is recording a somatosensory mismatch response (SMMR). The SMMR corresponds to extensively studied mismatch negativity (MMN) ERP component in auditory domain (Näätänen et al. 2007) and also to less studied MMN component in visual domain (Pazo-Alvarez, Cadaveira & Amenedo 2003). MMN represents cortical automatic change detection process and current theory suggests that repeatedly occurring standard stimulus creates a prediction of forthcoming events and the unexpected deviant event breaks this prediction creating a recordable non-conscious neurophysiological response representing brain's automatic capabilities of detecting changes in sensory environment (Kimura & Takeda 2015). In most MMN studies analysis is focused on the difference waveform, which is calculated by subtracting the standard from the deviant event-related field or potential. In the present study, difference waveforms were not used and analysis focused on the deviant and standard waveforms themselves approximating natural ongoing brain processes within the modeled time window. The term SMMR is used as it includes the mismatch phenomenon irrespective of the measurement method, e.g. MEG or EEG. The SMMR is reported to occur at 100-200 ms after stimulation onset as the deviant stimulation elicits stronger brain activation compared to standard stimulation (Kekoni et al. 1997, Shinozaki et al. 1998, Akatsuka et al. 2005). Also, an earlier component related to change detection has been reported to occur about 30-70 ms after stimulation with stronger brain activation after deviant stimulation (Shinozaki et al. 1998, Akatsuka et al. 2007a). Studies using MEG have localized the generation of these components in the SI and SII cortices (Akatsuka et al. 2007b, Naeije et al. 2018).

2.2.2 Nociceptive processing

The receptors, which respond to stimulus that can potentially damage tissue, are called nociceptors (free nerve endings), which respond to mechanical and thermal stimuli and indirectly to chemical stimuli (Strominger, Demarest & Laemle 2012; 157-158). Nociceptors are innervated with Aδ and C fibers, which have conduction velocities of 4-36 meters per second and 0.4-2.0 meters per second, respectively. The Aδ fibers produce short-latency pain, i.e. first pain, which can be described as sharp or pricking and the C fibers produce long-latency pain, i.e. second pain, described as dull or burning, and which is localized diffusively (Gardner & Johnson 2013). Nociceptive information is conveyed via anterolateral pathway, which comprise the spinomesencephalic, spinoreticular and spinothalamic tracts and this pathway decussates in the spinal cord before ascending to brain stem and thalamus and further to the cortex (Figure 2) (Gardner & Johnson 2013). Nociceptive processing and pain perception are

controlled by modulation of ascending and descending nociceptive pathways involved in a network of peripheral and central nervous system (Apkarian et al. 2005, Kuner & Flor 2017). In the human brain, this network is reported to consist of sensorimotor, limbic and associative brain areas (Duerden & Albanese 2013). In the cortical level, nociceptive processing has been suggested to involve a pain network of several cortical areas, which are consistently activated after noxious stimuli including primary and secondary somatosensory cortices, primary motor cortex, supplementary motor area, insula, anterior cingulate cortex, prefrontal cortex and thalamus (Apkarian et al. 2005, Kuner & Flor 2017). Brain areas involved in this network process also innocuous somatosensory information but the intensity of the network activation presumably differs according to different stimulation intensities (Kakigi, Watanabe & Yamasaki 2000).

Nociceptive processing can be studied using stimulation methods with MEG or EEG. Typical stimulation types are electrical stimulation (Kitamura et al. 1995, Kakigi, Watanabe & Yamasaki 2000), laser heat stimulation (Tarkka, Treede & Bromm 1992, Tarkka & Treede 1993) and even with cold stimulators (Leone et al. 2019). Thulium or CO_2 laser stimulation can be used to stimulate Aδ and C fibers rather selectively by application of different intensities and different sizes of the stimulation area (Hari 2011). Electrical stimulation is a simple method to use but the disadvantage is that electrical stimulation is more challenging to make specifically nociceptive as it tends to activate larger myelinated fibers that transmit tactile information, in addition to small myelinated nociceptive Aδ fibers (Kakigi, Watanabe & Yamasaki 2000). Nevertheless, electrical stimulation is successfully used investigating the somatosensory areas related to nociceptive processing (Kitamura et al. 1995, Inui et al. 2003).

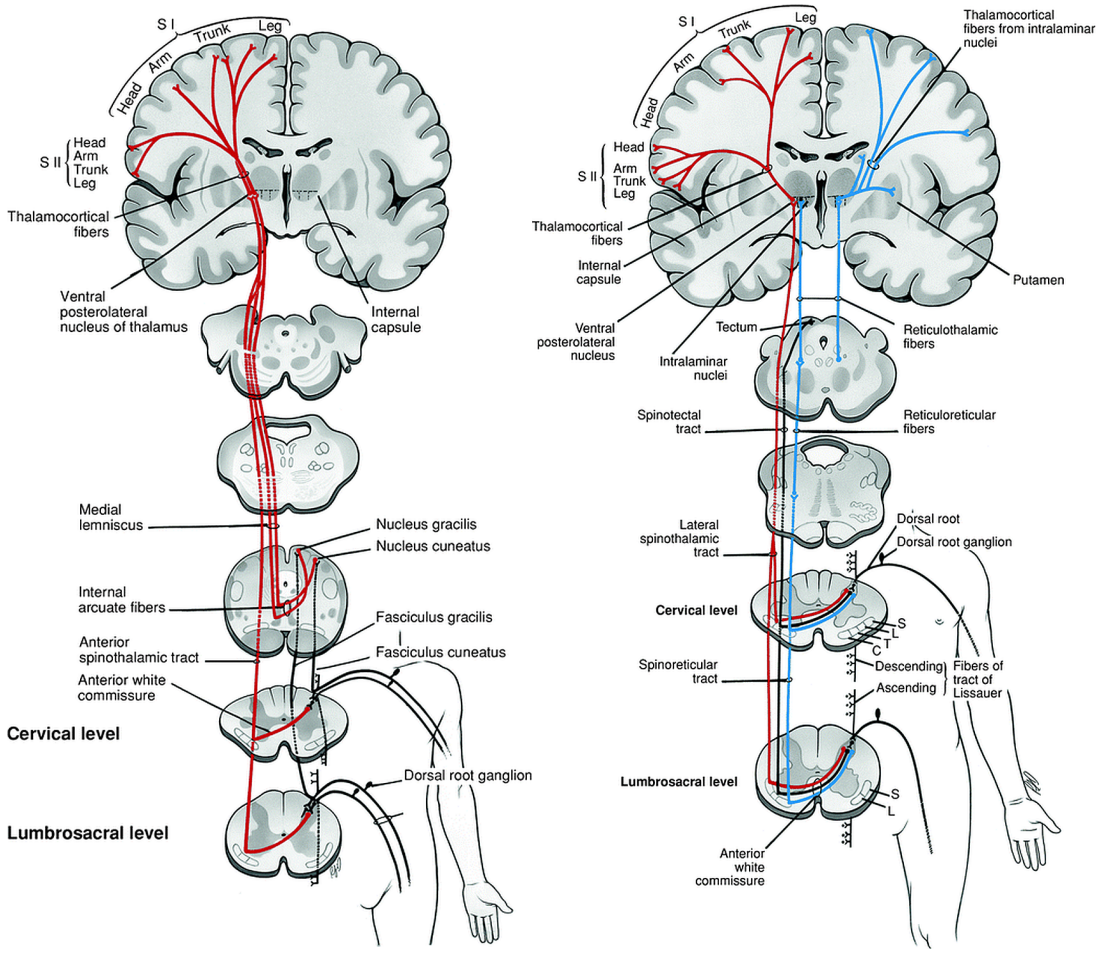

FIGURE 2 Somatosensory and nociceptive pathways. On the left, somatosensory pathways originating from spinal cord. Dorsal column-medial lemniscal pathway (black and red) arises on the ipsilateral side and decussates at the medulla (nucleus gracilis and cuneatus) reaching ventral posterolateral nucleus of thalamus and, further, SI and SII cortices. Additionally, anterior spinothalamic tract (red) mediates crude touch and movement sensation. On the right, pathways mediating pain and temperature. The lateral spinothalamic, spinomesencephalic (spitotectal) and spinoreticulothalamic tracts decussate at the lumbar or cervical level and arise on the contralateral side reaching thalamus. Further, projections from ventral posterolateral thalamic nucleus reach SI and SII cortices and the intralaminar thalamic nuclei project widely and diffusively to the cortex. (Adapted by permission from Springer Nature: Strominger, Demarest & Laemle (2012; 161, 179)).

2.3 Exercise effects on brain activity

During individual´s lifetime, the brain is subjected to many plastic changes as behaviour and experience as well as brain injuries and following recovery modulate brain´s structure and function (Nudo 2013, Mattson 2015). Physical activity has been shown to stimulate morphological brain differences in human

studies (Erickson et al. 2011, Hötting & Röder 2013, Erickson, Leckie & Weinstein 2014), and it has been associated with improved cognitive functioning (Erickson et al. 2019). Previous studies suggest connections between exercise and increased volume in hippocampus (Erickson et al. 2011), prefrontal cortex (Ruscheweyh et al. 2011) and improved white matter integrity (Strömmer et al. 2018). However, it is notable that the majority of the studies linking cognitive functioning to exercise has been conducted in older adults and research on young healthy adults currently available is insufficient (Erickson et al. 2019). Furthermore, research on exercise effects on other domains of brain function, such as somatosensory and nociceptive processing, is scarce.

Proper function of somatosensory system is paramount in our ability to interact with environment as we are subjected to constant sensory information. The brain is inherently able to gate irrelevant sensory information and this sensory gating is an important neurophysiological process modulating our responses to changes in environment (Bak et al. 2011). It can be speculated that persons participating in exercise are exposed to more diverse sensory stimulation and may be able to process the sensory information more efficiently (Tarkka et al. 2016). Previously sensory gating has been discussed in association also with processing of nociceptive information (Moayedi & Davis 2013).

Complex network of brain areas underlying pain perception and experience involve both somatosensory and nociceptive processing and somatosensory and nociceptive systems are closely linked. This can be observed with participation of SI and SII cortices in early phases of cortical activation after either innocuous somatosensory or higher intensity nociceptive stimulation (Peyron & Fauchon 2019). Pain symptoms in various chronic diseases are an important factor affecting the quality of life. Studies have even shown that prolonged pain symptoms can induce maladaptive neuroplastic effects on the central nervous system (Kuner & Flor 2017), for example, inducing cortical reorganization in the SI cortex (Flor et al. 1997). Treatment for pain mainly consists of pharmacological interventions (Tajerian & Clark 2017), however, exercise is used in rehabilitation and it has been reported to have hypoalgesic effects (Rice et al. 2019). Interestingly, athletes participating in exercise long-term have shown reduced pain perception (Tesarz et al. 2012).

Biological mechanisms that may be involved in exercise-induced hypoalgesia include endogenous opioid, endocannabinoid and serotonergic systems, however, these physiological mechanisms inducing exercise-induced hypoalgesia are still incompletely understood (Rice et al. 2019), especially very little is known of the possible early cortical involvement in hypoalgesic mechanisms. While studies have shown that exercise can induce beneficial neuroplastic (Voelcker-Rehage & Niemann 2013) and hypoalgesic effects (Rice et al. 2019), knowledge on associations between exercise, and somatosensory and nociceptive system is limited and require further research. The present dissertation focused on the early somatosensory and nociceptive cortical activity. Specifically, these studies concentrate on the neurophysiological features of

somatosensory and nociceptive processing and somatosensory change detection system and whether exercise may modulate these processes.

3 AIMS OF THE STUDY

The main objective of this dissertation was to study somatosensory function and nociceptive processing in the human brain and the influence of exercise on these processes. Functional neuroimaging methods with excellent temporal resolution and somatosensory and nociceptive stimuli were used to record cortical activity. Furthermore, acute exercise task design, and monozygotic twin-pair design with discordance in long-term exercise status within pair were used to measure exercise effects on cortical activity. The specific aims of individual studies were as follows:

I To assess whether brain functional and/or structural modulation associated with long-term physical activity is detectable using an exercise-discordant monozygotic male twin pair design.

II To assess somatosensory-driven automatic cortical change detection system elicited by different experimental somatosensory stimulations using magnetoencephalography.

III To analyze cortical processing of different types of innocuous and nociceptive electrical sensory stimulations with special reference to pain-related cortical sensory networks in young healthy participants.

IV To assess whether acute exercise task modulates cortical activity induced by experimental nociceptive stimulation.

4 METHODS

4.1 Ethical considerations

The participants gave written informed consent before any experimental session. Ethical approval for *Study I* was granted by the Ethical Review board for Human Research of the Central Finland Health Care District and for *Studies II-IV* by the Ethics Committee of the University of Jyväskylä. All studies were conducted in accordance with the Declaration of Helsinki. The measurements utilized somatosensory and nociceptive stimulation directed to the participants' hand or wrist. Stimulation may have caused discomfort and nociception, nonetheless the chosen method was essential for studying somatosensory and nociceptive processing in the human brain. During the measurements, the participants' wellbeing was constantly monitored and they were instructed that they had a right to abort the measurement at any moment. The participants' personal information was kept secret and separate from gathered data so that individuals cannot be identified in any reporting of the study results. The participants were volunteers and did not receive any compensation for taking part in the study.

4.2 Participants

The participants in all studies were healthy right-handed adults. In *Study I,* the participants were a subgroup from FITFATTWIN (Rottensteiner et al. 2015) study. Nine monozygotic twin pairs, 18 healthy men (mean age 34), who were long-term discordant within pair in their leisure-time physical activity were included in the study. The physical activity levels and within pair discordance were determined by a structured retrospective physical activity interview (Kujala et al. 1998, Waller, Kaprio & Kujala 2008, Leskinen et al. 2009) which takes into

account leisure-time physical activity, including commuting activity. Information from the interview was used to calculate the leisure-time metabolic equivalent (MET) index during past three years as MET hours/day (3-year-MET) for the physical activity assessment. Their weight, height, waist circumference and maximal oxygen uptake (VO_{2max}) were measured, body mass index (BMI) calculated and whole body composition measured after overnight fast using dual-energy X-ray absorptiometry (DXA Prodigy, GE Lunar Corp., Madison, WI, USA).

For *Studies II-IV*, the participants were recruited from university personnel and student body. *Study II* included 16 adults (six women, age range 18-36, mean age 29). *Study III* included 17 adults (seven women, age range 18-41, mean age 31) and in an additional recording five adults (two women, age range 28-39, mean age 34). Participants in *Studies II* and *III* mostly overlapped, while five additional women (age range 26-43, mean age 33) were recruited to participate in *Study IV*.

Before the MEG recordings in *Studies II-IV*, participants were seated in the MEG device and a short recording was conducted to ensure that no magnetic objects were present in the head or upper body, which could contaminate the MEG recording or generate artefacts. In *Studies II-IV*, RBDI mood questionnaire (Raitasalo 2007), a short version of the Beck Depression Inventory (BDI) (Beck et al. 1961) modified to Finnish language was used to verify the absence of depressive and anxiety symptoms among the participants. Additionally, any history of neurological or psychiatric diseases was ruled out by interview.

4.3 Stimulations

Both electrical and pneumatic tactile stimulations were utilized with SMMR and SEF experimental paradigms in the current studies. These experimental paradigms provide complementary information on features of primary and secondary somatosensory function. SEF, often considered as a gold standard in MEG research, focuses on SI and also SII activations and SMMR provides a more robust extension to somatosensory processing in secondary sensory areas. Furthermore, detailed SEF paradigms in Study III enabled development of the intracutaneous stimulus for experimental nociceptive stimulation.

In *Studies I* and *II*, a somatosensory peripheral stimulation was used to elicit somatosensory mismatch response (SMMR), as an automatic location change detection. SMMR stimulation protocol consisted of 1000 stimulations from which 10 percent were pseudorandomly delivered deviants. Stimulations were delivered in two halves. In the first half, standard stimulations were delivered to the right hand index finger and deviants to the fifth finger. In the second half, the stimulus locations were reversed, thus producing the mismatch in location during the flow of stimuli independent from finger. Interstimulus interval (ISI) was set at 600 ms in *Study I* and 500 ms in *Study II*. Electrical stimulation (*Study I*: model DS7A, Digitimer Ltd., Welwyn Garden City, UK; *Study II*: DeMeTec SCG30, DeMeTec GmbH, Langgöns, Germany) was delivered through flexible

non-magnetic ring electrodes (Technomed Europe Ltd., Maastricht, the Netherlands) placed on both fingers on the proximal and distal phalanges. The electrical stimulus was a monophasic square-wave pulse of 0.2 ms in duration. Stimulation intensities were set at two times the individual sensory threshold in *Study I* (second finger mean 4.5 (standard deviation ± 1.2) mA and fifth finger mean 4.3 (± 0.8) mA) and at least to a minimum of 120 percent in *Study II* (second finger mean 4.9 (± 1.0) mA and fifth finger mean 4.1 (± 0.9) mA) of the individual sensory threshold so that a clear sensation was perceived in both fingers.

Additionally, in *Study II*, a pneumatic tactile stimulation with the same SMMR stimulation protocol was used as a more natural stimulus to compare cortical responses to those elicited by electrical stimulation. Tactile stimulation was generated with an air-pressure stimulator built in-house, which produced 0.4 bar pressure pulse through plastic tubes (diameter 5 mm). The pressure pulse briefly inflated plastic membranes (surface area 2.0 cm^2 before membrane inflation) at the end of the tubes, which were attached to the second and fifth finger distal phalanges with lightweight plastic clips. The brief inflation of the plastic membrane generated a clear tactile sensation to the second and fifth fingertips.

In *Study III*, electrical stimulation (model DS7A, Digitimer Ltd., Welwyn Garden City, UK) was applied to different peripheral nerve areas on the right hand. Radial nerve area on the dorsal surface of the right hand was stimulated 80 times randomly within 4-6 second intervals. Stimulating electrodes (diameter 10 mm) were placed at the proximal end of the first metacarpal and on the distal head of the ulna. Stimulation intensity was set at two times the individual sensory threshold (mean 7.7 (± 2.2) mA). Median nerve was stimulated at the right hand wrist with a bipolar felt-pad stimulating electrode first with a short interstimulus interval of 200 ms (5 Hz stimulation frequency) 300 times and in an additional recording 80 times randomly within 4-6 second intervals to match the radial nerve stimulation ISI and stimulus count parameters. Intensity for the median nerve stimulation was set to individual motor threshold producing a weak thumb movement (mean 5.8 (± 1.4) mA).

Third type of stimuli in *Study III* was an intracutaneous electrical stimulation (modified from Kochs et al. (1996)) designed to deliver nociceptive stimuli. The stimulation was delivered to the third fingertip from where the superficial epidermal layers of the glabrous skin were lightly drilled with a small stainless steel drill (diameter of 1.5 mm). A non-magnetic copper tip electrode (diameter 1 mm, height 2 mm) was attached into the small skin hole with adhesive tape and a flexible non-magnetic metal ring return electrode (Technomed Europe Ltd., Maastricht, the Netherlands) was tightened in the metacarpophalangeal joint of the third finger. The delivered square-wave current pulse (duration 0.2 ms) activated the palmar digital branch of the median nerve and likely activated superficial nociceptive nerve terminals. The stimulation ISI and number of stimulations matched radial and median nerve stimulations. The stimulation intensity (mean 4.6 (± 2.2) mA) was set individually to each

participant so that the stimulation was rated as moderately painful, 6-7 on a visual analog scale (VAS 0-10).

The intracutaneous electrical stimulation was subsequently used in *Study IV* with intensity defined similarly as individually rated as moderately painful (mean 4.0 (± 1.8) mA). Stimulation interval was random within a range of 5.5 – 7.5 seconds and 30 repetitions were collected before and immediately after an acute exercise task. Between two MEG recordings with nociceptive intracutaneous stimulation to the right hand third fingertip, there was a 10-minute rest period to ensure the recovery of the primary afferent responsiveness and to prevent adaptation to the stimulation within session (LaMotte & Campbell 1978). The same individually adjusted stimulation intensity was used in both MEG recordings and the VAS scores were collected after each recording (mean before: 6.0 (± 0.5) and after: 6.6 (± 0.7)).

4.4 Tasks

In *Study I*, co-twins were recorded on the same day and during the EEG recording they listened to an engaging radio play while been instructed to concentrate on the play and ignore the stimuli. After recording, they were asked questions about the contents of the radio play. In *Study II*, task during the MEG recording was passive as the participants were asked to focus their gaze on a neutral mark approximately 1.5 meters in front of them and not pay attention to the stimuli.

In *Study III*, tasks were passive during median nerve and intracutaneous stimulation MEG recordings where the participants were asked not to pay attention to the stimuli and remain relaxed. In the first part of the study, during radial nerve stimulation the participants were asked to perform reaction time movement task defined as an index finger abduction after stimulation. The requested task occupied participant's attention. Previous research has shown that spatial attention towards the stimulated hand does not modulate the source strengths of early somatosensory evoked field (SEF) components (Mauguière et al. 1997a). Even though the radial nerve stimulation was followed by voluntary movement, only the early stages of cortical stimulation processing (up to 180 ms after stimulation and before the onset of voluntary movement) were compared between stimulation types. In the second part of the study, passive tasks were used in all stimulation conditions without attention task.

In *Study IV*, during recording the participants were instructed to remain still and focus their gaze on a neutral marker approximately 1.5 meters in front of them. Between two MEG recordings of intracutaneous stimulation, the participants performed an acute exercise task. The exercise task with the left hand was timed to the last three minutes of the 10-minute break period between the two recordings. The exercise task was a left hand three-minute isometric grip contraction using a hand dynamometer (Saehan SH5001, Saehan Inc., Korea). The force level was set at 30 percent of maximum voluntary contraction (MVC). Individual MVC force was measured (mean 262.8 (± 44.1) N) at the beginning of

the measurement session, at least 30 minutes before the MEG recording to ensure that any mild hypoalgesic effects from the MVC measurement would have subsided (Naugle, Fillingim & Riley 2012). The exercise task was strenuous and fatiguing and the rating of perceived exertion (RPE) resulted in a mean of 17.3 (± 1.5) on the Borg's RPE scale (6-20) (Borg 1970).

4.5 EEG, MRI and MEG data recording, preprocessing and analysis

4.5.1 EEG recording

In *Study I*, EEG was recorded with a 128-channel sensor net with a Cz reference (Electrical Geodesics, Inc., Portland, OR, USA) and for analysis re-referenced to average reference. EGI 128-channel Geodesic sensor net enables fast application and does not require scalp abrasion. Electrodes are embedded in small sponges filled with electrolyte solution and acceptable impedance being in the 50 – 100 kΩ range, though often 10 – 20 kΩ is obtained. Recording was done with 0.1 – 200 Hz bandpass filter and sampling rate of 500 Hz.

4.5.2 EEG data preprocessing and analysis

EEG data in *Study I* was analyzed with the Brain Electrical Source Analysis (BESA, Besa GmbH, Gräfelfing, Germany) software. The data was bandpass filtered with 1 – 35 Hz frequency range and segmented to epochs from -100 to 350 ms in relation to the stimulation onset. Epochs containing artefacts from eye-blinks, high amplitude potential shifts or movement were automatically rejected from further analysis. Artefact-free epochs were baseline corrected and averaged for each individual to form deviant event-related potential (ERP) and then same number of standard stimuli were picked and averaged to form the standard ERP waveform. The average amount per participant of analyzed deviant stimulations was 90 (± 8) from active and 91 (± 6) from inactive twins. Correspondingly, average amount of analyzed standard stimulations was 90 (± 10) from active and 92 (± 7) from inactive twins.

Grand average waveforms were formed from the individual averages separately for deviant and standard conditions. Inactive co-twins' deviant and standard grand averages were compared with those of active co-twins' grand averages. Topographic voltage maps were generated from the grand average waveforms and further source modelling was done with spatio-temporal multiple dipole source model. Modelling time window was from 0 to 350 ms where each source potential described the temporal variations in each dipole moment (i.e. its strength) while the equivalent dipole source maintained its location and orientation. An ellipsoidal head model with four shells was used and the proportion of the data not explained by the source model was displayed in residual variance (RV). First model was developed for the grand average

deviant waveform from the active twins starting from the waveform component with highest amplitude because source activities are easiest to dissociate when amplitudes are high and signal-to-noise ratio is good. The source model was a seven-dipole model where six dipoles explained cerebral activity and one dipole accounted for residual eye movements. Dipoles 1, 2, 3 and 5 were completely free during fitting and dipole 4 was symmetric to dipole 5 and dipole 6 was symmetric to dipole 2, and finally dipole 7, collecting residual eye movement activity, was fixed in location with free orientation. This model was applied to the deviant grand average of the inactive co-twins and to the standard grand averages of the active and inactive co-twins. When fitting this model to other grand averages, the source orientations were fitted but source locations were kept stationary. Further fitting or adding more dipoles did not improve the model. As the locations were kept the same when applying the source mode to other averages, the possible individual differences were observed in modulation of dipolar source potentials and in varying RVs. The differences in dipole moments were applied in statistical models.

4.5.3 MRI recording

In *Study I*, magnetic resonance imaging (MRI) scans were acquired from 18 individuals using a 1.5 Tesla whole body magnetic resonance scanner (Siemens Symphony, Siemens Medical Systems, Erlangen, Germany) on the same day as other data was collected. The 3D T1-weighted MPRAGE images of whole brain were collected with the following parameters: TR = 2180 ms, TE = 3.45 ms, TI = 1100 ms, flip angle = 15°, slice thickness = 1.0 mm, in-plane resolution 1.0 mm x 1.0 mm, and matrix size = 256 x 256.

4.5.4 MRI data preprocessing and analysis

Voxel-based morphometric (VBM) analyses of the MRI data in *Study I* were performed with VBM8 toolbox (http://dbm.neuro.uni-jena.de/vbm/) for Statistical Parametric Mapping 8 (SPM8) software (Wellcome Trust Center for Neuroimaging, UCL, London, UK) running on Matlab R2010a (Mathworks, Inc., Natick, MA, USA). The MRIs were first segmented into gray matter (GM), white matter (WM), and cerebrospinal fluid (CSF). Next, images were normalized to the Montreal Neurological Institute (MNI) brain template using a high-dimensional DARTEL algorithm. Nonlinearly modulated GM images were created to preserve relative differences in regional GM volume. Finally, the GM volumes were spatially smoothed with 12 mm full width at half maximum Gaussian kernel. GM, WM and CSF volumes were compared between co-twins as well as GM voxel counts of four regions on interest (ROI), suggested by the electrophysiological source model, from both hemispheres were compared between co-twins. The ROIs were defined using the WFU pickatlas toolbox (Wake Forest University, School of Medicine) (Maldjian et al. 2003, 2004) implemented in SPM8.

4.5.5 MEG recording

In *Studies II-IV*, MEG signals were recorded with a helmet-shaped 306-channel device covering the whole scalp (Elekta Neuromag®, Triux™, Stockholm, Sweden) using a bandpass filter of 0.1 – 330 Hz and digitized with a sampling frequency of 1000 Hz. The participants were seated comfortably in the MEG device, installed inside a magnetically shielded room (Vacuumschmelze GmbH, Hanau, Germany). The participant's head position in relation to the MEG sensors was determined with five head position indicator coils (HPI), placed on the participant's scalp and forehead. Prior to the MEG recording, the HPI coil locations were registered with a 3D digitizer (Fastrak®, Polhemus, Colchester, VT, USA) in relation to each participant's three anatomical landmarks (nasion and bilateral preauricular points). Additional digitized points were registered from the scalp surface, forehead and nose crest for accurate representation of the participant's individual head shape. The participants were instructed to keep their eyes open and to avoid blinking, eye movements and other voluntary movements, except when an active task was instructed. During the recording the participant's eye movements and blinks were continuously monitored with an electro-oculography (EOG). EOG electrodes were placed above the right eye above the zygomatic process of the frontal bone and below the right eye on the zygomatic bone. Collected MEG and EOG signals were stored for offline processing and analysis.

4.5.6 MEG data preprocessing and analysis

In *Studies II-IV*, the MEG data was first processed with the signal space separation method (Taulu, Kajola & Simola 2004) implemented in MaxFilter software (version 2.2; Elekta, Helsinki, Finland) to suppress environmental electromagnetic interference, and in *Studies II* and *IV* also for correcting head positions across participants. Since no individual structural MRIs were available in *Studies II-IV*, brain anatomy templates (MNI brain template in *Study II* and ICBM152 template in *Studies III* and *IV*) were used in source modelling. According to MEG guideline recommendations (Gross et al. 2013), an accurate digitization of the individual head shape is an appropriate method for source location analysis of electromagnetic activity. Instead of individual MRI, this head shape can be used to approximately align the participant's head to an anatomy template (Holliday et al. 2003) to allow for averaging across participants. The anatomy templates were aligned for each subject with the HPI data collected before the MEG recordings (Darvas et al. 2006). Different analysis software packages such as Brainstorm (Tadel et al. 2011) and Statistical Parametric Mapping 12 (SPM12) (Litvak et al. 2011) available in https://www.fil.ion.ucl.ac.uk/spm/ running on Matlab 2015a (Mathworks, Inc. Natick, MA, USA) were used depending on their applicability to planned analysis pathways. Different features of the used analysis software were utilized to complement each other.

4.5.6.1 MEG data preprocessing and analysis in *Study II*

In *Study II*, data preprocessing and analysis was conducted with SPM12 after converting the MEG raw data into SPM12 format. Stimulation delays (3 ms in electrical stimulation and 21 ms in tactile stimulation) were corrected. All 100 deviant stimulations and 100 standard stimulations preceding each deviant stimulation were picked for both electrical and tactile stimulation analyses. Data was epoched in relation to stimulation triggers to time windows from -500 ms to 750 ms including 400 ms buffers to avoid distortions from subsequent filtering. Data was highpass filtered at 0.1 Hz, lowpass filtered at 60 Hz and baseline correction was made using a time segment from -100 ms to 0 ms. Next, the trials were cropped including only the time window of interest from -100 to 350 ms. EOG artefacts were identified and trials where EOG amplitude exceeded 70 μV were excluded from further analysis. Average number of analyzed trials in electrical stimulation were: standard 86 (± 13.0) and deviant 86 (± 12.2) and in tactile stimulation: standard 82 (± 13.5) and deviant 81 (± 15.3). Further analysis was done first in sensor-level and second in source-level.

For sensor-level analysis, planar gradiometer channel pairs were combined into one value by taking root mean square (RMS) of the two gradiometers in each sensor location. In SPM12, scalp-time images were created from each individual combined gradiometer averages, using a time window from 0 to 300 ms, by projecting the sensor locations in 2D space and interpolating them, with time serving as the third dimension. These images were used to compare deviant stimulation between electrical and tactile conditions and deviant and standard stimulation within each condition. Differences detected in sensor-level analysis were used to determine time windows for source level analysis.

Source models were created with SPM12 group inversion using each participant's averaged trials including all 204 planar gradiometers and 102 magnetometers. Since no individual MRIs were available, a brain anatomy template (MNI brain), provided by SPM12, was used for head model with a cortical mesh size of 8196 vertices. Forward model was computed as a single sphere and inverse reconstruction was performed with SPM12 multiple sparse priors method for the whole trial time window from -100 to 350 ms. The source modelling results were transformed into cortical surface images for statistical analysis summarizing average activity from two time windows established in sensor-level analysis: from 40 to 58 ms and from 110 to 185 ms.

4.5.6.2 MEG data preprocessing and analysis in *Study III*

Data preprocessing and analysis in *Study III* was performed with Brainstorm software (version released 15th February 2017) and SPM12. Artefacts from eye movements and blinks were corrected with signal-space projection (SSP) method (Uusitalo & Ilmoniemi 1997). Stimulation delay of 3 ms was corrected. Next, as the shortest ISI was 200 ms, the data was segmented to epochs from -10 to 180 ms according to the stimulation onset and the first 10 ms of the time window served as a baseline. Averages of different conditions were computed for each individual from all artefact-free epochs. Source modelling was done using

distributed models. The forward model was computed with overlapping spheres method (Huang, Mosher & Leahy 1999) where one local sphere was assigned to each sensor. Source models were generated from each participant's averaged epochs using minimum-norm estimate in dynamic statistical parametric mapping (dSPM). Source dipole orientations were constrained normally to cortex and all gradiometer sensors were included.

From the dSPM source maps, ROIs were analyzed using Brainstorm's scout function for temporal analysis and SPM12 for regional and source strength analysis. The scouts were applied for each participant's source maps. Scout locations were determined by maximum amplitudes within four time windows indicated by gradiometer waveform components: 15-25, 25-35, 60-80 and 100-140 ms. Each scout was set to cover 20 vertices, corresponding to 3 cm^2 on average on the cortical surface. One scout represented mean activity in each source location and the scout waveforms were used to compare brain activities between conditions in temporal domain using time points of peak source field strength and mean amplitudes over 10 ms time windows after source action onsets. Source strengths and regional and hemispheric differences in the ROIs were compared between conditions in SPM12 utilizing extension toolbox WFU pickatlas (version 3.05) (Maldjian et al. 2003, 2004). Volumetric statistical parametric maps of the t-statistics were computed from each individual's source maps for 5 ms (short latency components) or 10 ms (middle and long latency components) time windows according to the peak source strength latencies identified from the scout waveforms. Atlas-based ROI masks (Lancaster et al. 1997, 2000) including bilateral post-central gyrus and bilateral insula were used for voxel-based statistical comparison.

4.5.6.3 MEG data preprocessing and analysis in *Study IV*

In *Study IV*, data preprocessing and analysis was performed with Brainstorm (version released 24th February 2019). The data was visually inspected for environmental and physiological artefacts, and artifacts from eye blinks were identified and corrected with SSP. The data was segmented to epochs surrounding the stimulation onset from -1500 to 2500 ms including 500 ms buffers at the beginning and end of the time window to avoid signal distortions caused by subsequent filtering. Stimulation delay of 3 ms, identified from the stimulation artefact, was corrected. The stimulation artefact was removed surrounding the stimulation onset from -4 to 8 ms by replacing the values in this short time period with linear interpolation. After preprocessing, two analysis pathways were adopted, namely event-related field analysis and oscillatory analysis based on spectral contents of the signals.

In the evoked field analysis, a 50 Hz notch filter was applied to remove the power line noise and then the data was filtered with a 70 Hz lowpass filter. The data was segmented to time windows from -200 to 500 ms according to the stimulation onset and baseline corrected (-200, -5 ms) before averaging. For source estimation, a forward model was computed using the overlapping spheres method. For each participant and both conditions, source maps were

produced from trial averages and derived from the minimum-norm estimate. Noise covariance statistics were derived from the empty room recordings collected before each measurement session. The orientations of the source dipoles were constrained normally to the cortical surface and all MEG channels were included. The current density source maps were normalized with Z-transformation with respect to the baseline and next, the source maps were smoothed spatially. ROIs were explored with the Brainstorm's scout function and the scouts were set to cover 20 vertices, corresponding to approximately 4 cm^2 on the cortical surface. Scout locations were determined in the source maps as the maximum source amplitudes using the evoked field waveform components as temporal cues.

Oscillatory analysis was performed by adopting the temporal spectral evolution (TSE) analysis (Salmelin & Hari 1994) to quantify the modulation of rhythmic activity in the ~20 Hz and ~10 Hz sensorimotor cortex rhythms. MEG signals were separately filtered through 15-25 Hz and 8-12 Hz frequency ranges and then rectified. Then, the signals were smoothed with 15 Hz lowpass filter, segmented to time window of interest from -500 to 2000 ms and finally each participant's data was averaged. The stimulus-related changes in both rhythms were quantified from one planar gradiometer channel in each hemisphere over sensorimotor regions. The gradiometer channels were selected based on their strongest reactivity, i.e. the largest change in amplitude from suppression to rebound. The suppression and rebound amplitudes were converted to relative values by calculating the percentage of the rhythms amplitude decrease and increase in relation to the reference baseline. Suppression and rebound strengths were determined as the mean amplitude ± 5 ms around the maximum value and latencies as the time points at maximum value of the suppression and rebound.

4.6 Statistical analyses

Statistical analysis in *Study I* was performed with IBM SPSS 22 (IBM, Armonk, NY, USA). Wilcoxon Signed Rank test was used to compare voxel counts in MRI ROIs. For dipole moment comparison point-to-point on source waveforms was performed with repeated measures ANOVA with 5(time) x 2(group) factorial design. Only group effects are reported. Significance was set at $p < 0.05$. Source waveform results include effect sizes in η_p^2 (partial eta-squared).

In *Study II*, statistical analysis was done in the SPM12 software as a regional field strength analysis. The group analysis of the MEG data was performed first in the sensor-level followed by source-level analysis. Group level differences within and between conditions were tested with paired samples t-test. The height threshold was set to $p < 0.001$ (uncorrected for multiple comparisons). Clusters surviving the primary threshold were regarded as significant when falling below family-wise error rate (FWE) corrected cluster-level threshold of 0.05. No minimum cluster size was determined.

Statistical analysis in *Study III* was performed with IBM SPSS 24 for temporal analysis and with SPM12 for regional field strength analysis. All group analysis of MEG data was done in source space. Temporal variables were compared with paired samples t-test, with significance threshold set at $p < 0.05$. Group level differences between identified brain regions were detected by voxel-level statistical analysis in SPM12 with two-sample t-test. Primary threshold was set to $p < 0.001$ or $p < 0.005$ (uncorrected for multiple comparisons) and corrected for multiple comparisons by the false discovery rate (FDR) method. Clusters were regarded as significant when falling below FDR-corrected cluster-level threshold of 0.05. No minimum cluster size was determined.

In *Study IV*, the measured electrophysiological parameters, peak latencies and amplitudes of the brain source activations, and oscillation reactivity were compared between conditions within participants using the paired samples t-test in IBM SPSS 24.

5 SUMMARY OF RESULTS

5.1 Study I

Study I examined whether brain functional and/or structural modulation associated with long-term physical activity is detectable using an exercise-discordant monozygotic male twin pair design. The co-twins differed in fitness and leisure-time activity levels, and fat percent revealing robust discordance in exercise history. The active twins fitness level (VO_{2max}, 43.1 (± 4) vs. 37.2 (± 3.5), $p < 0.008$) and activity level was higher (3-year-MET, 4.5 (± 2.1) vs. 1.4 (± 1.0), $p < 0.003$) and fat percent lower (20.3 (± 4) vs. 23.8 (± 5), $p < 0.04$) compared to their inactive brothers.

The seven-dipole source model is depicted in Figure 3. Source dipole (SD) 1 modeled major activity between 220 and 300 ms peaking with 20 nAm and SD 2 and 3 modeled unilateral (contralateral to stimulation) activity starting already at 24 ms with 9 and 11 nAm peak currents, respectively. SD 4 and 5 modeled bilateral activities between 100 and 300 ms in deeper brain areas peaking with 9 and 7 nAm currents, respectively. Finally, SD 6 modeled unilateral (ipsilateral to stimulation) activity between 74 and 272 ms peaking with 8 nAm. Approximate brain locations were estimated for SD 1 in the ventral anterior cingulate cortex, for SD2 in the contralateral postcentral gyrus with symmetrical SD6 in the ipsilateral postcentral gyrus. For SD3 the location was estimated in the frontal medial gyrus, for SD4 in the contralateral superior temporal gyrus with symmetrical SD5 in the ipsilateral superior temporal gyrus and finally, SD7 (not depicted in the Figure 3) explaining the excess eye movements. In the deviant grand average of the active co-twins, the RV was 6.9 % and when the model was introduced in the standard grand average, the RV was 25.1 %. In the inactive co-twins, the corresponding RVs were 5.7 % for the deviant grand average and 17.8 % for the standard grand average.

The deviant stimulus-elicited SMMR source waveforms were compared between active and inactive co-twins. Source SD2 showed a significant difference during 280-290 ms after stimulation ($F(1, 16) = 5.345$, $p = 0.034$, $\eta_p^2 = 0.250$) where

inactive co-twins had stronger amplitudes. In source SD3 there was a significant difference between 148-158 ms after stimulation ($F(1, 16) = 8.200$, $p = 0.011$, $\eta_p^2 = 0.339$) where again inactive co-twins had stronger amplitudes. Source SD4 had two instances, first at 86-96 ms ($F(1, 16) = 5.780$, $p = 0.029$, $\eta_p^2 = 0.265$), where again inactive co-twins had stronger amplitudes. The second difference in SD4 occurred at 252-262 ms after stimulation ($F(1, 16) = 5.538$, $p = 0.032$, $\eta_p^2 = 0.257$) where active co-twins had stronger amplitudes. Source SD1 did not show differences between co-twins. Additionally, the standard stimulations dipole source waveforms were compared and there, in source SD6, was significant difference at 252-262 ms ($F(1, 16) = 4.811$, $p = 0.043$, $\eta_p^2 = 0.231$) where active co-twins had stronger amplitudes. Dipole moments with significant differences are depicted in Figure 4. Comparison of normalized images of structural MRIs did not show differences between co-twins in total GM, WM and CSF volumes. Further analysis with ROIs, based on the above described multiple dipole source model, revealed GM voxel count difference in the right anterior cingulate (inactive 544 ± 9 vs. active 536 ± 12, $p = 0.046$) between co-twins where inactive co-twins showed larger voxel count. Overall, these results demonstrated that long-term physical activity selectively modulated specific early somatosensory functional brain responses and may have selectively modified specific cortical structures.

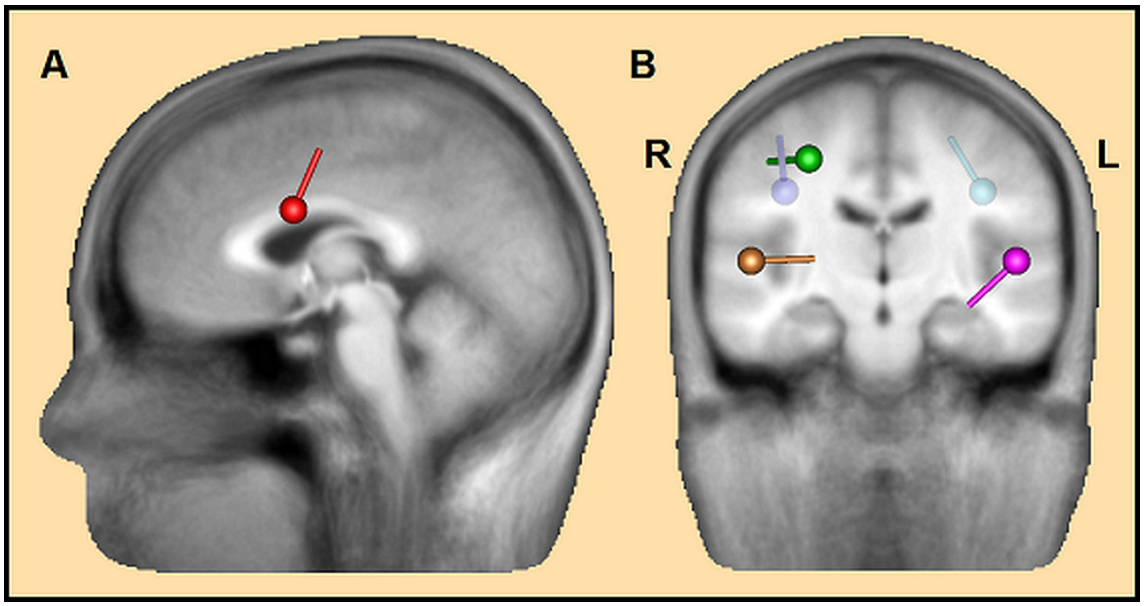

FIGURE 3 Seven-dipole source model generated from the grand average deviant waveform in *Study I*. Dipole model is presented in an average MRI provided in BESA in sagittal (A) and verticofrontal (B) planes. Six dipoles are visible in these depicted planes, one dipole accounting for eye movement activity is not visible here. SD1 = red, SD2 = light purple, SD3 = green, SD4 = magenta, SD5 = brown and SD6 = blue. (Figure as originally published in Hautasaari et al. 2017).

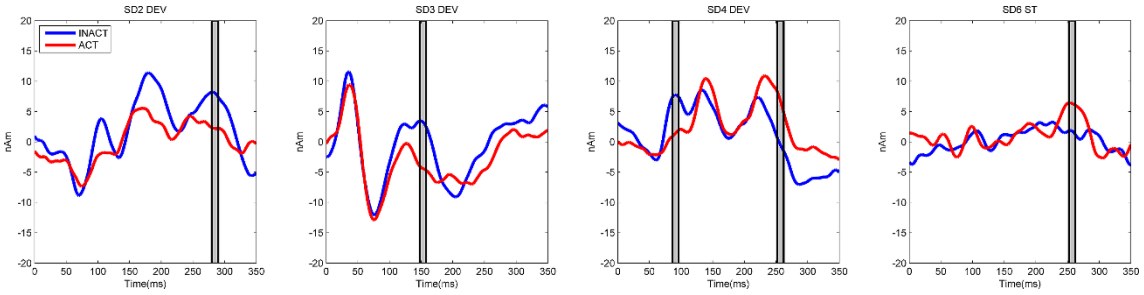

FIGURE 4 Source moments of individual dipoles of the developed source model explaining deviant data sets in *Study I*. Time windows of detected significant differences between groups are shown (inactive twins in blue and active twins in red). Source SD2 for deviant (first from left, light purple in Fig. 3), difference during 280–290 ms from stimulus onset. Source SD3 for deviant (second from left, green in Fig. 3), difference during 148–158 ms from stimulus onset. Source SD4 for deviant (third from left, magenta in Fig. 3), differences during 86–96 and 252–262 after stimulus onset. Standard stimuli data were also modeled and source SD6 (fourth from left, light blue in Fig. 3) shows standard stimulus data sets where difference during 252–262 ms after stimulus onset was found. Significant differences between inactive and active twins are indicated with gray bars and zero time-point is the stimulus onset. (Figure as originally published in Hautasaari et al. 2017).

5.2 Study II

Study II examined somatosensory-driven automatic cortical change detection system elicited by different experimental somatosensory stimulations using MEG. The results revealed that both electrical and tactile stimulation can be used to detect somatosensory mismatch response (SMMR). On sensor-level, both types of deviant stimulation generated two prominent waveform components around 50 ms after stimulation (M50) and in the range of 110 – 185 ms (SMMR) in the channels approximately corresponding to contra- and ipsilateral parietal areas. Both of these components had stronger amplitudes after deviant compared to standard stimulation (Figure 5). Source-level results revealed that the M50 component is generated in the primary somatosensory cortex (SI) while the SMMR component is generated in the secondary somatosensory cortex (SII) and the source strengths were stronger after deviant compared to standard stimulation in both components (Figure 6). Comparison of deviant stimulations between electrical and tactile stimulation on sensor-level showed stronger activation on ipsilateral channels after tactile stimulation. Furthermore, on source-level, tactile stimulation showed long-latency bilateral SI activation during the SMMR component whereas analysis did not reveal this bilateral long-latency SI activation after electrical stimulation. Overall, these results demonstrated that, in addition to electrical stimulation, more natural tactile stimulation is a feasible method to elicit SMMR. Furthermore, with MEG, the SMMR processing can be localized in the SI and SII cortices.

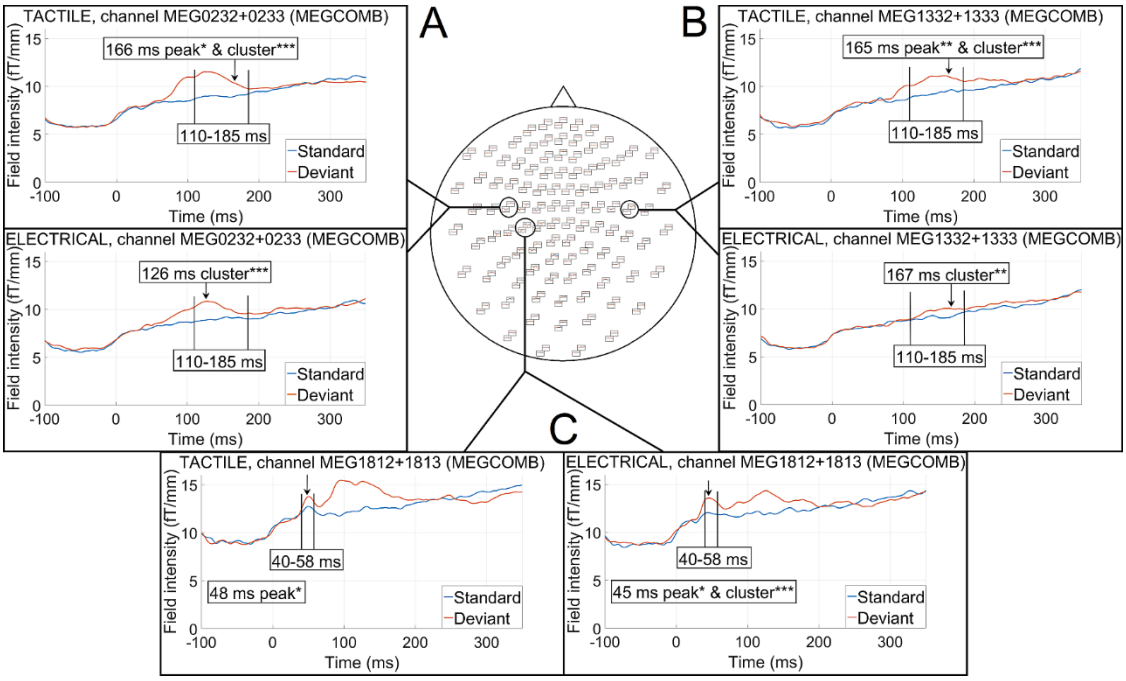

FIGURE 5 Grand average combined gradiometer RMS waveforms from representative channels for tactile and electrical stimulation conditions in *Study II*. Average waveforms illustrating differences between deviant and standard stimulations. The locations of the representative channels approximately correspond to contra- and ipsilateral parietal cortical areas. Arrows indicate cluster and/or peak-level time points of statistical differences. Vertical lines illustrate the time windows, determined for source-level analysis, enclosing early latency contralateral (C) and long-latency bilateral (A & B) waveform components. (*$p < 0.05$, **$p < 0.01$ & ***$p < 0.001$). (Figure as originally published in Hautasaari et al. 2019).

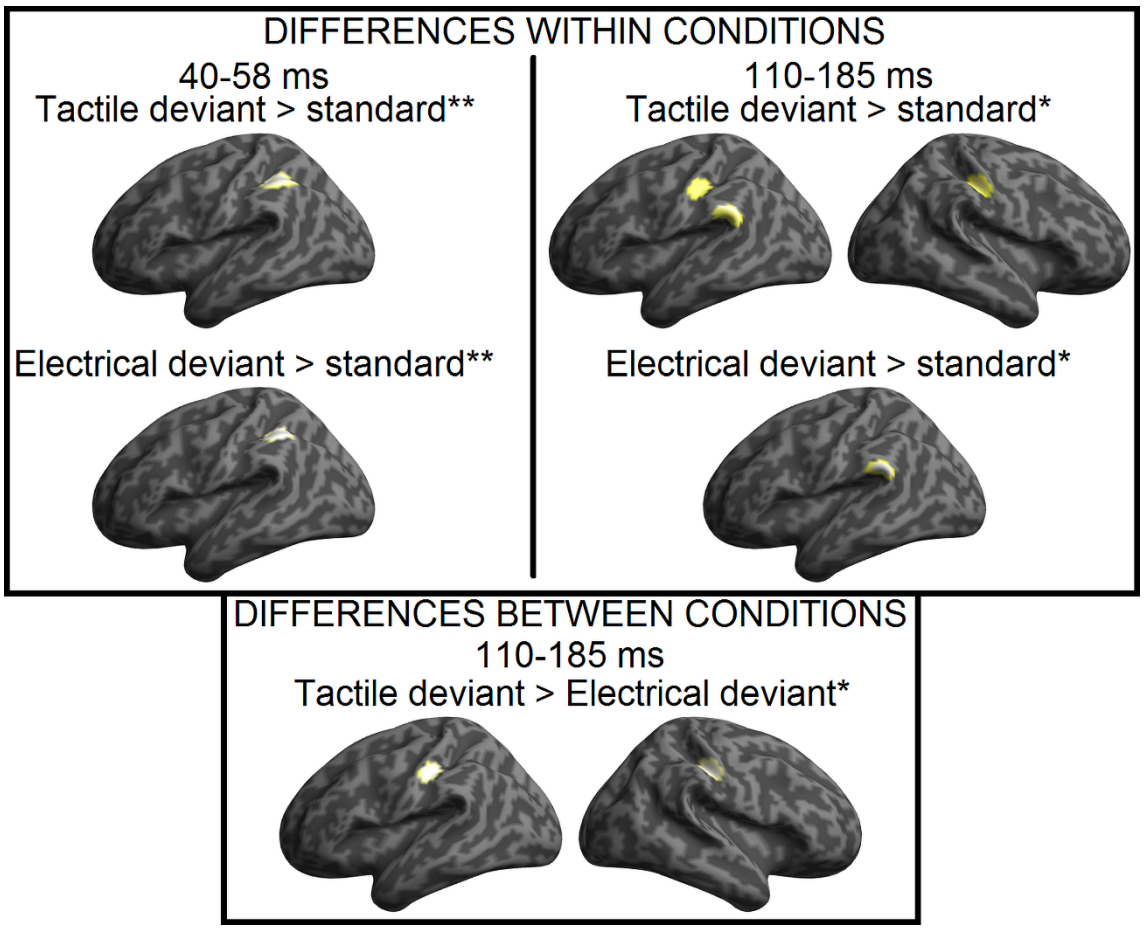

FIGURE 6 Differences in brain activation within and between conditions in *Study II*. Within conditions comparison showing significantly different activation in the contralateral SI cortex during the 40–58 ms time window after tactile and electrical deviant stimulations, respectively, compared to standard stimulation. During the 110–185 ms time window when compared to standard stimulation, tactile deviant stimulation evoked significantly different brain activations in bilateral SI cortices and contralateral SII cortex, while electrical deviant stimulation showed significantly different activation in the contralateral SII cortex. Differences between conditions, as shown in the lower part of the figure, revealed the significantly different activation in the bilateral SI cortices during the 110–185 ms time window after tactile deviant stimulation when comparing deviant stimulations between conditions. (> in figure indicates the direction of the stronger activation. *$p < 0.05$, **$p < 0.01$ & ***$p < 0.001$). (Figure as originally published in Hautasaari et al. 2019).

5.3 Study III

Study III examined cortical processing of different types of innocuous and nociceptive electrical sensory stimulations with special reference to pain-related cortical sensory networks in young healthy participants. In the first part of this study, the main brain activations were identified from averaged gradiometer

waveforms and dSPM activation maps from 17 participants (Figure 7). Median nerve stimulation showed first activation peaking at 20 (± 2.0) ms in the postcentral gyrus. First activation after radial nerve stimulation showed later peak latency at 32 (± 4.9) ms also in the postcentral gyrus. Middle latency activations peaked also in the postcentral gyrus with similar peak latencies at 65 (± 7.0) ms after median nerve stimulation and at 67 (± 4.8) ms after radial nerve stimulation. Subsequent prominent long latency activations did not occur after median nerve stimulation when ISI was short (200 ms). After radial nerve stimulation, with ISI range of 4-6 s, long latency activations were identified in the contralateral posterior operculo-insular area at 112 (± 11.6) ms and in the ipsilateral posterior operculo-insular area at 130 (± 21.7) ms and this hemispheric difference in latency was significantly different ($p = 0.001$, $t = -4.45$, $df = 16$). This hemispheric difference was also present in the onset of bilateral posterior operculo-insular area activations as the contralateral activation started significantly earlier ($p = 0.003$, $t = 3.51$, $df = 16$). Although, the radial nerve stimulation was followed by motor task in the first part of the study, the reaction time measured from stimulation to movement onset in electromyography (EMG) was 221 (± 51) ms indicating that no on-going motor activity was present during the analysis time window from stimulation onset to 180 ms. Furthermore, radial nerve stimulation without motor task, in the second part of the study, elicited corresponding activation.

In the second part of the study with five subjects, the short and middle latency activations were replicated. The first activation after median nerve stimulation occurred earlier at 20 (± 2.2) ms in the postcentral gyrus compared to first activation after radial nerve stimulation at 26.6 (± 5.6) ms. Furthermore, median nerve stimulation with long ISI activated bilateral posterior operculo-insular areas similarly to radial nerve stimulation with the same ISI. The intracutaneous nociceptive stimulation used in the second part of the study produced activations comparable to those of radial nerve stimulation with first activation occurring at 25.2 (± 2.6) ms followed by middle and long latency activation resembling those of radial nerve stimulation. Overall, these results demonstrated longer latency of the first activation in the postcentral gyrus after peripheral stimulation to purely sensory areas (i.e. radial nerve area on the dorsal hand surface and intracutaneous stimulation to fingertip) compared to mixed nerve (median nerve) on the wrist. Furthermore, the data showed temporal differences in peak activation between hemispheres in the posterior operculo-insular area demonstrating possible callosal transmission.

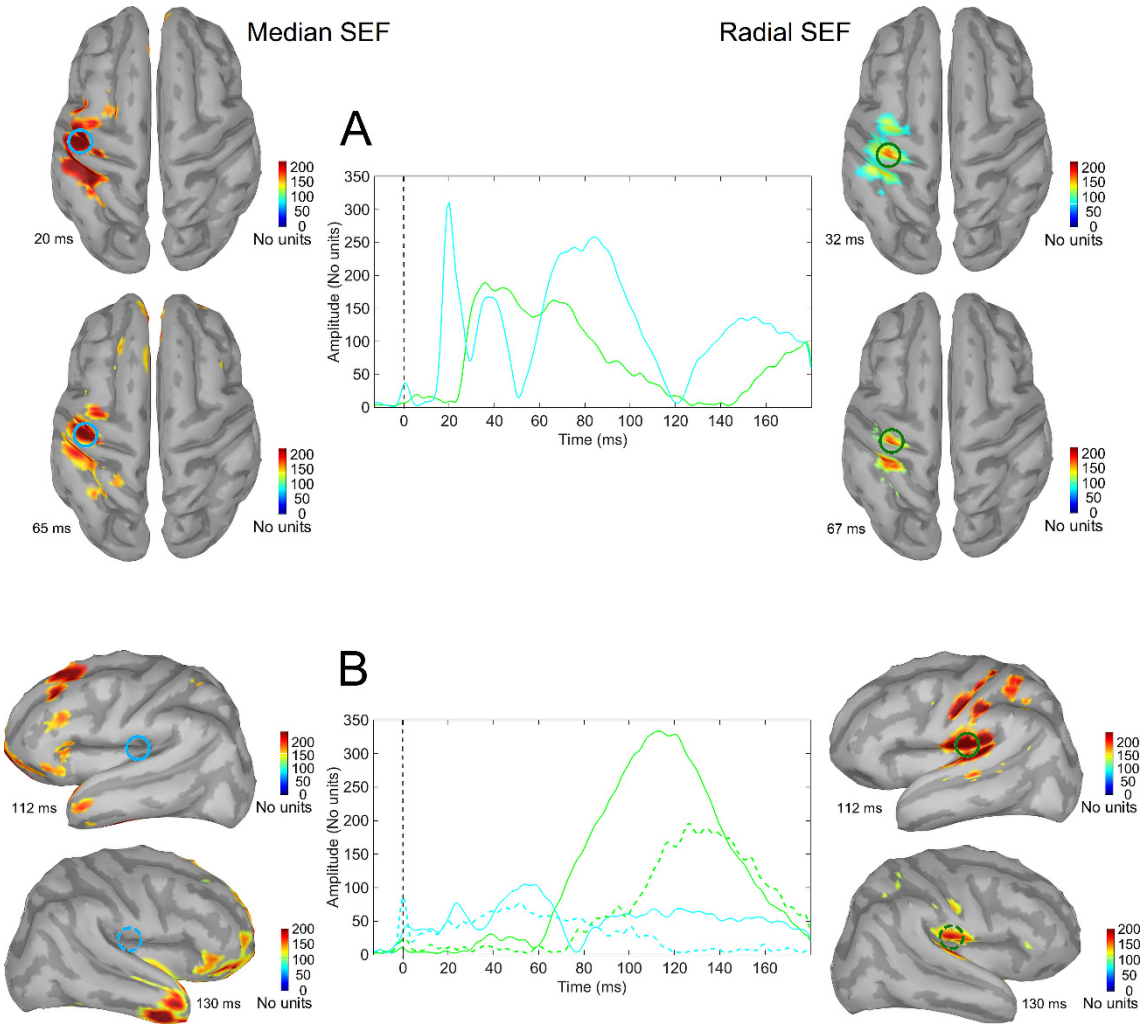

FIGURE 7 Grand average source locations and waveforms after median nerve and radial nerve stimulation from the original experiment in *Study III*. Initial components at 20 ms (median) and 32 ms (radial), following components at 65 ms (median) and 67 ms (radial) (A) and bilateral components at 112 and 130 ms (B) are shown for median and radial nerve stimulations from the original experiments. Dynamic statistical parametric mapping (dSPM) source maps illustrate the activations at mean peak time points in contralateral postcentral gyrus (A) and bilateral operculo-insular areas (B). Temporal differences in source activities between median SEF (cyan) and radial SEF (green) are illustrated in the middle (A) corresponding to postcentral gyrus and (B) to bilateral operculo-insular area activation time courses. Contralateral side to stimulated hand is shown in solid circle superimposed on activation on dSPM maps and the corresponding time course with solid line (A and B) and ipsilateral side is similarly shown with dashed circles and lines (B). Note, the figure depicts median nerve stimulation with short ISI without showing prominent long latency activations. (Figure as originally published in Hautasaari et al. 2018).

5.4 Study IV

Study IV examined whether an acute exercise task modulates cortical activity induced by experimental nociceptive stimulation. The experiments were performed before and after exercise task. Evoked field analysis revealed main cortical activations in the SI and bilateral SII areas after stimulation with maximum amplitudes peaking on average in the SI cortex at 45 (± 10) ms before and at 48 (± 7) ms after exercise task. Maximum amplitudes peaked on average in the contralateral SII area at 101 (± 17.2) ms before and at 103 (± 16.9) ms after exercise task and, furthermore, in the ipsilateral SII area at 103 (± 15.7) ms before and at 106 (± 17.8) ms after exercise task. The results from evoked field analysis did not reveal exercise-induced modulation on the peak amplitudes or latencies in these cortical sources.

The oscillation analysis revealed that acute exercise modulates stimulation-elicited sensorimotor ~20 Hz rhythm (Figure 8). This effect was seen as a statistically significant increase in the amplitude of the stimulation-elicited ~20 Hz rhythm suppression in the contralateral hemisphere after exercise (before: 33.2 ± 7.7% and after: 41.8 ± 11.3%, $t(4) = 2.807$, $p = 0.048$). Additionally, the data showed a trend towards increased suppression amplitude in the ipsilateral hemisphere and towards decreased rebound amplitude in both hemispheres. Similar trends were seen in contralateral hemisphere suppression and bilateral hemisphere rebound amplitudes in the sensorimotor ~10 Hz rhythm however, without statistically significant differences (Figure 9). Peak latencies of the ~20 Hz suppression fell within a range of 260 – 351 ms and rebound within a 798 – 982 ms range with no statistically significant latency differences between conditions. Similar result was seen in the ~10 Hz rhythm, where the average peak suppression latencies fell within a 431 – 468 ms range, and rebound latencies within a 941 – 1342 ms range.

Overall, this study revealed modulation in the oscillatory nociceptive processing in the sensorimotor cortex after acute exercise task and this modulation was observable in the ~20 Hz motor cortex rhythm. Furthermore, these results support previous research showing that nociceptive stimulation is a powerful modulator of the ~20 Hz and ~10 Hz sensorimotor rhythms.

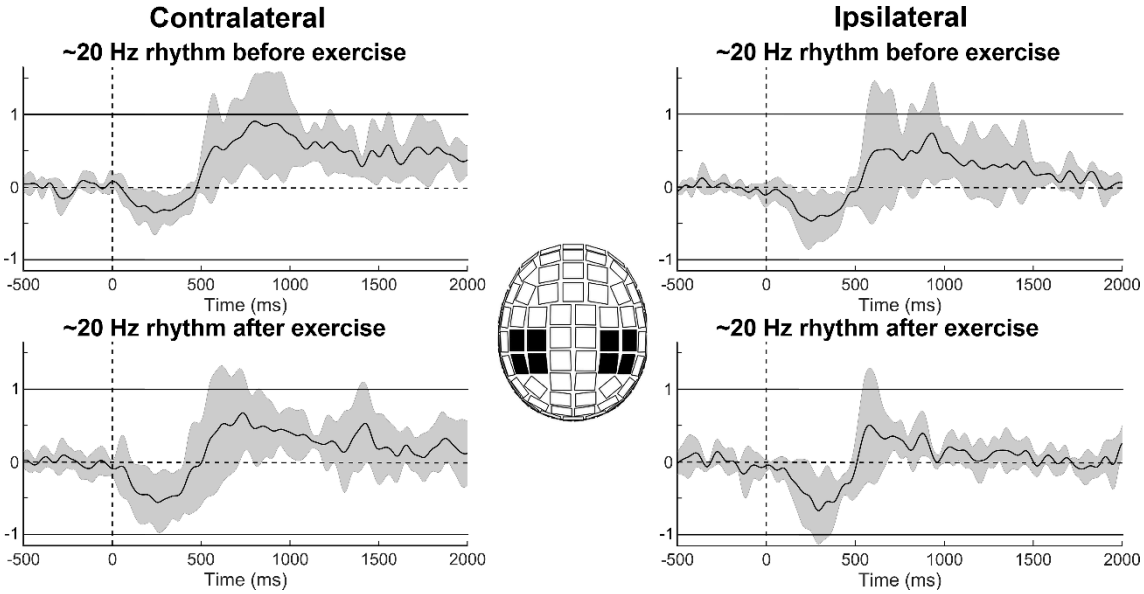

FIGURE 8 Average waveforms showing modulation on ~20 Hz rhythm after intracutaneous stimulation in *Study IV*. Effect of intracutaneous stimulation on the level of the ~20 Hz rhythm in the contralateral (left) and ipsilateral (right) hemispheres (mean ± standard deviation over 5 participants). Figures on top showing effects before exercise and figures below showing effects after exercise. Zero denotes the stimulation onset. Y-axis depicts arbitrary scales, same for both conditions. Filled squares in the sensor map (middle) show sensor locations among which the most reactive sensor was analyzed for each individual.

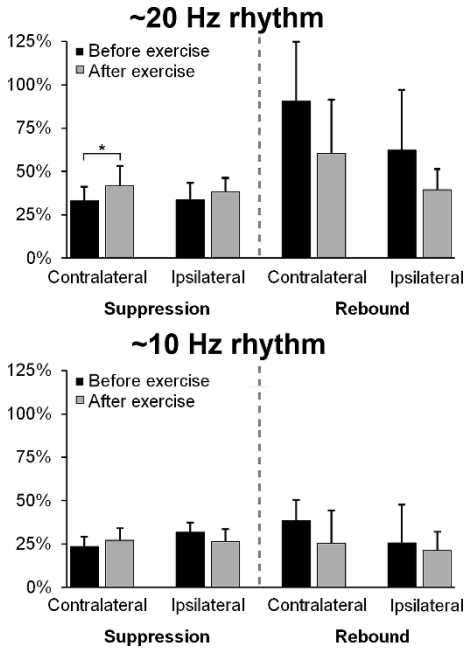

FIGURE 9 Relative ~20 Hz and ~10 Hz rhythm stimulation-elicited suppression and rebound amplitudes before and after exercise in *Study IV*. Mean (± standard deviation) amplitudes of the ~20 Hz rhythm (top) and ~10 Hz rhythm (below) suppression and rebound. Contralateral and ipsilateral hemispheres depicted separately and comparison between before and after exercise. (*$p < 0.05$).

6 DISCUSSION

The present dissertation investigated cortical somatosensory and nociceptive processing and how exercise might influence these processes in healthy young adults. In *Study I*, the somatosensory change detection mechanism was studied by EEG and measuring ERPs with electrical stimulation of fingers in young monozygotic twins. The SMMR processing was modelled with a seven-dipole source model where the inactive co-twins showed stronger amplitudes in source strengths related to processing of deviant stimulation. Further, a small but significant modulation in GM voxel count in the right anterior cingulate was discovered as the inactive twin showed larger voxel count. This twin-pair design showed that leisure-time physical activity has an effect on automatic somatosensory cortical function and may selectively modulate sensory-related cortical areas. In *Study II*, the somatosensory change detection system was further studied using MEG method with electrical and more natural tactile stimulation. These results indicated that the primary and secondary somatosensory cortices are involved in SMMR processing and both types of stimulations are feasible for studying this processing.

Cortical somatosensory processing was investigated in *Study III* with MEG by using electrical stimulation to different peripheral nerve areas. Additionally, an intracutaneous electrical stimulation was implemented as a nociceptive stimulation. These results revealed temporal dissociation in brain activations between peripheral stimulations to slightly diverging hand areas. Mixed (median) nerve stimulation had a faster propagation latency seen as an earlier activation in the postcentral gyrus compared to sensory (radial) nerve stimulation or intracutaneous stimulation to the third fingertip. Further, the data revealed latency differences in onset and peak activation times between contralateral and ipsilateral posterior operculo-insular areas suggesting transmission through the corpus callosum between these brain areas. To further elucidate these results, the intracutaneous nociceptive stimulation was utilized in *Study IV* to investigate effects of acute exercise on nociceptive processing. While the evoked field component and source analysis results did not reveal exercise-induced difference to early activations in the SI cortex and SII area, a modulation was seen in the

oscillatory function where ~20 Hz sensorimotor cortex oscillation showed increased stimulation-induced suppression amplitude after exercise task and a trend towards decreased rebound. This data suggests that acute exercise may have an effect on nociceptive processing in the sensorimotor cortex on oscillatory level.

6.1 Somatosensory and nociceptive cortical processing

6.1.1 Somatosensory evoked fields after innocuous and nociceptive stimulation

Stimulation to the median nerve at the wrist is a common and robust method for eliciting somatosensory evoked fields (SEF) with MEG and evoked potentials (SEP) with EEG. Other peripheral nerve areas are used as well and, for example, intracutaneous stimulation or stimulation of the radial nerve area at the dorsum of the hand can be used to activate only sensory afferents (Kimura 2001; 148-151) while the median nerve at the wrist is a mixed nerve and its stimulation activates also motor fibers (Kimura 2001; 131-141). Thus, stimulating an area innervated selectively with sensory afferents could be advantageous when studying somatosensory system or in diagnostic purposes in neuropathology. In *Study III*, the data replicated previous studies (Tiihonen, Hari & Hämäläinen 1989, Hari et al. 1993, Kakigi 1994) showing the first SEF waveform component peaking at 20 ms after median nerve stimulation, however, the first waveform component after radial nerve stimulation peaked at 32 ms, similarly to previous study by Inui et al. (2003) and the intracutaneous stimulation in the present study showed similar activations than the radial nerve stimulation. This latency difference could be due to dissimilar conduction velocities in peripheral nerve fibers as the stimulation to the lateral dorsal aspect of the hand activates sensory branch of the radial nerve and stimulation to the median nerve at the wrist activates both sensory and motor afferents. While the first waveform component peaked later after radial nerve stimulation, middle latency component around 60 ms occurred at similar latencies after all stimulations. These early and middle latency activations located in the postcentral gyrus and corresponded well with previous research (Srisa-an, Lei & Tarkka 1996, Mauguière et al. 1997b, Kakigi et al. 2000, Barba et al. 2008).

Subsequent long latency waveform component after radial nerve stimulation peaked at 112 ms in the contralateral hemisphere and corresponding activation was identified also in the ipsilateral hemisphere peaking at 130 ms. Similar activations were identified also after median nerve stimulation with longer interstimulus interval and after intracutaneous stimulation. These activations located in the parietal operculum in both hemispheres, a brain region which is usually considered as the SII area (zu Eulenburg et al. 2013). Although, the complexity of this brain area involved in somatosensory processing is highlighted by previous research (Eickhoff et al. 2006a, Eickhoff et al. 2006b) dissociating the parietal operculum to four different anatomically and

physiologically distinct cytoarchitectonic areas. Furthermore, posterior insula locates adjacent to SII area which is reciprocally connected to the SII area and receives projections also from the SI cortex (Augustine 1985, Friedman et al. 1986). The long latency bilateral activations in this data could not be distinguished to separate brain areas, although, overlapping SII and posterior insula activation is possible due to their close proximity of location and activation latencies (Inui et al. 2003, Liberati et al. 2016). The Montreal Neurological Institute (MNI) coordinates also indicate the activation of the posterior operculo-insular cortex. In this data, the regional analysis with SPM12 revealed peak MNI coordinates within cluster in contralateral (left) hemisphere as -44, -19, 15 and in the ipsilateral hemisphere as 44, -19, 15 after radial nerve stimulation. Further, after intracutaneous nociceptive stimulation the MNI coordinates within cluster localized more medially as -38, -24, 20 in the contralateral and as 32, -24, 20 in the ipsilateral hemispheres. These MNI coordinates correspond rather well with the center of gravity coordinates in posterior insula cytoarchitectonic areas Ig1 (left: -34, -28, 14 and right: 35, -27, 11) or Ig2 (left: -38, -22, 11 and right: 38, -21, 10) defined by Kurth et al. (2010) and also with operculum 1 area center of gravity mean coordinates (left: -52, -27, 27 and right: 58, -26, 26) from Eickhoff et al. (2006b) who proposed operculum 1 area as the most likely SII area in humans. Although digitized individual head shapes together with MRI templates allow source localization, it has to be noted that the present data did not include individual structural MRIs, which limits the accuracy of the source analysis. However, prior research have robustly reported SI and SII sources. Based on this knowledge, these source could be localized rather confidently in the current research.

This data also revealed 15-18 ms latency difference between contra- and ipsilateral peak activations in the posterior operculo-insular areas after radial nerve and intracutaneous stimulation. Corresponding latency differences between hemispheres has been reported previously by studies using non-nociceptive transcutaneous electrical stimulation to radial nerve area (Inui et al. 2003) and using peripheral vibrotactile stimulation with intracerebral recording (Liberati et al. 2016). This interhemispheric delay has been attributed to callosal transmission between contra- and ipsilateral hemispheres (Frot & Mauguière 1999, Karhu & Tesche 1999) but also direct thalamo-cortical connection to ipsilateral hemispheres has been suggested (Forss et al. 1999). Information flow between somatosensory cortices has been reported to occur in parallel (Liang, Mouraux & Iannetti 2011) or serial (Khoshnejad et al. 2014) manner. However, the nature of this processing is still under debate while a study by Klingner et al. (2016), using combination of fMRI and MEG, demonstrated that early neural activity, first 100 ms after somatosensory stimulus, is best explained by parallel and subsequent activity by serial processing route.

Based on results in *Study III*, we used the intracutaneous nociceptive electrical stimulation subsequently in *Study IV* replicating the activations in the SI and bilateral operculo-insular (SII) areas. While the electrical stimulation is a simple method to use, its disadvantage as a pain model is that it activates larger myelinated fibers concurrently with small myelinated nociceptive Aδ-fibers

(Kakigi, Watanabe & Yamasaki 2000). In other words, this type of stimulation is not pain-specific stimulation. However, previous studies have shown that increasing the electrical stimulus intensity to moderate or more painful levels increases the waveform component amplitudes and source amplitudes in the SII areas (Kitamura et al. 1995, Valeriani et al. 2000). This is also clearly demonstrated in our data when comparing transcutaneous electrical stimulation with ring electrodes to second finger with innocuous stimulation intensity and intracutaneous stimulation to third finger with moderately painful intensity (Figure 10). Interestingly, in a recent review, Peyron and Fauchon (2019) suggest that the posterior operculo-insular area may be the starting point of the nociceptive-related networks as it is consistently activated by noxious stimulation across studies (Peyron & Fauchon 2019). These findings suggest that the intracutaneous electrical stimulation used in this study may be a satisfactory method for investigating early phases of cortical nociceptive processing.

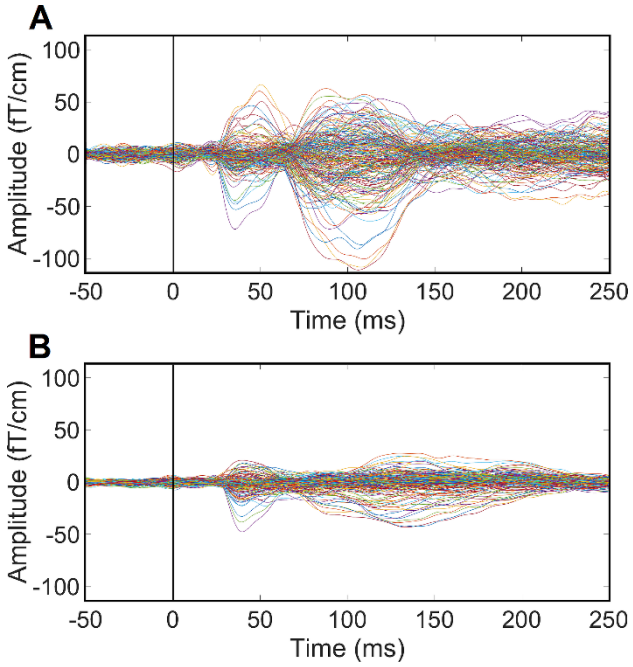

FIGURE 10 Grand average gradiometer waveforms of electrical intracutaneous nociceptive stimulation and innocuous transcutaneous stimulation with similar stimulation intensities. Note, intracutaneous stimulation (A) eliciting stronger 50 ms and 100 ms waveform component amplitudes compared to transcutaneous stimulation (B).

6.1.2 Somatosensory mismatch responses

Previously the current SMMR experiment set-up has been reliably used with EEG recordings by electrically eliciting SMMR for a location difference in the hand and its modulation has been observed in ageing and in persons in different physical activity categories (Strömmer, Tarkka & Astikainen 2014, Tarkka et al. 2016). In *Study I*, a 3D source model was developed to approximate the cerebral sources of the SMMR registered with EEG. The source model attempted to

incorporate cortical sources from stimulus onset to 350 ms in order to describe the process of detecting somatosensory mismatch. Most mismatch negativity (MMN) studies use analysis of difference waveform, which is calculated by subtracting the standard from the deviant event-related field or potential. The analysis in the current study focused on the deviant and standard waveforms approximating natural condition where most of the ongoing brain processes are taken into consideration within the modeled time window. The source model consisted of seven dipoles, of which six modeled brain activity and one eye movements and blinks. One dipole, SD1, was localized to the right ventral anterior cingulate gyrus, which is associated with a variety of phenomena related to executive control with numerous projections to motor areas (Devinsky, Morrell & Vogt 1995). Two dipoles, SD2 and SD6, were localized bilaterally to the postcentral gyrus, SI cortex, which is specifically related to somatosensory processing, e.g. to the sensation of touch, position sense and pressure (Strominger, Demarest & Laemle 2012; 436-438). One dipole, SD3, was localized to the frontal medial gyrus in the right hemisphere, an area with connections to postcentral gyrus and functional links to spatial attention and top-down control of attentional focus (Talati & Hirsch 2005, Strominger, Demarest & Laemle 2012; 433-436). Finally, two dipoles, SD4 and SD5, were localized bilaterally to the superior temporal gyrus, an area which is heavily implicated in auditory processes, but may also contribute to amodal, likely multisensory, and memory-related aspects on MMN response (Näätänen et al. 2007).

In *Study II*, the SMMR was investigated with MEG recording using two different types of somatosensory stimuli, electrical and pneumatically produced tactile stimulation. Both types of stimuli produced two distinct waveform components, M50 within 40 – 58 ms time window and SMMR component within 110 – 185 ms time window after deviant stimulation. Previous studies have also reported earlier enhanced M50 component after deviant stimulation at similar latency (Shinozaki et al. 1998, Akatsuka et al. 2005, Akatsuka et al. 2007a) and source location in the SI cortex (Akatsuka et al. 2007b). The SMMR component latency corresponded well with previous research (Kekoni et al. 1997, Shinozaki et al. 1998, Akatsuka et al. 2005, Strömmer, Tarkka & Astikainen 2014) and also source location in SII cortex was consistent with previous studies (Akatsuka et al. 2007b, Naeije et al. 2018). The earlier M50 component has been speculated to be enhanced during tasks where the participant can clearly discriminate the stimulations while the enhancement of the longer latency SMMR component may occur when a fine discrimination is required between the sensory stimuli (Akatsuka et al. 2005).

In the current data, after the tactile stimulation, also a SI activation was detected during the SMMR component bilaterally. Akatsuka et al. (2007a) reported, using a single dipole analysis, that contralateral SI, in addition to contralateral SII, contributed to their late component within 150-250 ms time window and they concluded that this component may be generated by two or more sources. While the contralateral SI activation is robustly reported, the ipsilateral SI activation has been more elusive to record after somatosensory

stimulation. Previous studies have reported ipsilateral SI activation and possible factors for more difficult detection may be the interindividual variability or that a larger amplitude response from ipsilateral SII may mask the weaker SI activation in the recording (Allison et al. 1989, Korvenoja et al. 1995). Hadoush et al. (2010) reported, similar to the current data, bilateral SI activation after mechanical tactile stimulation and they hypothesized that, in contrast to electrical stimulation, the ipsilateral SI activation could be recorded more consistently after mechanical stimulation due to more selective tactile input. A recent review by Tamè et al. (2016) suggested that, in addition to the contralateral SI activation, the ipsilateral SI is involved in bilateral integration of tactile stimuli. They emphasized the concept that during tactile processing there may already occur an early bilateral involvement of the SI cortex in tactile processing (Tamè et al. 2016).

This data demonstrates that EEG and MEG methods and utilization of different somatosensory stimulus types e.g. electrical or tactile, are feasible methods for studying somatosensory change detection mechanism in healthy individuals and potentially also in clinical research. Furthermore, tactile stimulation could have benefits when studying patient groups with altered sensory processing. Tactile stimulation is closer to natural touch and it may be more tolerable and patient-friendly, including for small children, compared to electrical stimulation. MMN studies in auditory domain have reported changes in the automatic change detection system revealing usually an attenuated auditory MMN amplitude in diverse disorders e.g. in dyslexia, autism or Parkinson's disease, however, the potential of utilizing somatosensory MMR in clinical studies has so far been under-utilized (Näätänen 2009). Nonetheless, previous study has reported abnormal SMMR processing in patients with cerebellar damage (Restuccia et al. 2007). Interestingly, a recent study by Chen et al. (2018) reported abnormal somatosensory MMN processing in cervical dystonia patients while their auditory MMN processing was normal compared to healthy controls. This finding highlights the benefit of using domain specific experimental design, e.g. somatosensory MMR, when studying disorders presenting with somatosensory domain pathologies. In addition to basic research on mechanisms of the SMMR and SEF processing in healthy participants and their potential in clinical and diagnostic studies, SMMR and SEF experiments are suitable for investigating exercise effects on automatic somatosensory and nociceptive cortical function.

6.2 Exercise effects on cortical function

6.2.1 Associations between exercise and SMMR

So far, more studies have focused on exercise effects to brain structure (Rovio et al. 2010, Erickson, Leckie & Weinstein 2014), especially in cognition-related brain areas e.g. hippocampus (Erickson et al. 2011, Firth et al. 2018) in aging population,

while research on how exercise could affect somatosensory brain function is scarce. In *Study I*, the data demonstrated that long-term physical activity may modulate specific early somatosensory functional brain processes and may modify brain structure. The differences in functional brain responses occurred during the SMMR processing where the inactive co-twins showed larger automatic neural activation in source dipoles approximated to SI and SII regions and in the frontal medial gyrus. SI and SII activity correspond to primary and secondary somatosensory processing but the frontal medial gyrus activity and the difference detected in this dipole may indicate more complex automatic somatosensory mismatch processing.

The frontal medial gyrus has been reported to participate in motor planning and non-motor tasks e.g. decision making, discrimination and in convergence of sensory information for high-level processes related to coordination of motor activity (Erdler et al. 2000, Eimer & Driver 2001, Hirsch, Moreno & Kim 2001). Furthermore, frontal medial gyrus has been reported to be active during cognitive tasks when the participant have to decide "where" in the body the target is (Talati & Hirsch 2005) and furthermore, this region has been implicated to participate in sensory gating (Bak et al. 2011). Thus, the source dipole amplitude differences may be explained by differences in sensory gating emerging from different levels of physical activity and the larger amplitudes in inactive co-twins may reflect the deviant information ascending from the body automatically alerting more the inactive co-twins. Relating to the current results, Popovich and Staines (2015) reported modulation of late somatosensory component, especially LLP in their work, in attended and unattended conditions after one acute bout of aerobic exercise. Their suggestion was that this modulation could be associated with improvement in selective attentional processing and sensory gating of task-irrelevant stimuli. The result for unattended condition in Popovich and Staines (2015) is comparable to the current data. Our SMMR occurred at similar time window as in Popovich and Staines (2015) with the inactive co-twins showing larger amplitudes. This may imply improved sensory gating in the active twins, however, the indications from the current data are much stronger than in Popovich and Staines (2015) showing long-term exercise effect with discordance between the co-twins for at least three years.

The structural analysis based on ROIs derived from the dipole locations in *Study I* also indicated possible structural change in right hemisphere anterior cingulate cortex (ACC) with higher voxel count in the inactive twins. The data implies that the ACC is, at least to some extent, functionally involved in somatosensory deviant detection. As the ACC is connected to sensation regulation (Apkarian et al. 2005), it is possible that the sensation from the electrical stimulation, at least in part, was automatically assessed in this brain area.

The current results implying functional and structural changes in the brain of the healthy co-twins only differing in their long-term exercise history leads toward a viewpoint of brain plasticity in adults. Cortical plasticity has been

assessed in patients recovering from brain insults such as cerebrovascular stroke (Tarkka, et al. 2008, Nudo et al. 2013, Julkunen et al. 2016). It may be that many principles found in the recovery process may also apply to long-term intensive activity, e.g. physical exercise. Previous studies have reported association between higher cardiorespiratory fitness levels and reduced loss of GM and WM volumes in the frontal, prefrontal and temporal areas and hippocampi in older adults (Colcombe et al. 2003, Erickson et al. 2011, Erickson, Leckie & Weinstein 2014) and exercise has been shown to induce neuro- and angiogenesis e.g. in hippocampus in rodents (Pereira et al. 2007). Still, further research is clearly needed to elucidate the factors involved in exercise-induced plasticity, however, overall it seems that physical exercise is effective as a neuroprotective formula and modulator of brain plasticity.

6.2.2 Associations between exercise and sensorimotor oscillations

In addition to somatosensory processing, the current thesis implies that acute exercise may have an effect on cortical nociceptive processing. In *Study IV*, the data revealed modulation in the oscillatory nociceptive processing over sensorimotor cortex after acute exercise which was observable in the ~20 Hz motor cortex rhythm. Additionally, the data support previous findings (Raij et al. 2004) showing that nociceptive stimulation modulates both ~20 Hz and ~10 Hz sensorimotor rhythms. In the evoked field analysis, two major waveform components at about 50 ms and 100 ms could be confidently localized to the SI and SII cortices respectively. However, with a limited number of participants, no modulation was observed in latency or amplitude in these sources and it must be noted that the current intracutaneous electrical stimulation was not specific to nociceptive Aδ or C-fibers. Comparably, Jones et al. (2016) was not able to find consistent exercise-induced modulation in their SEPs measured with EEG and speculated if the contribution of non-nociceptive pathways could be the reason for the lack of clear modulation to their SEPs. It may be that the evoked fields and corresponding sources peaking before 200 ms may be sensitive to stimulation intensity but not yet involved in the integration of nociceptive information towards coherent pain perception.

After acute exercise, the stimulation-induced ~20 Hz rhythm suppression was found to be stronger followed by a tendency towards weaker rebound. The somatosensory stimulation-induced modulation to the ~20 Hz rhythm has been localized to the primary motor cortex (MI) bilaterally (Hari et al. 1997, Salenius et al. 1997, Cheyne et al. 2003, Gaetz & Cheyne 2006). The finding in the current study can be interpreted that the MI cortex excitability increased (stronger suppression) and following inhibition decreased (weaker rebound). Furthermore, previous studies have implicated MI activation after nociceptive stimulation (Melzack & Wall 1965, Raij et al. 2004, Duerden & Albanese 2013) that may imply probable activation of the sensory and motor systems in preparation to react to relevant adverse stimuli (Gaetz & Cheyne 2006, Ploner et al. 2006).

Since research is scarce in this area, studies using other methods, such as transcranial magnetic stimulation (TMS), may help in interpreting this result.

High-frequency repetitive TMS (rTMS) to MI cortex has been reported to have an analgesic effect (Leo & Latif 2007). The mechanism of this effect is not yet clear, however, it is suggested that the modulation to the MI activity after rTMS may spread from a local site down to thalamic nuclei and ascending nociceptive information may be suppressed in part in the spinothalamic tract (Leo & Latif 2007). Previous studies report that high-frequency rTMS modulates neuronal activity by inducing increased excitability in the stimulated brain area (Pascual-Leone et al. 1998) and may initiate following decrease in intracortical inhibition (Kozyrev, Eysel & Jancke 2014). Similar effect has been reported with single pulse TMS studies showing that fatiguing exercise increases MI excitability and decreases intracortical inhibition (Otieno et al. 2019). Furthermore, Granovsky et al. (2019) reported recently using conditioned pain modulation (CPM), that increased MI corticospinal excitability is associated with more efficient inhibitory pain modulation. These results correspond with the current study in showing similar changes to cortical excitability, however, comparison between MEG and TMS parameters should be interpreted with caution due to limited research in this area (Mäkelä et al. 2015).

Based on the current result demonstrating modulation of the stimulation-induced ~20 Hz oscillation after acute exercise in the cortical level, we can speculate, that the changes in cortical oscillatory activity may be a part of the exercise-induced modulation of nociceptive processing via top-down pathways. Top-down pain modulation has been suggested to function as descending pain modulatory circuit with input from multiple cortical brain areas, including MI, feeding to the midbrain and further to the medulla (Ossipov, Dussor & Porreca 2010, De Felice & Ossipov 2016). Beta band, i.e. ~20 Hz rhythm, has been suggested to have a role in neural communication between cortical and subcortical networks (Hari et al. 1997, Cheyne 2013). Additionally, intracranial MI stimulation has been reported to relieve neuropathic pain, possibly via endogenous opioid secretion from the periaqueductal gray and anterior and middle cingulate cortices, which are reported to receive projections from the MI cortex (Maarrawi et al. 2007, Peyron et al. 2007) and have a high density of opioid receptors (Jones et al. 1991). Furthermore, in trained athletes, Scheef et al. (2012) suggest that aerobic exercise may mediate antinociceptive mechanism possibly by an elevated opioidergic tone in the brain resulting from long-term exercise. In conclusion, it can be speculated that, in a centralized pain inhibitory response, increased motor system activity may have an important role via exercise (Koltyn & Umeda 2007, Scheef et al. 2012, Paris et al. 2013) or via external cortical stimulation (Leo & Latif 2007, Granovsky, Sprecher & Sinai 2019).

6.3 Methodological considerations and limitations

The current thesis has some limitations that could be addressed in future studies. Although the results in *Study I* suggest modulation in co-twins somatosensory processing due to exercise history, it still may be that acquired differences from

various exposures and experiences, unrelated to exercise, may play a role in the observed differences. Hence, the direction of causality is difficult to determine. However, twin pair design's ability in *Study I* to control for familial and genetic confounders and differences observed between monozygotic twins is noteworthy. In *Study IV*, individual pain experience was measured using VAS-scores. With the current small sample size in *Study IV*, VAS-scores are not sufficiently accurate measure to interpret acute exercise effects on individual pain experience. Future studies would benefit from acquiring more information about the individual participant pain experience and sensory testing using e.g. pressure pain threshold measures and quantitative sensory testing. Additionally, although the intracutaneous electrical stimulation was used as a painful stimulus, it is not specific to nociceptive Aδ or C-fibers and this could be remedied by using e.g. laser heat stimulation. The current experiment in *Study IV* is limited in its ability to detect changes in internal state of brain oscillation, because it concentrated only on stimulus-induced modulation on oscillation. Cortical oscillations are complex phenomena and can be influenced by a variety of factors. Previous research have associated decrease of power in alpha (~10 Hz) and beta (~20 Hz) bands with increased stimulation intensity (Nickel et al. 2017) but also with pain perception (Bunk et al. 2018). This demonstrates the challenge in interpreting findings on oscillation-level. With small sample sizes, caution must be applied to generalizing the results and larger sample sizes would make the results more generalizable. It has to be noted that to compare observed differences between long-term and acute exercise is rather difficult.

One limitation involved in all electrophysiological functional analysis is the lack of individual structural MRIs. This limits the accuracy of source localization. However, with MEG studies, according to MEG recording and analysis guidelines (Gross et al. 2013), the digitization of individual head shape can be used with MRI templates to allow source localization. In the present MEG measurements the focus was in the early phases of somatosensory and nociceptive processing involving SI and SII cortices. These sources are reported robustly in prior research and based on this, the SI and SII source activations could be reported rather confidently in the current thesis. MEG is inherently biased towards tangential sources closer to sensors, i.e. in the cortical surface, however, emerging studies show possibilities for localizing also deeper sources with MEG (Samuelsson et al. 2019). This could allow more accurate localization of sources, for example, involved in the pain network locating in deeper brain regions. On the other hand, EEG detects more readily radial and deeper and also tangential sources. When applying source localization procedures, EEG is spatially less accurate than MEG due to volume conduction. These both methods have high temporal accuracy and can be used to complement each other, for example, in combined MEG/EEG measurement.

6.4 Conclusions and future directions

The results from this dissertation align with previous research demonstrating that SEF and SMMR experimental designs with MEG and EEG are robust methods for studying early cortical activations in somatosensory and nociceptive systems. The present results also demonstrate interaction between exercise and cortical somatosensory and nociceptive processing. The observed differences in SMMR processing between co-twins may be linked to differences in exercise history between these twin brothers. Smaller SMMR amplitude in active co-twins may imply more efficient gating of somatosensory stimuli, in other words, it may be that the deviant stimulus alerted more the inactive co-twins. Additionally, acute exercise modulated the stimulation-induced response in the sensorimotor ~20 Hz oscillations. This finding indicates that the modulation of excitability in MI, demonstrated in ~20 Hz oscillation, may be in part associated with the top-down modulation of nociceptive information. While these results demonstrate interaction between exercise and somatosensory and nociceptive cortical functions, further research is necessary for better understanding of the neurophysiological mechanisms underlying this interaction and linking this information to designing optimal rehabilitation paradigms.

Methodological advancements in the future, especially using MEG method with potential for localization of deeper sources and new sensor technology (optically-pumped magnetometers) with tolerance to higher temperatures and direct application to scalp, may assist in increasing understanding of somatosensory and nociceptive systems in the human brain. As the present study focused on the early cortical activations, it would be interesting for future studies to target brain processes occurring at longer latency and even delineating activation time courses of the multiple brain areas involved in the pain network. The results revealed modulation after acute exercise in the stimulation-induced nociceptive oscillatory beta (~20 Hz) rhythm activity over sensorimotor cortex. This rhythm may be involved in processing stimulation intensity and location. Interestingly, frontal gamma rhythm has been indicated to have possible contribution on pain perception. Hence, interesting future research targets could be if the frontal gamma rhythm could be modulated by exercise, is there interplay between brain oscillations in the somatosensory and nociceptive processing and if the brain oscillations act as mediators within an involved cortical network.

YHTEENVETO (FINNISH SUMMARY)

Liikunnan vaikutukset aivojen automaattiseen somatosensoriseen ja nosiseptiiviseen prosessointiin

Liikunta on osa terveellistä elämäntapaa. Liikunnan on osoitettu edistävän fyysistä toimintakykyä sekä vaikuttavan positiivisesti useiden kroonisten sairauksien riskitekijöihin. Liikunnan yhteyttä sydän- ja verisuonitauteihin on tutkittu mittavasti. Vasta viime vuosina tutkimus on lisääntynyt myös liikunnan ja aivotoiminnan välisten yhteyksien selvittämiseksi. Valtaosa tästä tutkimuksesta on kohdistunut ikääntyneiden kognitiivisten toimintojen tutkimiseen ja liikunnalla näyttäisi olevan positiivinen vaikutus näihin toimintoihin, mutta vähemmän tiedetään liikunnan vaikutuksesta muihin neuraalisiin järjestelmiin kuten somatosensoriseen ja nosiseptiiviseen aivotoimintaan. Nämä neurofysiologiset järjestelmät osallistuvat muun muassa kivun prosessointiin. Kipu on olennainen oire useissa kroonisissa sairauksissa ja kroonisen kivun on osoitettu muuntavan aivotoimintaa negatiiviseen suuntaan. Toisaalta liikunnalla on todettu positiivisia vaikutuksia aivotoimintaan, muun muassa muistitoimintoihin, sekä liikunnan on havaittu vaikuttavan positiivisesti koettuun kipuun. Erityisesti liikunnan vaikutusta kivun hallintamekanismien taustalla olevaan neurofysiologiaan ei kuitenkaan vielä täysin ymmärretä ja tämä alue vaatii lisätutkimusta.

Tämän väitöskirjatutkimuksen tarkoitus oli tutkia somatosensorista ja nosiseptiivistä aivotoimintaa ja selvittää vaikuttaako liikunta tässä työssä mitattuihin toimintoihin. Tutkimuksessa käytettiin toiminnallisia aivokuvantamismenetelmiä rekisteröimällä lyhytlatenttisia somatosensorisia ja nosiseptiivisiä aivovasteita hyödyntäen somatosensorisia ja nosiseptiivisiä stimulaatiomenetelmiä. Tutkimusaineisto muodostui *tutkimuksessa I* identtisistä kaksospareista, jotka poikkesivat parin sisällä liikuntatottumuksiltaan vuosien ajan sekä *tutkimuksissa II-IV* aineistona oli terveitä aikuisia. Liikunnan yhteyksiä aivotoimintaan tutkittiin mittaamalla sekä akuutin liikuntasuorituksen vaikutusta, että kaksospareilla pitkäkestoisen liikunnan aiheuttamia eroja.

Tutkimuksessa I tutkittiin aivojen automaattista somatosensorista muutoksen havaitsemissysteemiä EEG:lla ja pitkäkestoisen liikunnan harjoittamisen vaikutusta tähän systeemiin. Kyseinen aineisto koostui identtisistä kaksospareista, jotka parin sisällä poikkesivat vuosien ajan liikuntatottumuksiltaan. Tuloksissa havaittiin, että liikunta vaikuttaa tiettyihin somatosensorisiin aivovasteisiin siten, että passiivisilla kaksosilla muutoksenhavaitsemisvaste oli voimakkaampi. *Tutkimuksessa II* tarkasteltiin aivojen muutoksenhavaitsemisvastetta MEG:lla hyödyntäen sähköistä ja taktiilia stimulaatiota. Tuloksien perusteella molemmat stimulaatiotavat ovat luotettavia keinoja tuottamaan muutoksenhavaitsemisvaste MEG:lla. Lisäksi tulokset vahvistavat aiempia tutkimuksia osoittaen primaarisen ja sekundaarisen somatosensorisen aivokuoren osallistuvan muutoksen havaitsemismekanismiin. *Tutkimuksessa III* selvitettiin MEG:lla mitkä uni- ja bilateraaliset aivoalueet osallistuvat lyhytlatenttiseen somatosensoriseen prosessointiin.

Tässä hyödynnettiin sekä vaimeata että nosiseptiivista sähköstimulaatiota. Tulokset osoittivat aktiivisten aivolähteiden sijainnissa ja ajoituksessa eroja käden eri alueille kohdistettujen eri voimakkuuksisten sähköstimulaatioiden jälkeen. *Tutkimuksessa IV* tutkittiin akuutin liikuntasuorituksen vaikutusta nosiseptiiviseen prosessointiin ja sensorimotorisen aivokuoren ärtyvyyteen. Tulokset osoittivat akuutin liikuntasuorituksen vaikuttavan nosiseptiiviseen prosessointiin liittyvään aivorytmiin sensorimotorisella aivokuorella. Primaarisen motorisen aivokuoren ~20 Hz:n aivorytmissä havaittiin voimakkaampi nosiseptiivisen stimulaation tuottama amplitudin lasku vastaten aivokuoren ärtyvyyden kasvua ja viitteitä heikompaan amplitudin palautumiseen vastaten vähentynyttä inhibitiota.

Väitöskirjan tulokset osoittavat tarkasteltujen somatosensoristen ja nosiseptiivisten stimulaatiomenetelmien olevan menetelmällisesti vahvoja tutkittaessa lyhytlatenttisia somatosensorisia ja nosiseptiivisiä vasteita EEG:lla ja MEG:lla. Tutkimuksen tulokset osoittavat myös selkeästi yhteyden liikunnan ja aivokuoren somatosensorisen ja nosiseptiivisen prosessoinnin välillä. Identtisillä kaksosilla havaittiin eroja somatosensorisessa muutoksenhavaitsemisvasteessa. Havaitut erot voivat olla yhteydessä kaksosparien keskinäiseen eroon liikunnan harrastamisessa. Ero muutoksenhavaitsemisvasteessa mahdollisesti osoittaa, että liikunnallisesti aktiivisemmalla kaksosella somatosensoristen ärsykkeiden automaattinen säätely toimii tehokkaammin, toisin sanoen, poikkeava sensorinen ärsyke automaattisesti ”varoitti” enemmän liikunnallisesti passiivista kaksosta. Akuutin liikuntasuorituksen jälkeen havaittu vaikutus primaarin motorisen aivokuoren ~20 Hz:n aivorytmiin on mahdollisesti osatekijä nosiseption top-down säätelyssä. Vaikka näiden tutkimusten tulokset osoittavat yhteyden liikunnan ja aivokuoren somatosensorisen ja nosiseptiivisen prosessoinnin välillä, lisätutkimus on kuitenkin tarpeen tämän monimutkaisen vuorovaikutuksen neurofysiologisten mekanismien ymmärtämiseksi sekä tämän tiedon yhdistämiseksi myös osaksi optimaalisten kuntoutuskäytäntöjen suunnittelua.

REFERENCES

Ahlfors, S. P., Han, J., Belliveau, J. W. & Hämäläinen, M. S. 2010. Sensitivity of MEG and EEG to source orientation. Brain Topography 23 (3), 227-232.

Akatsuka, K., Wasaka, T., Nakata, H., Inui, K., Hoshiyama, M. & Kakigi, R. 2005. Mismatch responses related to temporal discrimination of somatosensory stimulation. Clinical Neurophysiology 116 (8), 1930-1937.

Akatsuka, K., Wasaka, T., Nakata, H., Kida, T. & Kakigi, R. 2007a. The effect of stimulus probability on the somatosensory mismatch field. Experimental Brain Research 181 (4), 607-614.

Akatsuka, K., Wasaka, T., Nakata, H., Kida, T., Hoshiyama, M., Tamura, Y. & Kakigi, R. 2007b. Objective examination for two-point stimulation using a somatosensory oddball paradigm: an MEG study. Clinical Neurophysiology 118 (2), 403-411.

Allison, T., McCarthy, G., Wood, C. C., Williamson, P. D. & Spencer, D. D. 1989. Human cortical potentials evoked by stimulation of the median nerve. II. Cytoarchitectonic areas generating long-latency activity. Journal of Neurophysiology 62 (3), 711-722.

Apkarian, A. V., Bushnell, M. C., Treede, R. & Zubieta, J. 2005. Human brain mechanisms of pain perception and regulation in health and disease. European Journal of Pain 9 (4), 463-484.

Augustine, J. R. 1985. The insular lobe in primates including humans. Neurological Research 7 (1), 2-10.

Baillet, S. 2010. The dowser in the fields: searching for MEG sources. In P. C. Hansen, M. L. Kringelbach & R. Salmelin (Eds.) MEG: an introduction to methods. New York, NY: Oxford University Press, 83-123.

Bak, N., Glenthoj, B. Y., Rostrup, E., Larsson, H. B. & Oranje, B. 2011. Source localization of sensory gating: a combined EEG and fMRI study in healthy volunteers. NeuroImage 54 (4), 2711-2718.

Barba, C., Valeriani, M., Colicchio, G. & Mauguière, F. 2008. New depth short-latency somatosensory evoked potential (SEP) component recorded in human SI area. Neuroscience Letters 432 (3), 179-183.

Beck, A. T., Ward, C. H., Mendelson, M. M., Mock, J. J. & Erbaugh, J. J. 1961. An inventory for measuring depression. Archives of General Psychiatry 4 (6), 561-571.

Berger, H. 1929. Über das Elektrenkephalogramm des Menschen. Archiv für Psychiatrie und Nervenkrankheiten 87 (1), 527-570.

Borg, G. 1970. Perceived exertion as an indicator of somatic stress. Scandinavian Journal of Rehabilitation Medicine 2 (2), 92-98.

Braeutigam, S. 2013. Magnetoencephalography: fundamentals and established and emerging clinical applications in radiology. ISRN Radiology 2013, 529463.

Bunk, S. F., Lautenbacher, S., Rüsseler, J., Müller, K., Schulz, J. & Kunz, M. 2018. Does EEG activity during painful stimulation mirror more closely the

noxious stimulus intensity or the subjective pain sensation? Somatosensory & Motor Research 35 (3-4), 192-198.

Chen, J., Macerollo, A., Sadnicka, A., Lu, M., Tsai, C., Korlipara, P., Bhatia, K., Rothwell, J. C. & Edwards, M. J. 2018. Cervical dystonia: normal auditory mismatch negativity and abnormal somatosensory mismatch negativity. Clinical Neurophysiology 129 (9), 1947-1954.

Cheyne, D., Gaetz, W., Garnero, L., Lachaux, J., Ducorps, A., Schwartz, D. & Varela, F. J. 2003. Neuromagnetic imaging of cortical oscillations accompanying tactile stimulation. Cognitive Brain Research 17 (3), 599-611.

Cheyne, D. O. 2013. MEG studies of sensorimotor rhythms: a review. Experimental Neurology 245, 27-39.

Cohen, D. 1968. Magnetoencephalography: evidence of magnetic fields produced by alpha-rhythm currents. Science 161 (3843), 784-786.

Colcombe, S. J., Erickson, K. I., Raz, N., Webb, A. G., Cohen, N. J., McAuley, E. & Kramer, A. F. 2003. Aerobic fitness reduces brain tissue loss in aging humans. The Journals of Gerontology. Series A, Biological Sciences and Medical Sciences 58 (2), 176-180.

Darvas, F., Ermer, J. J., Mosher, J. C. & Leahy, R. M. 2006. Generic head models for atlas-based EEG source analysis. Human Brain Mapping 27 (2), 129-143.

De Felice, M. & Ossipov, M. H. 2016. Cortical and subcortical modulation of pain. Pain Management 6 (2), 111-120.

Devinsky, O., Morrell, M. J. & Vogt, B. A. 1995. Contributions of anterior cingulate cortex to behaviour. Brain 118 (1), 279-306.

Duerden, E. G. & Albanese, M. 2013. Localization of pain-related brain activation: a meta-analysis of neuroimaging data. Human Brain Mapping 34 (1), 109-149.

Eickhoff, S. B., Schleicher, A., Zilles, K. & Amunts, K. 2006a. The human parietal operculum. I. Cytoarchitectonic mapping of subdivisions. Cerebral Cortex 16 (2), 254-267.

Eickhoff, S. B., Amunts, K., Mohlberg, H. & Zilles, K. 2006b. The human parietal operculum. II. Stereotaxic maps and correlation with functional imaging results. Cerebral Cortex 16 (2), 268-279.

Eimer, M. & Driver, J. 2001. Crossmodal links in endogenous and exogenous spatial attention: evidence from event-related brain potential studies. Neuroscience and Biobehavioral Reviews 25 (6), 497-511.

Erdler, M., Beisteiner, R., Mayer, D., Kaindl, T., Edward, V., Windischberger, C., Lindinger, G. & Deecke, L. 2000. Supplementary motor area activation preceding voluntary movement is detectable with a whole-scalp magnetoencephalography system. NeuroImage 11 (6), 697-707.

Erickson, K. I., Voss, M. W., Prakash, R. S., Basak, C., Szabo, A., Chaddock, L., Kim, J. S., Heo, S., Alves, H., White, S. M., Wojcicki, T. R., Mailey, E., Vieira, V. J., Martin, S. A., Pence, B. D., Woods, J. A., McAuley, E., Kramer, A. F. & Gage, F. 2011. Exercise training increases size of hippocampus and improves memory. Proceedings of the National Academy of Sciences of the United States of America 108 (7), 3017-3022.

Erickson, K. I., Leckie, R. L. & Weinstein, A. M. 2014. Physical activity, fitness, and gray matter volume. Neurobiology of Aging 35, S20-S28.

Erickson, K. I., Hillman, C., Stillman, C. M., Ballard, R. M., Bloodgood, B., Conroy, D. E., Macko, R., Marquez, D. X., Petruzzello, S. J., Powell, K. E. & The 2018 Physical Activity Guidelines Advisory Committee. 2019. Physical activity, cognition, and brain outcomes: a review of the 2018 physical activity guidelines. Medicine & Science in Sports & Exercise 51 (6), 1242-1251.

Firth, J., Stubbs, B., Vancampfort, D., Schuch, F., Lagopoulos, J., Rosenbaum, S. & Ward, P. B. 2018. Effect of aerobic exercise on hippocampal volume in humans: a systematic review and meta-analysis. NeuroImage 166, 230-238.

Flor, H., Braun, C., Elbert, T. & Birbaumer, N. 1997. Extensive reorganization of primary somatosensory cortex in chronic back pain patients. Neuroscience Letters 224 (1), 5-8.

Forss, N., Hietanen, M., Salonen, O. & Hari, R. 1999. Modified activation of somatosensory cortical network in patients with right-hemisphere stroke. Brain 122 (10), 1889-1899.

Friedman, D. P., Murray, E. A., O'Neill, J. B. & Mishkin, M. 1986. Cortical connections of the somatosensory fields of the lateral sulcus of macaques: evidence for a corticolimbic pathway for touch. The Journal of Comparative Neurology 252 (3), 323-347.

Frot, M. & Mauguière, F. 1999. Timing and spatial distribution of somatosensory responses recorded in the upper bank of the sylvian fissure (SII area) in humans. Cerebral Cortex 9 (8), 854-863.

Gaetz, W. & Cheyne, D. 2006. Localization of sensorimotor cortical rhythms induced by tactile stimulation using spatially filtered MEG. NeuroImage 30 (3), 899-908.

Gardner, E. P. & Johnson, K. O. 2013. The somatosensory system: receptors and central pathways. In E. R. Kandel, J. H. Schwartz, T. M. Jessell, S. A. Siegelbaum & A. J. Hudspeth (Eds.) Principles of Neural Science. (Fifth edition). New York, NY: McGraw Hill, 475-487.

Granovsky, Y., Sprecher, E. & Sinai, A. 2019. Motor corticospinal excitability: a novel facet of pain modulation? Pain Reports 4 (2), e725.

Gross, J., Baillet, S., Barnes, G. R., Henson, R. N., Hillebrand, A., Jensen, O., Jerbi, K., Litvak, V., Maess, B., Oostenveld, R., Parkkonen, L., Taylor, J. R., van Wassenhove, V., Wibral, M. & Schoffelen, J. 2013. Good practice for conducting and reporting MEG research. NeuroImage 65, 349-363.

Hadoush, H., Inoue, K., Nakanishi, K., Kurumadani, H., Sunagawa, T. & Ochi, M. 2010. Ipsilateral primary sensorimotor cortical response to mechanical tactile stimuli. NeuroReport 21 (2), 108-113.

Hari, R., Karhu, J., Hämäläinen, M., Knuutila, J., Salonen, O., Sams, M. & Vilkman, V. 1993. Functional organization of the human first and second somatosensory cortices: a neuromagnetic study. European Journal of Neuroscience 5 (6), 724-734.

Hari, R., Salmelin, R., Mäkelä, J. P., Salenius, S. & Helle, M. 1997. Magnetoencephalographic cortical rhythms. International Journal of Psychophysiology 26 (1), 51-62.

Hari, R. & Forss, N. 1999. Magnetoencephalography in the study of human somatosensory cortical processing. Philosophical Transactions of the Royal Society. Series B, Biological Sciences 354 (1387), 1145-1154.

Hari, R., Parkkonen, L. & Nangini, C. 2010. The brain in time: insights from neuromagnetic recordings. Annals of the New York Academy of Sciences 1191 (1), 89-109.

Hari, R. 2011. Magnetoencephalography: methods and applications. In E. Niedermeyer, D. L. Schomer & F. H. Lopes da Silva (Eds.) Niedermeyer's Electroencephalography: Basic principles, Clinical applications, and Related fields. (Sixth edition). Philadelphia, PA: Wolters Kluwer/Lippincott Williams & Wilkins Health, 865-900.

Hari, R. & Salmelin, R. 2012. Magnetoencephalography: from SQUIDs to neuroscience. Neuroimage 20th anniversary special edition. NeuroImage 61 (2), 386-396.

Hirsch, J., Moreno, D. R. & Kim, K. H. S. 2001. Interconnected large-scale systems for three fundamental cognitive tasks revealed by functional MRI. Journal of Cognitive Neuroscience 13 (3), 389-405.

Holliday, I. E., Barnes, G. R., Hillebrand, A. & Singh, K. D. 2003. Accuracy and applications of group MEG studies using cortical source locations estimated from participants' scalp surfaces. Human Brain Mapping 20 (3), 142-147.

Huang, M. X., Mosher, J. C. & Leahy, R. M. 1999. A sensor-weighted overlapping-sphere head model and exhaustive head model comparison for MEG. Physics in Medicine and Biology 44 (2), 423-440.

Hämäläinen, M., Hari, R., Ilmoniemi, R. J., Knuutila, J. & Lounasmaa, O. V. 1993. Magnetoencephalography—theory, instrumentation, and applications to noninvasive studies of the working human brain. Reviews of Modern Physics 65 (2), 413-497.

Hötting, K. & Röder, B. 2013. Beneficial effects of physical exercise on neuroplasticity and cognition. Neuroscience and Biobehavioral Reviews 37 (9), 2243-2257.

Inui, K., Tran, T. D., Qiu, Y., Wang, X., Hoshiyama, M. & Kakigi, R. 2003. A comparative magnetoencephalographic study of cortical activations evoked by noxious and innocuous somatosensory stimulations. Neuroscience 120 (1), 235-248.

Jackson, A. F. & Bolger, D. J. 2014. The neurophysiological bases of EEG and EEG measurement: a review for the rest of us. Psychophysiology 51 (11), 1061-1071.

Jones, A. K. P., Qi, L. Y., Fujirawa, T., Luthra, S. K., Ashburner, J., Bloomfield, P., Cunningham, V. J., Itoh, M., Fukuda, H. & Jones, T. 1991. In vivo distribution of opioid receptors in man in relation to the cortical projections of the medial and lateral pain systems measured with positron emission tomography. Neuroscience Letters 126 (1), 25-28.

Jones, M. D., Taylor, J. L., Booth, J. & Barry, B. K. 2016. Exploring the mechanisms of exercise induced hypoalgesia using somatosensory and laser evoked potentials. Frontiers in Physiology 7, 581.

Jousmäki, V. 2000. Tracking functions of cortical networks on a millisecond timescale. Neural Networks 13 (8-9), 883-889.

Joutsa, J. 2018. Isotooppimenetelmät. In E. Mervaala, E. Haaksiluoto, S. Himanen, S. Jääskeläinen, M. Kallio & S. Vanhatalo (Eds.) Kliininen neurofysiologia. Helsinki: Kustannus Oy Duodecim, knf02908.

Julkunen, P., Könönen, M., Määttä, S., Tarkka, I. M., Hiekkala, S. H., Säisänen, L., Vanninen, R., Karhu, J. & Jäkälä, P. 2016. Longitudinal study on modulated corticospinal excitability throughout recovery in supratentorial stroke. Neuroscience Letters 617, 88-93.

Kakigi, R. 1994. Somatosensory evoked magnetic fields following median nerve stimulation. Neuroscience Research 20 (2), 165-174.

Kakigi, R., Hoshiyama, M., Shimojo, M., Naka, D., Yamasaki, H., Watanabe, S., Xiang, J., Maeda, K., Lam, K., Itomi, K. & Nakamura, A. 2000. The somatosensory evoked magnetic fields. Progress in Neurobiology 61 (5), 495-523.

Kakigi, R., Watanabe, S. & Yamasaki, H. 2000. Pain-related somatosensory evoked potentials. Journal of Clinical Neurophysiology 17 (3), 295-308.

Kakigi, R. & Forss, N. 2010. Somatosensory and motor function. In P. C. Hansen, M. L. Kringelbach & R. Salmelin (Eds.) MEG: an introduction to methods. New York, NY: Oxford University Press, 300-345.

Karhu, J. & Tesche, C. D. 1999. Simultaneous early processing of sensory input in human primary (SI) and secondary (SII) somatosensory cortices. Journal of Neurophysiology 81 (5), 2017-2025.

Kekoni, J., Hämäläinen, H., Saarinen, M., Gröhn, J., Reinikainen, K., Lehtokoski, A. & Näätänen, R. 1997. Rate effect and mismatch responses in the somatosensory system: ERP-recordings in humans. Biological Psychology 46 (2), 125-142.

Khoshnejad, M., Piché, M., Saleh, S., Duncan, G. & Rainville, P. 2014. Serial processing in primary and secondary somatosensory cortex: a DCM analysis of human fMRI data in response to innocuous and noxious electrical stimulation. Neuroscience Letters 577, 83-88.

Kimura, J. 2001. Electrodiagnosis in diseases of nerve and muscle: principles and practice. (Third edition). New York, NY: Oxford University Press.

Kimura, M. & Takeda, Y. 2015. Automatic prediction regarding the next state of a visual object: electrophysiological indicators of prediction match and mismatch. Brain Research 1626, 31-44.

Kitamura, Y., Kakigi, R., Hoshiyama, M., Koyama, S., Shimojo, M. & Watanabe, S. 1995. Pain-related somatosensory evoked magnetic fields. Electroencephalography and Clinical Neurophysiology 95 (6), 463-474.

Klingner, C. M., Brodoehl, S., Huonker, R. & Witte, O. W. 2016. The processing of somatosensory information shifts from an early parallel into a serial

processing mode: a combined fMRI/MEG study. Frontiers in Systems Neuroscience 10, 103.

Kochs, E., Scharein, E., Möllenberg, O., Bromm, B. & Schulte am Esch, J. 1996. Analgesic efficacy of low-dose ketamine. Somatosensory-evoked responses in relation to subjective pain ratings. Anesthesiology 85 (2), 304-314.

Koltyn, K. F. & Umeda, M. 2007. Contralateral attenuation of pain after short-duration submaximal isometric exercise. Journal of Pain 8 (11), 887-892.

Koltyn, K. F., Brellenthin, A. G., Cook, D. B., Sehgal, N. & Hillard, C. 2014. Mechanisms of exercise-induced hypoalgesia. Journal of Pain 15 (12), 1294-1304.

Korvenoja, A., Wikström, H., Huttunen, J., Virtanen, J., Laine, P., Aronen, H., Seppäläinen, A. & llmoniemi, R. 1995. Activation of ipsilateral primary sensorimotor cortex by median nerve stimulation. NeuroReport 6 (18), 2589-2593.

Kozyrev, V., Eysel, U. T. & Jancke, D. 2014. Voltage-sensitive dye imaging of transcranial magnetic stimulation-induced intracortical dynamics. Proceedings of the National Academy of Sciences of the United States of America 111 (37), 13553-13558.

Kraus, W. E., Powell, K. E., Haskell, W. L., Janz, K. F., Cambell, W. W., Jakicic, J. M., Troiano, R. P., Sprow, K., Torres, A., Piercy, K. L. & The 2018 Physical Activity Guidelines Advisory Committee 2019. Physical activity, all-cause and cardiovascular mortality, and cardiovascular disease. Medicine & Science in Sports & Exercise 51 (6), 1270-1281.

Kujala, U. M., Kaprio, J., Sarna, S. & Koskenvuo, M. 1998. Relationship of leisure-time physical activity and mortality: the Finnish twin cohort. Journal of the American Medical Association 279 (6), 440-444.

Kujala, U. M. 2009. Evidence on the effects of exercise therapy in the treatment of chronic disease. British Journal of Sports Medicine 43 (8), 550-555.

Kuner, R. & Flor, H. 2017. Structural plasticity and reorganisation in chronic pain. Nature Reviews: Neuroscience 18 (1), 20-30.

Kurth, F., Eickhoff, S. B., Schleicher, A., Hoemke, L., Zilles, K. & Amunts, K. 2010. Cytoarchitecture and probabilistic maps of the human posterior insular cortex. Cerebral Cortex 20 (6), 1448-1461.

Könönen, M., Vanninen, R. & Halme, H. 2018. Funktionaalinen magneettikuvaus, fMRI. In E. Mervaala, E. Haaksiluoto, S. Himanen, S. Jääskeläinen, M. Kallio & S. Vanhatalo (Eds.) Kliininen neurofysiologia. Helsinki: Kustannus Oy Duodecim, knf02904.

LaMotte, R. H. & Campbell, J. N. 1978. Comparison of responses of warm and nociceptive C-fiber afferents in monkey with human judgments of thermal pain. Journal of Neurophysiology 41 (2), 509-528.

Lancaster, J. L., Rainey, L. H., Summerlin, J. L., Freitas, C. S., Fox, P. T., Evans, A. C., Toga, A. W. & Mazziotta, J. C. 1997. Automated labeling of the human brain: a preliminary report on the development and evaluation of a forward-transform method. Human Brain Mapping 5 (4), 238-242.

Lancaster, J. L., Woldorff, M. G., Parsons, L. M., Liotti, M., Freitas, C. S., Rainey, L., Kochunov, P. V., Nickerson, D., Mikiten, S. A. & Fox, P. T. 2000. Automated Talairach atlas labels for functional brain mapping. Human Brain Mapping 10 (3), 120-131.

Lee, I. M., Shiroma, E. J., Lobelo, F., Puska, P., Blair, S. N., Katzmarzyk, P. T. & Lancet Physical Activity Series Working Group 2012. Effect of physical inactivity on major non-communicable diseases worldwide: an analysis of burden of disease and life expectancy. Lancet 380 (9838), 219-229.

Leo, R. J. & Latif, T. 2007. Repetitive transcranial magnetic stimulation (rTMS) in experimentally induced and chronic neuropathic pain: a review. Journal of Pain 8 (6), 453-459.

Leone, C., Dufour, A., Di Stefano, G., Fasolino, A., Di Lionardo, A., La Cesa, S., Galosi, E., Valeriani, M., Nolano, M., Cruccu, G. & Truini, A. 2019. Cooling the skin for assessing small-fibre function. Pain 160 (9), 1967-1975.

Leskinen, T., Waller, K., Mutikainen, S., Aaltonen, S., Ronkainen, P. H., Alén, M., Sipilä, S., Kovanen, V., Perhonen, M., Pietiläinen, K. H., Cheng, S., Suominen, H., Kainulainen, H., Kaprio, J. & Kujala, U. M. 2009. Effects of 32-year leisure time physical activity discordance in twin pairs on health (TWINACTIVE Study): aims, design and results for physical fitness. Twin Research and Human Genetics 12 (1), 108-117.

Liang, M., Mouraux, A. & Iannetti, G. D. 2011. Parallel processing of nociceptive and non-nociceptive somatosensory information in the human primary and secondary somatosensory cortices: evidence from dynamic causal modeling of functional magnetic resonance imaging data. Journal of Neuroscience 31 (24), 8976-8985.

Liberati, G., Klöcker, A., Safronova, M. M., Ferrão Santos, S., Ribeiro Vaz, J., Raftopoulos, C. & Mouraux, A. 2016. Nociceptive local field potentials recorded from the human insula are not specific for nociception. PLoS Biology 14 (1), e1002345.

Litvak, V., Mattout, J., Kiebel, S., Phillips, C., Henson, R., Kilner, J., Barnes, G., Oostenveld, R., Daunizeau, J., Flandin, G., Penny, W. & Friston, K. 2011. EEG and MEG data analysis in SPM8. Computational Intelligence and Neuroscience 2011, 852961.

Lopes da Silva, F. H. 2010. Electrophysiological basis of MEG signals. In P. C. Hansen, M. L. Kringelbach & R. Salmelin (Eds.) MEG: an introduction to methods. New York, NY: Oxford University Press, 1-23.

Lopes da Silva, F. H. 2011 Event-related potentials: general aspects of methodology and quantification. In E. Niedermeyer, D. L. Schomer, & F. H. Lopes da Silva (Eds.) Niedermeyer's Electroencephalography: Basic principles, Clinical applications, and Related fields. (Sixth edition). Philadelphia, PA: Wolters Kluwer/Lippincott Williams & Wilkins Health, 923-934.

Lopes da Silva, F. H. & Van Rotterdam, A. 2011. Biophysical aspects of EEG and magnetoencephalogram generation. In E. Niedermeyer, D. L. Schomer & F. H. Lopes da Silva (Eds.) Niedermeyer's Electroencephalography: Basic

principles, Clinical applications, and Related fields. (Sixth edition). Philadelphia, PA: Wolters Kluwer/Lippincott Williams & Wilkins Health, 91-110.

Maarrawi, J., Peyron, R., Mertens, P., Costes, N., Magnin, M., Sindou, M., Laurent, B. & Garcia-Larrea, L. 2007. Motor cortex stimulation for pain control induces changes in the endogenous opioid system. Neurology 69 (9), 827-834.

Maldjian, J. A., Laurienti, P. J., Kraft, R. A. & Burdette, J. H. 2003. An automated method for neuroanatomic and cytoarchitectonic atlas-based interrogation of fMRI data sets. NeuroImage 19 (3), 1233-1239.

Maldjian, J. A., Laurienti, P. J. & Burdette, J. H. 2004. Precentral gyrus discrepancy in electronic versions of the Talairach atlas. NeuroImage 21 (1), 450-455.

Mattson, M. P. 2015. Lifelong brain health is a lifelong challenge: from evolutionary principles to empirical evidence. Ageing Research Reviews 20, 37-45.

Mauguière, F., Merlet, I., Forss, N., Vanni, S., Jousmäki, V., Adeleine, P. & Hari, R. 1997a. Activation of a distributed somatosensory cortical network in the human brain: a dipole modelling study of magnetic fields evoked by median nerve stimulation. Part II: effects of stimulus rate, attention and stimulus detection. Electroencephalography and Clinical Neurophysiology 104 (4), 290-295.

Mauguière, F., Merlet, I., Forss, N., Vanni, S., Jousmäki, V., Adeleine, P. & Hari, R. 1997b. Activation of a distributed somatosensory cortical network in the human brain. A dipole modelling study of magnetic fields evoked by median nerve stimulation. Part I: location and activation timing of SEF sources. Electroencephalography and Clinical Neurophysiology 104 (4), 281-289.

Melzack, R. & Wall, P. D. 1965. Pain mechanisms: a new theory. Science 150 (3699), 971-979.

Michel, C. M. & He, B. 2011. EEG Mapping and source imaging. In E. Niedermeyer, D. L. Schomer & F. H. Lopes da Silva (Eds.) Niedermeyer's Electroencephalography: Basic principles, Clinical applications, and Related fields. (Sixth edition). Philadelphia, PA: Wolters Kluwer/Lippincott Williams & Wilkins Health, 1179-1202.

Moayedi, M. & Davis, K. D. 2013. Theories of pain: from specificity to gate control. Journal of Neurophysiology 109 (1), 5-12.

Mäkelä, J. P. 2010. The use of MEG in clinical setting. In P. C. Hansen, M. L. Kringelbach & R. Salmelin (Eds.) MEG: an introduction to methods. New York, NY: Oxford University Press, 373-402.

Mäkelä, J. P., Lioumis, P., Laaksonen, K., Forss, N., Tatlisumak, T., Kaste, M. & Mustanoja, S. 2015. Cortical excitability measured with nTMS and MEG during stroke recovery. Neural Plasticity 2015, 309546.

Naeije, G., Vaulet, T., Wens, V., Marty, B., Goldman, S. & De Tiège, X. 2018. Neural basis of early somatosensory change detection: a magnetoencephalography study. Brain Topography 31 (2), 242-256.

Naugle, K. M., Fillingim, R. B. & Riley, J. L. 2012. A meta-analytic review of the hypoalgesic effects of exercise. Journal of Pain 13 (12), 1139-1150.

Nevalainen, P. 2018. MEG:n periaatteet. In E. Mervaala, E. Haaksiluoto, S. Himanen, S. Jääskeläinen, M. Kallio & S. Vanhatalo (Eds.) Kliininen neurofysiologia. Helsinki: Kustannus Oy Duodecim, knf01701.

Nickel, M. M., May, E. S., Tiemann, L., Schmidt, P., Postorino, M., Ta Dinh, S., Gross, J. & Ploner, M. 2017. Brain oscillations differently encode noxious stimulus intensity and pain intensity. NeuroImage 148, 141-147.

Nudo, R. J. 2013. Recovery after brain injury: mechanisms and principles. Frontiers in Human Neuroscience 7, 887.

Näätänen, R., Paavilainen, P., Rinne, T. & Alho, K. 2007. The mismatch negativity (MMN) in basic research of central auditory processing: a review. Clinical Neurophysiology 118 (12), 2544-2590.

Näätänen, R. 2009. Somatosensory mismatch negativity: a new clinical tool for developmental neurological research? Developmental Medicine and Child Neurology 51 (12), 930-931.

Ossipov, M. H., Dussor, G. O. & Porreca, F. 2010. Central modulation of pain. The Journal of Clinical Investigation 120 (11), 3779-3787.

Otieno, L. A., Opie, G. M., Semmler, J. G., Ridding, M. C. & Sidhu, S. K. 2019. Intermittent single-joint fatiguing exercise reduces TMS-EEG measures of cortical inhibition. Journal of Neurophysiology 121 (2), 471-479.

Paris, T. A., Misra, G., Archer, D. B. & Coombes, S. A. 2013. Effects of a force production task and a working memory task on pain perception. Journal of Pain 14 (11), 1492-1501.

Pasanen, T., Tolvanen, S., Heinonen, A. & Kujala, U. M. 2017. Exercise therapy for functional capacity in chronic diseases: an overview of meta-analyses of randomised controlled trials. British Journal of Sports Medicine 51 (20), 1459-1465.

Pascual-Leone, A., Tormos, J., Keenan, J., Tarazona, F., Cañete, C. & Catalá, M. 1998. Study and modulation of human cortical excitability with transcranial magnetic stimulation. Journal of Clinical Neurophysiology 15 (4), 333-343.

Pazo-Alvarez, P., Cadaveira, F. & Amenedo, E. 2003. MMN in the visual modality: a review. Biological Psychology 63 (3), 199-236.

Pedersen, B. K. & Saltin, B. 2015. Exercise as medicine – evidence for prescribing exercise as therapy in 26 different chronic diseases. Scandinavian Journal of Medicine & Science in Sports 25 (S3), 1-72.

Pereira, A. C., Huddleston, D. E., Brickman, A. M., Sosunov, A. A., Hen, R., McKhann, G. M., Sloan, R., Gage, F. H., Brown, T. R. & Small, S. A. 2007. An in vivo correlate of exercise-induced neurogenesis in the adult dentate gyrus. Proceedings of the National Academy of Sciences of the United States of America 104 (13), 5638-5643.

Peyron, R., Faillenot, I., Mertens, P., Laurent, B. & Garcia-Larrea, L. 2007. Motor cortex stimulation in neuropathic pain. Correlations between analgesic effect and hemodynamic changes in the brain. A PET study. NeuroImage 34 (1), 310-321.

Peyron, R. & Fauchon, C. 2019. The posterior insular-opercular cortex: an access to the brain networks of thermosensory and nociceptive processes? Neuroscience Letters 702, 34-39.

Pfurtscheller, G. & Lopes da Silva, F. H. 2011. EEG event-related desynchronization (ERD) and event-related synchronization (ERS). In E. Niedermeyer, D. L. Schomer & F. H. Lopes da Silva (Eds.) Niedermeyer's Electroencephalography: Basic principles, Clinical applications, and Related fields. (Sixth edition). Philadelphia, PA: Wolters Kluwer/Lippincott Williams & Wilkins Health, 935-948.

Ploner, M., Gross, J., Timmermann, L., Pollok, B. & Schnitzler, A. 2006. Pain suppresses spontaneous brain rhythms. Cerebral Cortex 16 (4), 537-540.

Popovich, C. & Staines, W. R. 2015. Acute aerobic exercise enhances attentional modulation of somatosensory event-related potentials during a tactile discrimination task. Behavioural Brain Research 281, 267-275.

Proudfoot, M., Woolrich, M. W., Nobre, A. C. & Turner, M. R. 2014. Magnetoencephalography. Practical Neurology 14 (5), 336-343.

Puce, A. & Hämäläinen, M. S. 2017. A review of issues related to data acquisition and analysis in EEG/MEG studies. Brain Sciences 7 (6), E58.

Raij, T. T., Forss, N., Stancák, A. & Hari, R. 2004. Modulation of motor-cortex oscillatory activity by painful Aδ- and C-fiber stimuli. NeuroImage 23 (2), 569-573.

Raitasalo, R. 2007. Mielialakysely: Suomen oloihin Beckin lyhyen depressiokyselyn pohjalta kehitetty masennusoireilun ja itsetunnon kysely. Sosiaali- ja terveysturvan tutkimuksia 86. Helsinki: Kelan tutkimusosasto.

Restuccia, D., Marca, G. D., Valeriani, M., Leggio, M. G. & Molinari, M. 2007. Cerebellar damage impairs detection of somatosensory input changes. A somatosensory mismatch-negativity study. Brain 130 (1), 276-287.

Rice, D., Nijs, J., Kosek, E., Wideman, T., Hasenbring, M. I., Koltyn, K., Graven-Nielsen, T. & Polli, A. 2019. Exercise-induced hypoalgesia in pain-free and chronic pain populations: state of the art and future directions. The Journal of Pain (Epub ahead of print).

Rottensteiner, M., Leskinen, T., Niskanen, E., Aaltonen, S., Mutikainen, S., Wikgren, J., Heikkilä, K., Kovanen, V., Kainulainen, H., Kaprio, J., Tarkka, I. M. & Kujala, U. M. 2015. Physical activity, fitness, glucose homeostasis, and brain morphology in twins. Medicine and Science in Sports and Exercise 47 (3), 509-518.

Rovio, S., Spulberg, G., Nieminen, L. J., Niskanen, E., Winblad, B., Tuomilehto, J., Nissinen, A., Soininen, H. & Kivipelto, M. 2010. The effect of midlife physical activity on structural brain changes in the elderly. Neurobiology of Aging 31 (11), 1927-1936.

Ruscheweyh, R., Willemer, C., Kruger, K., Duning, T., Warnecke, T., Sommer, J., Volker, K., Ho, H. V., Mooren, F., Knecht, S. & Floel, A. 2011. Physical activity and memory functions: an interventional study. Neurobiology of Aging 32 (7), 1304-1319.

Salenius, S., Schnitzler, A., Salmelin, R., Jousmäki, V. & Hari, R. 1997. Modulation of human cortical rolandic rhythms during natural sensorimotor tasks. NeuroImage 5 (3), 221-228.

Salmelin, R. & Hari, R. 1994. Spatiotemporal characteristics of sensorimotor neuromagnetic rhythms related to thumb movement. Neuroscience 60 (2), 537-550.

Salmelin, R. & Parkkonen, L. 2010. Experimental design. In P. C. Hansen, M. L. Kringelbach & R. Salmelin (Eds.) MEG: an introduction to methods. New York, NY: Oxford University Press, 75-82.

Samuelsson, J. G., Khan, S., Sundaram, P., Peled, N. & Hämäläinen, M. S. 2019. Cortical signal suppression (CSS) for detection of subcortical activity using MEG and EEG. Brain Topography 32 (2), 215-228.

Scheef, L., Jankowski, J., Daamen, M., Weyer, G., Klingenberg, M., Renner, J., Mueckter, S., Schürmann, B., Musshoff, F., Wagner, M., Schild, H. H., Zimmer, A. & Boecker, H. 2012. An fMRI study on the acute effects of exercise on pain processing in trained athletes. Pain 153 (8), 1702-1714.

Seeck, M., Koessler, L., Bast, T., Leijten, F., Michel, C., Baumgartner, C., He, B. & Beniczky, S. 2017. The standardized EEG electrode array of the IFCN. Clinical Neurophysiology 128 (10), 2070-2077.

Shinozaki, N., Yabe, H., Sutoh, T., Hiruma, T. & Kaneko, S. 1998. Somatosensory automatic responses to deviant stimuli. Cognitive Brain Research 7 (2), 165-171.

Srisa-an, P., Lei, L. & Tarkka, I. M. 1996. Middle latency somatosensory evoked potentials: noninvasive source analysis. Journal of Clinical Neurophysiology 13 (2), 156-163.

Strominger, N. L., Demarest, R. J. & Laemle, L. B. 2012. Noback's Human Nervous System, Seventh Edition: Structure and Function. (Seventh edition). Totowa, NJ: Humana Press.

Strömmer, J. M., Davis, S. W., Henson, R. N., Tyler, L. K. & Campbell, K. L. 2018. Physical activity predicts population-level age-related differences in frontal white matter. Journals of Gerontology: Series A, Biological Sciences and Medical Sciences (Epub ahead of print.).

Strömmer, J. M., Tarkka, I. M. & Astikainen, P. 2014. Somatosensory mismatch response in young and elderly adults. Frontiers in Aging Neuroscience 6, 293.

Tadel, F., Baillet, S., Mosher, J. C., Pantazis, D. & Leahy, R. M. 2011. Brainstorm: a user-friendly application for MEG/EEG analysis. Computational Intelligence and Neuroscience 2011, 879716.

Tajerian, M. & Clark, J. D. 2017. Nonpharmacological interventions in targeting pain-related brain plasticity. Neural Plasticity 2017, 2038573.

Talati, A. & Hirsch, J. 2005. Functional specialization within the medial frontal gyrus for perceptual go/no-go decisions based on "what," "when," and "where" related information: an fMRI study. Journal of Cognitive Neuroscience 17 (7), 981-993.

Tamè, L., Braun, C., Holmes, N. P., Farnè, A. & Pavani, F. 2016. Bilateral representations of touch in the primary somatosensory cortex. Cognitive Neuropsychology 33 (1-2), 48-66.

Tarkka, I. M., Könönen, M., Pitkänen, K., Sivenius, J. & Mervaala, E. 2008. Alterations in cortical excitability in chronic stroke after constraint-induced movement therapy. Neurological Research 30 (5), 504-510.

Tarkka, I. M., Savić, A., Pekkola, E., Rottensteiner, M., Leskinen, T., Kaprio, J. & Kujala, U. M. 2016. Long-term physical activity modulates brain processing of somatosensory stimuli: evidence from young male twins. Biological Psychology 117, 1-7.

Tarkka, I. M. & Treede, R. D. 1993. Equivalent electrical source analysis of pain-related somatosensory evoked potentials elicited by a CO2 laser. Journal of Clinical Neurophysiology 10 (4), 513-519.

Tarkka, I. M., Treede, R. D. & Bromm, B. 1992. Sensory and movement-related cortical potentials in nociceptive and auditory reaction time tasks. Acta Neurologica Scandinavica 86 (4), 359-364.

Taulu, S., Kajola, M. & Simola, J. 2004. Suppression of interference and artifacts by the signal space separation method. Brain Topography 16 (4), 269-275.

Tesarz, J., Schuster, A. K., Hartmann, M., Gerhardt, A. & Eich, W. 2012. Pain perception in athletes compared to normally active controls: a systematic review with meta-analysis. Pain 153 (6), 1253-1262.

Tiihonen, J., Hari, R. & Hämäläinen, M. 1989. Early deflections of cerebral magnetic responses to median nerve stimulation. Electroencephalography and Clinical Neurophysiology/Evoked Potentials Section 74 (4), 290-296.

Tyndall, A. V., Clark, C. M., Anderson, T. J., Hogan, D. B., Hill, M. D., Longman, R. S. & Poulin, M. J. 2018. Protective effects of exercise on cognition and brain health in older adults. Exercise and Sport Sciences Reviews 46 (4), 215-223.

Uusitalo, M. A. & Ilmoniemi, R. J. 1997. Signal-space projection method for separating MEG or EEG into components. Medical and Biological Engineering and Computing 35 (2), 135-140.

Valeriani, M., Le Pera, D., Niddam, D., Arendt-Nielsen, L. & Chen, A. C. N. 2000. Dipolar source modeling of somatosensory evoked potentials to painful and nonpainful median nerve stimulation. Muscle & Nerve 23 (8), 1194-1203.

Vanhatalo, S., Lauronen, L., Heinonen, H., Kallio, M. & Mervaala, E. 2018. EEG:n perusta. In E. Mervaala, E. Haaksiluoto, S. Himanen, S. Jääskeläinen, M. Kallio & S. Vanhatalo (Eds.) Kliininen neurofysiologia. Helsinki: Kustannus Oy Duodecim, knf00801.

van Middelkoop, M., Rubinstein, S. M., Verhagen, A. P., Ostelo, R. W., Koes, B. W. & van Tulder, M. W. 2010. Exercise therapy for chronic nonspecific low-back pain. Best Practice & Research Clinical Rheumatology 24 (2), 193-204.

Voelcker-Rehage, C. & Niemann, C. 2013. Structural and functional brain changes related to different types of physical activity across the life span. Neuroscience and Biobehavioral Reviews 37 (9 Pt B), 2268-2295.

Waller, K., Kaprio, J. & Kujala, U. M. 2008. Associations between long-term physical activity, waist circumference and weight gain: a 30-year longitudinal twin study. International Journal of Obesity 32 (2), 353-361.

zu Eulenburg, P., Baumgärtner, U., Treede, R. D. & Dieterich, M. 2013. Interoceptive and multimodal functions of the operculo-insular cortex: Tactile, nociceptive and vestibular representations. NeuroImage 83, 75-86.

ORIGINAL PAPERS

I

SOMATOSENSORY BRAIN FUNCTION AND GRAY MATTER REGIONAL VOLUMES DIFFER ACCORDING TO EXERCISE HISTORY: EVIDENCE FROM MONOZYGOTIC TWINS

by

Hautasaari, P., Savić, A. M., Loberg, O., Niskanen, E., Kaprio, J., Kujala, U. M. & Tarkka, I. M. 2017.

Brain Topography 30 (1), 77-86

Somatosensory brain function and gray matter regional volumes differ according to exercise history: Evidence from monozygotic twins

Pekka Hautasaari[1], Andrej M. Savić[2,3] Otto Loberg[4], Eini Niskanen[5], Jaakko Kaprio[6], Urho M. Kujala[1] and Ina M. Tarkka [1]

[1]Department of Health Sciences, University of Jyväskylä, Jyväskylä, Finland, [2]University of Belgrade, School of Electrical Engineering, Belgrade, Serbia and [3]Tecnalia Serbia Ltd., Belgrade, Serbia, [4]Department of Psychology, University of Jyväskylä, Jyväskylä, Finland, [5]Department of Applied Physics, University of Eastern Finland, Kuopio, Finland, [6]Department of Public Health, University of Helsinki, and National Institute for Health and Welfare, and Institute for Molecular Medicine (FIMM) University of Helsinki, Helsinki, Finland

Address for correspondence:

Ina M. Tarkka, PhD
University of Jyväskylä
Rautpohjankatu 8
40014 Jyväskylä,
Finland
Tel. +358 408053596
E-mail: Ina.Tarkka@jyu.fi

ABSTRACT

Associations between long-term physical activity and cortical function and brain structure are poorly known. Our aim was to assess whether brain functional and/or structural modulation associated with long-term physical activity is detectable using a discordant monozygotic male twin pair design. Nine monozygotic male twin pairs were carefully selected for an intrapair difference in their leisure-time physical activity of at least three years duration (mean age 34±1 y). We registered somatosensory mismatch response (sMMR) in EEG to electrical stimulation of fingers and whole brain MR images. We obtained exercise history and measured physical fitness and body composition. Equivalent electrical dipole sources of sMMR as well as gray matter (GM) voxel counts in regions of interest (ROI) indicated by source analysis were evaluated. SMMR dipolar source strengths differed between active and inactive twins within twin pairs in postcentral gyrus, medial frontal gyrus and superior temporal gyrus and in anterior cingulate (AC) GM voxel counts differed similarly. Compared to active twins, their inactive twin brothers showed greater dipole strengths in short periods of the deviant-elicited sMMR and larger AC GM voxel counts. Stronger activation in early unattended cortical processing of the deviant sensory signals in inactive co-twins may imply less effective gating of somatosensory information in inactive twins compared to their active brothers. Present findings indicate that already in 30's long-term physical activity pattern is linked with specific brain indices, both in functional and structural domains.

Key words: Twin research; Brain electrophysiology; Somatosensory cortex; Mismatch negativity; Brain structure; Physical activity

1. Introduction

Physical activity is known to have many beneficial physiological effects on the human body, e.g. cardiovascular system, endocrine system and skeletal muscle function enhance because of physical activity and, in addition, physical activity has a significant role in reducing risk for several chronic diseases (Kujala, Kaprio, Sarna, & Koskenvuo, 1998; Reiner, Niermann, Jekauc, & Woll, 2013). However, less is known about the effects of physical activity on brain structure and function in healthy adults. Recently we showed that increased levels of physical activity that are associated with beneficial alterations of several known cardio-metabolic disease risk factors were associated with structural modulation cortical gray matter (GM) volumes independent of genetic background (Rottensteiner et al., 2015). Our aim in the present study is to investigate further electrophysiological functional differences in early sensory processing and their possible link to regional brain structures using a monozygotic twin pair design to adjust for known and unknown, including familial and/or genetic confounders of the association between physical activity and brain function and structure. We recruited young healthy male twins who were discordant long-term, for the past 3 years, in their physical activity habits. Our cohort was selected in order to avoid effects of chronic diseases, medications or possible prodromal phases of diseases.

Exercise has an effect on brain structure and cognitive function in humans (Hillman, Erickson, & Kramer, 2008; Ruscheweyh et al., 2011). Accumulating evidence suggests connections between better executive functioning and increased volume in prefrontal and insular cortex (Ruscheweyh et al., 2011) and between exercise and increased hippocampal (Erickson et al., 2011), prefrontal and temporal GM as well as anterior white matter (WM) volume (Hillman et al., 2008). Most of previous research has been conducted in older adults.

Much less has been done with children and especially among young adults on exercise effects on brain. In our recent study we detected larger GM volume in non-dominant striatal and prefrontal structures based on whole brain MRI analysis in active young healthy adult male twins compared to their inactive twin brothers (Rottensteiner et al., 2015).

Mismatch negativity (MMN) is a comprehensively studied component of the auditory evoked potential most often registered using EEG (for review, see (Näätänen, Paavilainen, Rinne, & Alho, 2007)). It is generated by a cortical automatic change-detection process and it is elicited by any discernible auditory change when the ongoing auditory input differs from the preceding auditory stimulus (Näätänen et al., 2007). Less frequently studied somatosensory mismatch response (sMMR) is a corresponding change detection mechanism where various stimuli can be used to elicit sMMR including electrical or vibratory stimuli (Akatsuka, Wasaka, Nakata, Kida, & Kakigi, 2007; Spackman, Boyd, & Towell, 2007). Regardless of the stimulus type, violations to previous stimulus array are necessary to elicit the mismatch response (Akatsuka et al., 2005; Kekoni et al., 1997). SMMR determinants are not yet widely studied however, we recently detected differences between young and elderly healthy adults using electrical stimuli in a location mismatch design in the hand (Strömmer, Tarkka, & Astikainen, 2014). Our previous finding suggested attenuated later phase of SMMR in the elderly compared to young adults. SMMR is, by definition, an early precognitive, sensory-driven, automatic activation of change detection system. Of high relevance is the interesting recent report by Popovich and Staines (2015). They investigated the effect of acute bout of exercise in several components of somatosensory evoked potential in attended and unattended conditions (Popovich & Staines, 2015). Their oddball design involved attention paid to the specific finger where deviant stimuli were delivered allowing afterwards analysis during attention or ignore (unattended) conditions. Their unattended

condition resulted in enhanced N140 component in the parietal area. This component may resemble an early part of sMMR of our previous work however, we never requested any voluntary response in our experiments (Strömmer et al., 2014). Popovich and Staines (2015) allocated the effect they found of acute bout of moderate intensity aerobic exercise to improvement of selective attentional processing by enhancing involuntary shifts of attention from task-irrelevant stimuli post-exercise (Popovich & Staines, 2015). That may explain the effect after one acute exercise session however, it does not answer the question regarding effects of long-term physical activity. Popovich and Staines (2015) also analyzed later component, which they call LLP component, (175-250 ms window) and show suppressed LLP after acute exercise in unattended condition. They allocated this suppression to increased sensory gating of task-irrelevant stimuli (Popovich & Staines, 2015). Their amplitude modulations (N140 and LLP) occurred within the same time window as our sMMR (Strömmer et al., 2014; Tarkka et al., 2016). Our recent data implied modulation in few electrode locations on the somatosensory cortical area, where inactive individuals showed larger components, and we allocated this difference between inactive and active ones to enhanced gating of aberrant somatosensory stimuli in active co-twin compared to inactive co-twin (Tarkka et al., 2016).

There is wide inter-individual variability in known metabolic and cardiorespiratory responses to regular physical activity, e.g. in plasma triglycerides, fasting insulin levels and cardiorespiratory fitness levels (Bouchard et al., 2012). Twin studies provide a pathway to study associations between physical activity vs. inactivity in functional and structural measures in strong study design where genetic background and mostly also childhood environment is controlled. In the present study, we analyse in detail cerebral sources of sMMR and related brain structures in MR images in a rare set of healthy twin pairs who are

long-term discordant in physical activity. We aim to recognize if possible functional differences are in any way reflected in structural brain indices.

2. Methods

2.1. Participants

Participants were a subgroup from FITFATTWIN (Rottensteiner et al. 2014) study. A total of 18 healthy men from nine monozygotic twin pairs participated such that each pair was long-term discordant in their leisure-time physical activity. The mean age of participants was about 35 years. In FITFATTWIN study we identified pairs who were long-term discordant for physical activity in order to investigate the effects of physical activity. We selected only men because before this age pregnancies have a major influence on physical activity fluctuations and irregularities related to menstrual cycle also influence many biological parameters targeted in our study. FITFATTWIN study participants were initially identified from FinnTwin16 Cohort, which is a population based, longitudinal study of Finnish twins born between October 1974 and December 1979 (Kaprio, Pulkkinen, & Rose, 2002). Selection of the twin pairs to the present study is described in detailed in Rottensteiner et al. 2015 (Rottensteiner et al., 2015). In short, the twins participated in web-based questionnaire after which there was a telephone interview and finally interview at the laboratory and medical examination. Physical activity levels and pairwise discordance was based on structured retrospective physical activity interview (Kujala et al., 1998; Leskinen et al., 2009; Waller, Kaprio, & Kujala, 2008) which we conducted and which takes into account leisure-time physical activity, including commuting activity, one-year intervals over the past six years. This information was used to define pairwise discordance. The mean leisure-time

metabolic equivalent (MET) index during the past three years (3-yr-LTMET index as MET hours/day) was calculated and used as a criterion to assess leisure-time physical activity level. Weight, height, waist circumference and maximal oxygen uptake (VO_{2max}) were measured, body mass index (BMI) was calculated, and the whole body composition was determined after an overnight fast using dual-energy X-ray absorptiometry (DXA Prodigy; GE Lunar Corp., Madison, Wisconsin) (Table 1.).

(Table 1. around here)

Study procedure and test protocols were approved by the Ethical Review Board for Human Research of the Central Finland Health Care District (9/29/2011) and the study was conducted following the tenets of the Declaration of Helsinki. All participants volunteered, received no financial benefit and provided a written informed consent prior to participation.

2.2. SMMR protocol

Somatosensory electrical stimuli were delivered (Digitimer Ltd., model DS7A, Welvyn Garden City, UK) to left index and little fingers through flexible metal ring electrodes (stimulating cathode electrode placed above the proximal phalanx and anode electrode above the distal phalanx, Technomed Europe Ltd, Maastricht, Netherlands) to elicit somatosensory mismatch response, sMMR, as an automatic location deviance detection. The somatosensory stimulation was divided into two parts: in the first part standard stimuli were applied to the index finger and deviant stimuli to the little finger and in the second part standard and deviant stimuli locations were reversed thus producing mismatch in location during the flow of stimuli independent from finger. Stimulus intensity was set twice the individual sensory threshold separately for each finger. Electrical stimulus duration was 200 μs. Total of 1000 stimuli were delivered, 10 % were randomly delivered deviants. The inter-stimulus interval was 600 ms. Both co-twins were recorded on the same day. Participants were listening to an

engaging radio play and they were asked to ignore stimuli and concentrate on the play. Participants were observed via a video camera during recording and they were asked questions of the contents of the radio play afterwards.

EEG was continuously recorded with 128-channel sensor net with Cz reference (Electrical Geodesics, Inc., Portland, Oregon) and for analysis re-referenced to average reference. The sampling rate was 500 Hz with 0.1 Hz - 200 Hz bandpass filtering at recording. For offline analysis, EEG data was bandpass filtered in a range 1Hz - 35 Hz and segmented to 450 ms epochs (100 ms baseline preceding the stimulus onset and 350 ms post stimulus onset). Epochs containing artifacts with high amplitude potential shifts and eye-blinks and/or movement artifacts were automatically rejected. Noise-free epochs were baseline corrected and averaged to form the deviant wave form event-related potential (ERP) and then same amount of standard stimuli as the individual's deviant stimuli were picked from those standards that follow deviants in order to form the standard wave form for each participant. The minimum number of accepted deviants was 66 per participant (Table 1).

2.3. ERP analysis

Grand averages were formed for deviant and standard stimulus conditions each for inactive and active co-twins. Topographic voltage maps were plotted from deviant and standard grand average wave forms. Further data processing was performed with Brain Electrical Source Analysis (BESA, Besa GmbH, Gräfelfing, Germany). Spatio-temporal multiple dipole source models were developed. In this kind of a model, each source potential described the temporal variations in each dipole moment (i.e. its strength), while the equivalent dipole source maintained a stationary location and orientation in the modeling time window (0-350 ms from the stimulus onset). The proportion of the data not explained by the model was displayed in

residual variance (RV). An ellipsoidal head model with four shells was used. First the grand average waveform with highest amplitude was chosen as a starting point for modeling because source activities are easiest to dissociate when amplitudes are high and signal-to-noise ratio is good. Thus first model was developed for the deviant wave form grand average data set of the active twins. This was a seven-dipole model, where six dipoles explained cerebral activity and one dipole accounted for residual eye movements. Dipole 1 modeled major activity between 220-300 ms peaking with 20 nAm and dipoles 2 and 3 modeled unilateral (contralateral to stimulation) activity starting already at 24 ms with 9 nAm and 11 nAm peak currents, respectively. Dipoles 4 and 5 modeled bilateral activities between 100-300 ms in deeper brain areas peaking with 9 nAm and 7 nAm currents, respectively. Finally dipole 6 modeled unilateral (ipsilateral to stimulation) activity between 74-272 ms peaking with 8 nAm. Dipoles 1, 2, 3 and 5 were completely free during fitting and dipole 4 was symmetric to dipole 5 and dipole 6 was symmetric to dipole 2, and finally dipole 7, collecting residual eye movement activity, was fixed in location with free orientation. We applied this model to the data of the deviant grand average of inactive twins, and in addition, to the standard grand average wave forms of both groups. Always when applying first model to other data sets, the equivalent electrical dipole source orientations were fitted but no source locations were allowed to change. We tested that further fitting or adding more dipoles did not result in any substantial improvement of the model. As the locations were kept similar when applying the model in other data sets, the possible individual differences were observed in modulation of dipolar source potentials and in varying RVs. The differences in dipole moments were applied in statistical models.

2.4. MRI recording and preprocessing

Brain magnetic resonance imaging (MRI) scans were acquired using a 1.5 T whole body magnetic resonance (MR) scanner (Siemens Symphony, Siemens Medical Systems, Erlangen, Germany) on the same day as other data was collected. The 3D T1-weighted MPRAGE images of whole brain were collected with the following parameters: TR = 2180 ms, TE = 3.45 ms, TI = 1100 ms, flip angle = 15˚, slice thickness = 1.0 mm, in-plane resolution 1.0 mm × 1.0 mm, and matrix size = 256 × 256. Voxel-based morphometric (VBM) analyses were performed with VBM8 toolbox (http://dbm.neuro.uni-jena.de/vbm/) for SPM8 (Wellcome Trust Center for Neuroimaging, UCL, UK) running under Matlab R2010a (The Mathworks Inc., Natick, MA, USA). First, the MR images were segmented into gray matter (GM), white matter (WM), and cerebrospinal fluid (CSF). Images were then normalized to the Montreal Neurological Institute brain template using a high-dimensional DARTEL algorithm. Nonlinearly modulated GM images were created to preserve relative differences in regional GM volume. Finally, the GM volumes were spatially smoothed with 12 mm full width at half maximum Gaussian kernel. GM, WM and CSF volumes were compared between co-twins as well as GM voxel counts of four regions of interest (ROI), suggested by the source model, from both hemispheres were compared between co-twins. The ROIs were defined using the WFUPickAtlas-tool (Wake Forest University, School of Medicine) implemented in SPM8 (Maldjian, Laurienti, Kraft, & Burdette, 2003; Maldjian, Laurienti, & Burdette, 2004). The locations of WFU atlas ROIs used here for comparison between co-twins are given in Fig. 4.

2.5.Statistical analysis

Wilcoxon Signed Rank Test was used to compare voxel counts in MRI ROIs. For dipole moment comparison statistical analysis point-to-point on source waveforms was performed in SPSS 22 with repeated measures ANOVA with 5(time) x 2(group) factorial design. Only

group effects are reported. Significance was set at $p \leq 0.05$. Source waveform results include effect sizes in η_p^2 (partial eta-squared).

3. Results

The characteristics of the 18 twins from nine twin pairs are shown in Table 1. Inactive and active co-twins differed in their fat% and VO_2max, as anticipated. The mean activity level of the active twins was 321% higher than that of their inactive brothers (3-yr-leisuretime MET), while their fitness levels were 132% higher (VO_{2max}) (Rottensteiner et al., 2015; Tarkka et al., 2016). We did not see any difference in the number of successful ERP recordings and brain segmented morphologic volumes between active and inactive co-twins. SMMR grand average waveforms of inactive and active co-twins are depicted in Fig. 1, where all 128 channels are superimposed to allow visualisation of similarities and differences between the co-twins in an illustrative window from -100 to 500 ms. In Fig.1, 0 denotes the stimulus onset and selected time points (90 ms, 150 ms, 244 ms and 280 ms) are shown in topographic maps to facilitate comparison.

(Figure 1. around here)

Equivalent electrical dipole source model developed in BESA is shown in Fig. 2, where the same model is illustrated in sagittal (A) and verticofrontal (B) planes. The model consisted of 7 source dipoles (SD), though the dipole explaining eye activity is not visible in the planes shown in Fig. 2. The 3D dipole location coordinates of the model are given in Table 2 as well as the approximate brain areas which the dipole coordinates represent. The model RV in the grand average of the deviant of active co-twins was 6.9% and the same model, when introduced in standard grand average, gave RV 25.1%. When this model was

introduced in the grand average of the deviant of inactive co-twins the RV was 5.7% and when it was introduced in standard grand average of inactive co-twins RV was 17.8%. When the model was introduced in any data sets, SD orientations were fitted but locations were not. The subsequent relatively minor orientation variations are not shown. Source wave forms of the models for deviant stimulus-elicited sMMRs were compared between inactive and active co-twins. For source SD2 we found significant difference during 280 to 290 ms post stimulus ($F(1, 16) = 5.345$, $p = 0.034$, $\eta_p^2 = 0.250$) where inactive co-twins had stronger amplitudes. In source SD3 there was significant difference between 148-158 ms after stimulus onset ($F(1, 16) = 8.200$, $p = 0.011$, $\eta_p^2 = 0.339$) where again inactive co-twins had stronger amplitudes. Source SD4 differed at two periods: first at 86 to 96 ms ($F(1, 16) = 5.780$, $p = 0.029$, $\eta_p^2 = 0.265$) where again inactive co-twins had stronger amplitudes. The later difference in SD4 was in the window from 252 to 262 ms ($F(1, 16) = 5.538$, $p = 0.032$, $\eta_p^2 = 0.257$) where active co-twins had stronger amplitudes. Source SD1 did not show differences. Also the standard stimulus equivalent dipole source waveforms were compared, and there for source SD6 we found significant difference during 252 to 262 ms ($F(1, 16) = 4.811$, $p = 0.043$, $\eta_p^2 = 0.231$) where active co-twins had stronger amplitudes. Fig. 3 details the differences in SD moments.

(Table 2 and Figures 2 and 3 around here)

Total GM, WM and CSF volumes estimated from non-normalized images did not differ between the co-twins in structural MRI analysis (see Table 1). Multiple dipole source model suggested ROIs (anterior cingulate, postcentral gyrus, frontal medial gyrus and superior temporal gyrus) where GM voxel count was performed. The exact 3D regional counts in MRI were performed using WFU Atlas, see cortical surface rendering of ROIs in Fig. 4. GM voxel count differed in one ROI, the right anterior cingulate, (inactive 544±9 vs. active 536±12, $p=0.046$) between inactive and active co-twins where inactive co-twins showed

larger voxel count (see Table 3 for all tested ROIs). Right anterior cingulate ROI is illustrated in averaged MR image in Fig. 5.

(Table 3. and Figures 4 and 5 around here)

4. Discussion

Our present results demonstrate that long-term physical activity selectively modulates specific early sensory functional brain responses and may selectively modify cortical structures. Three-dimensional source analysis indicated short time windows where specific sMMR cerebral sources were stronger, and GM voxel count in structural MR image was higher in the right anterior cingulate ROI, both distinctions in inactive co-twins compared to their active co-twins. The purpose of studying young, healthy male twins is to see whether possible dissimilarities in physical activity, at an age when chronic diseases, medications or prodromal disease processes are unlikely yet to be present, are associated with functional and/or structural modulation in the brain. The monozygotic twin design with discordant brothers provides a unique experimental opportunity allowing adjustment for known and unknown confounders of the association between physical activity and brain markers.

Previously we have shown that sMMR is reliably electrically elicited by a location difference in the hand and its modulations can be observed in ageing and in persons in different physical activity categories (Strömmer et al., 2014; Tarkka et al., 2016). The cerebral sources of auditory mismatch negativity (MMN), the apparent close relative of sMMR, have been located in bilateral temporal cortices and frontal cortex (Giard, Perrin, Pernier, & Bouchet, 1990; Naatanen & Kahkonen, 2009; Näätänen et al., 2007). In the

present study, we developed a 3D source model to approximate the cerebral sources of the electrically registered sMMR. Previously, equivalent current dipole source for the sMMR component in the window of 150-250 ms was located in the primary (SI) or secondary somatosensory cortex (SII) contralateral to stimulated hand by Akatsuka et al. (2007) in their magnetoencephalograhic study (Akatsuka et al., 2007). Kekoni et al. (1992) have also localized somewhat earlier middle-latency somatosensory magnetic fields in contralateral SI and SII (Kekoni et al., 1997). We, however, attempted to incorporate the sources of cortical activity from stimulus onset to 350 ms in order to describe the complete process of detecting sensory mismatch. Our model was developed for the deviant waveform even though mismatch negativity studies often investigate difference waveforms. In contrast to difference waveform analysis, our model approximates sources in a natural condition where most of the ongoing brain processes are taken into consideration within the modeled window.

Our source model has seven dipoles, six of which are in the brain. SD1 source located in the right ventral anterior cingulate gyrus, location associated with large variety of phenomena related to executive control with numerous projections to motor areas (Devinsky, Morrell, & Vogt, 1995). SD:s 2, 3 and 6 located in areas more specifically related to somatosensory processing as SD 2 and 6 were located in postcentral gyrus, part of the area known as primary somatosensory cortex, SI, responsible for processing sensation of touch (Noback, Strominger, Demarest, & Ruggiero, 2005). Furthermore, SD 3 located in frontal medial gyrus in the right hemisphere, area with connections to postcentral gyrus and functional links to spatial attention and top-down control of attentional focus (Fox et al., 2014). SD4 and SD5 were located in left and right superior temporal gyri (bilaterally in BA 22), in areas which are heavily implicated in auditory processing, but may also contribute to amodal, likely multisensory, and memory-related aspects of MMN response (Näätänen et al., 2007).

Those sMMR differences, that indicated larger automatic neural activation in inactive co-twins compared to their active brothers, located in contralateral SI and SII regions and in the frontal medial gyrus (Fig. 3, Source Dipole 2, Source Dipole 3). The SI and SII activity likely cover primary and secondary somatosensory processing and also some somatosensory associative function, however, difference observed in activation in frontal medial gyrus may well indicate more complex automatic sensory mismatch processing. Frontal medial gyrus is known to contribute to a number of associative and executive functions and is active also in cognitive task when subjects have to decide "where" in the body the target is (Talati & Hirsch, 2005). This region is implicated in motor planning and non-motor tasks such as decision making, discrimination and especially in convergence of sensory information for high-level processes related to coordination of motor activity (Bak, Glenthoj, Rostrup, Larsson, & Oranje, 2011; Noback et al., 2005). Thus, frontal medial gyrus may play a role in automatically alerting inactive co-twins more than the active co-twins of deviant information ascending from the body. Sensory gating using different electrical stimulation paradigm has been applicably studied in psychiatry where source modeling has implicated frontal medial gyrus as an important player in gating (Bak et al., 2011; Jensen, Oranje, Wienberg, & Glenthoj, 2008). Thus it may be that amplitude differences we have observed are explained by differences in sensory gating emerging from different levels of physical activity.

First source dipole (SD1) of the present model located close to midline and likely accounted for activity in rather large bilateral region in ventral anterior cingulate. No difference was observed in the source moment of this dipole associated with level of physical activity. This dipole mainly accounted for late activity within the model, approximately from 220 to 280 ms. As the electrical stimulus intensity in the fingers were twice sensory

threshold, the stimuli were distinctive and not pleasant. It is plausible that SD1 accounted for activity registering the unpleasantness of stimuli as ventral anterior cingulate area is known for processing painful stimuli (Apkarian, Bushnell, Treede, & Zubieta, 2005; Devinsky et al., 1995; Tarkka & Treede, 1993). Anterior cingulate is activated in various acute pain stimulus paradigms (Apkarian et al., 2005) and thus it is conceivable that co-twins responded similarly to the unpleasantness of electrical stimuli but their interpretations varied depending on their accustomed level of physical activity. Tesarz et al (2013) recently elegantly showed that pain inhibitory system may be less responsive in athletes than in non-athletes (Tesarz, Gerhardt, Schommer, Treede, & Eich, 2013). Applied to our condition, their conclusion may support our view of the present data, i.e. both twins recognized the unpleasantness similarly but active co-twins automatically assessed it less meaningful. Popovich and Staines (2015) found that only one acute bout of exercise modulated late somatosensory component (especially LLP in their work) in attended and unattended conditions, and they suggested that this modulation was associated with improvement in selective attentional processing and sensory gating of task-irrelevant stimuli (Popovich & Staines, 2015). Our findings on sMMR occurred in the same time window with corresponding results to Popovich and Staines's unattended condition and our inactive twins showed stronger amplitudes compared to their active co-twins. However, our data shows long-term exercise effect as the co-twins were discordant in their physical activity for at least three years.

As the functional modeling of sMMR revealed distinctions between co-twins, a comparison of structural brain images of co-twins was performed. It was based on the regions where active sources were identified (see Table 3). Atlas-based ROIs were used in GM voxel count comparison where a difference in the right hemisphere anterior cingulate was detected indicating higher voxel count in inactive co-twins. We were astonished that only right

anterior cingulate region showed this structural difference. Yet it should be remembered that these atlas ROIs are rather large (Fig. 4.) and inevitably these areas participate in many different functions which may or may not modulate GM morphology in young healthy men. Our data imply that anterior cingulate region is, at least to some extent, functionally involved in somatosensory deviant detection and it shows morphological difference associated with long-term exercise history. We can speculate that physical activity may have somewhat corresponding structural brain effects as is suggested by Fox et al. (2014) analyzing morphometric neuroimaging studies in meditation practitioners (Fox et al., 2014). That large meta-analysis found eight brain regions consistently altered in meditators compared to non-meditators, including anterior and mid cingulate and sensory cortices and insula. Sensation regulation is connected with anterior cingulate (Apkarian et al., 2005; Fox et al., 2014) and it is likely that the unpleasantness of electrical stimuli was automatically assessed, at least in part, in this region.

Establishing modulations in both MR revealed morphology and functional source analysis in healthy twin males who differ only in their long-term exercise history leads towards emerged point of view in brain research, namely brain plasticity in adults. Most studies assess cortical plasticity during recovery processes after brain insults, such as cerebrovascular stroke (Julkunen et al., 2016; Nudo & McNeal, 2013; Nudo, 2013; Tarkka, Könönen, Pitkänen, Sivenius, & Mervaala, 2008), however many principles found in recovery processes may also apply to any intensive long-term activity, in our case physical exercise. Number of factors influence dose-response of physical exercise in brain plasticity, ranging from molecular and cellular cascades to points of saturation of effect, most of which are poorly known. However, it seems likely that behavioral experience, in the present case it being mostly aerobic exercise, is a powerful modulator of brain plasticity.

In conclusion, we showed multiple brain areas involved in sensory discrimination and integration of sensory inputs in the early time period where conscious processing of stimuli was most unlikely. Furthermore, we demonstrated differences between monozygotic co-twins, discordant in physical activity, in the tested automatic sensory processing. Our experimental design verified that attentional or motivational factors did not contaminate our result. Though we control for familial and genetic confounders, we cannot firmly establish the direction of causation, even though we consider physical activity as the more likely driver of the neurophysiological changes than vice versa. The small number of monozygotic twin pairs discordant in long-term physical activity is clearly a limitation of the present study and thus more research is needed to confirm the present results. It is, however, very difficult to identify larger numbers of twin pairs sufficiently discordant for leisure-time physical activity and fitness who are also healthy and free of medications and other potential confounders. We essentially screened all available pairs from five birth cohorts aged in the mid-thirties in Finland. We had only structural MR images in the present study, and thus it would be interesting to relate electrically elicited sMMR and functional MR imaging, yet any brain structural differences between healthy monozygotic twins is noteworthy.

Acknowledgements

Authors wish to thank the participants of the study and laboratory personnel and students at the University of Jyväskylä who contributed to this study. Support from the Juho Vainio Foundation (Helsinki) is acknowledged (to I M Tarkka). Data collection in the twin cohort has been supported by National Institute of Alcohol Abuse and Alcoholism (grants AA-12502, AA-00145, and AA-09203 to R J Rose) and the Academy of Finland (grants 100499, 265240, 263278 and 264146 to J Kaprio).

References

Akatsuka, K., Wasaka, T., Nakata, H., Inui, K., Hoshiyama, M., & Kakigi, R. (2005). Mismatch responses related to temporal discrimination of somatosensory stimulation. *Clinical Neurophysiology : Official Journal of the International Federation of Clinical Neurophysiology, 116*(8), 1930-1937. doi:10.1016/j.clinph.2005.04.021

Akatsuka, K., Wasaka, T., Nakata, H., Kida, T., & Kakigi, R. (2007). The effect of stimulus probability on the somatosensory mismatch field. *Experimental Brain Research, 181*(4), 607-614. doi:10.1007/s00221-007-0958-4

Apkarian, A. V., Bushnell, M. C., Treede, R. D., & Zubieta, J. K. (2005). Human brain mechanisms of pain perception and regulation in health and disease. *European Journal of Pain (London, England), 9*(4), 463-484. doi:S1090-3801(04)00148-X [pii]

Bak, N., Glenthoj, B. Y., Rostrup, E., Larsson, H. B., & Oranje, B. (2011). Source localization of sensory gating: A combined EEG and fMRI study in healthy volunteers. *NeuroImage, 54*(4), 2711-2718. doi:10.1016/j.neuroimage.2010.11.039 [doi]

Bouchard, C., Blair, S. N., Church, T. S., Earnest, C. P., Hagberg, J. M., Hakkinen, K., . . . Rankinen, T. (2012). Adverse metabolic response to regular exercise: Is it a rare or common occurrence? *PloS One, 7*(5), e37887. doi:10.1371/journal.pone.0037887 [doi]

Devinsky, O., Morrell, M. J., & Vogt, B. A. (1995). Contributions of anterior cingulate cortex to behaviour. *Brain : A Journal of Neurology, 118 (Pt 1)*(Pt 1), 279-306.

Erickson, K. I., Voss, M. W., Prakash, R. S., Basak, C., Szabo, A., Chaddock, L., . . . Kramer, A. F. (2011). Exercise training increases size of hippocampus and improves memory.

Proceedings of the National Academy of Sciences of the United States of America, 108(7), 3017-3022. doi:10.1073/pnas.1015950108 [doi]

Fox, K. C., Nijeboer, S., Dixon, M. L., Floman, J. L., Ellamil, M., Rumak, S. P., . . . Christoff, K. (2014). Is meditation associated with altered brain structure? A systematic review and meta-analysis of morphometric neuroimaging in meditation practitioners. *Neuroscience and Biobehavioral Reviews, 43*, 48-73. doi:10.1016/j.neubiorev.2014.03.016 [doi]

Giard, M. H., Perrin, F., Pernier, J., & Bouchet, P. (1990). Brain generators implicated in the processing of auditory stimulus deviance: A topographic event-related potential study. *Psychophysiology, 27*(6), 627-640.

Hillman, C. H., Erickson, K. I., & Kramer, A. F. (2008). Be smart, exercise your heart: Exercise effects on brain and cognition. *Nature Reviews.Neuroscience, 9*(1), 58-65. doi:10.1038/nrn2298

Jensen, K. S., Oranje, B., Wienberg, M., & Glenthoj, B. Y. (2008). The effects of increased serotonergic activity on human sensory gating and its neural generators. *Psychopharmacology, 196*(4), 631-641. doi:10.1007/s00213-007-1001-y [doi]

Julkunen, P., Kononen, M., Maatta, S., Tarkka, I. M., Hiekkala, S. H., Saisanen, L., . . . Jakala, P. (2016). Longitudinal study on modulated corticospinal excitability throughout recovery in supratentorial stroke. *Neuroscience Letters, 617*, 88-93. doi:S0304-3940(16)30082-9 [pii]

Kaprio, J., Pulkkinen, L., & Rose, R. J. (2002). Genetic and environmental factors in health-related behaviors: Studies on finnish twins and twin families. *Twin Research : The*

Official Journal of the International Society for Twin Studies, 5(5), 366-371. doi:10.1375/136905202320906101 [doi]

Kekoni, J., Hämäläinen, H., Saarinen, M., Grohn, J., Reinikainen, K., Lehtokoski, A., & Näätänen, R. (1997). Rate effect and mismatch responses in the somatosensory system: ERP-recordings in humans. *Biological Psychology, 46*(2), 125-142. doi:S0301-0511(97)05249-6 [pii]

Kujala, U. M., Kaprio, J., Sarna, S., & Koskenvuo, M. (1998). Relationship of leisure-time physical activity and mortality: The finnish twin cohort. *Jama, 279*(6), 440-444. doi:joc71682 [pii]

Leskinen, T., Waller, K., Mutikainen, S., Aaltonen, S., Ronkainen, P. H., Alen, M., . . . Kujala, U. M. (2009). Effects of 32-year leisure time physical activity discordance in twin pairs on health (TWINACTIVE study): Aims, design and results for physical fitness. *Twin Research and Human Genetics : The Official Journal of the International Society for Twin Studies, 12*(1), 108-117. doi:10.1375/twin.12.1.108 [doi]

Maldjian, J. A., Laurienti, P. J., & Burdette, J. H. (2004). Precentral gyrus discrepancy in electronic versions of the talairach atlas. *NeuroImage, 21*(1), 450-455. doi:S1053811903005755 [pii]

Maldjian, J. A., Laurienti, P. J., Kraft, R. A., & Burdette, J. H. (2003). An automated method for neuroanatomic and cytoarchitectonic atlas-based interrogation of fMRI data sets. *NeuroImage, 19*(3), 1233-1239. doi:S1053811903001691 [pii]

Naatanen, R., & Kahkonen, S. (2009). Central auditory dysfunction in schizophrenia as revealed by the mismatch negativity (MMN) and its magnetic equivalent MMNm: A

review. *The International Journal of Neuropsychopharmacology / Official Scientific Journal of the Collegium Internationale Neuropsychopharmacologicum (CINP), 12*(1), 125-135. doi:10.1017/S1461145708009322 [doi]

Näätänen, R., Paavilainen, P., Rinne, T., & Alho, K. (2007). The mismatch negativity (MMN) in basic research of central auditory processing: A review. *Clinical Neurophysiology : Official Journal of the International Federation of Clinical Neurophysiology, 118*(12), 2544-2590. doi:10.1016/j.clinph.2007.04.026

Noback, C., Strominger, N., Demarest, R., & Ruggiero, D. (2005). *The human nervous system, structure and function* (Sixth Edition ed.). Totowa, New Jersey, USA: Humana Press.

Nudo, R. J. (2013). Recovery after brain injury: Mechanisms and principles. *Frontiers in Human Neuroscience, 7*, 887. doi:10.3389/fnhum.2013.00887 [doi]

Nudo, R. J., & McNeal, D. (2013). Plasticity of cerebral functions. *Handbook of Clinical Neurology, 110*, 13-21. doi:10.1016/B978-0-444-52901-5.00002-2 [doi]

Popovich, C., & Staines, W. R. (2015). Acute aerobic exercise enhances attentional modulation of somatosensory event-related potentials during a tactile discrimination task. *Behavioural Brain Research, 281*, 267-275. doi:10.1016/j.bbr.2014.12.045 [doi]

Reiner, M., Niermann, C., Jekauc, D., & Woll, A. (2013). Long-term health benefits of physical activity - a systematic review of longitudinal studies. *BMC Public Health, 13*, 813-2458-13-813. doi:10.1186/1471-2458-13-813; 10.1186/1471-2458-13-813

Rottensteiner, M., Leskinen, T., Niskanen, E., Aaltonen, S., Mutikainen, S., Wikgren, J., . . . Kujala, U. M. (2015). Physical activity, fitness, glucose homeostasis, and brain

morphology in twins. *Medicine and Science in Sports and Exercise, 47*(3), 509-518. doi:10.1249/MSS.0000000000000437 [doi]

Ruscheweyh, R., Willemer, C., Kruger, K., Duning, T., Warnecke, T., Sommer, J., . . . Floel, A. (2011). Physical activity and memory functions: An interventional study. *Neurobiology of Aging, 32*(7), 1304-1319. doi:10.1016/j.neurobiolaging.2009.08.001 [doi]

Spackman, L. A., Boyd, S. G., & Towell, A. (2007). Effects of stimulus frequency and duration on somatosensory discrimination responses. *Experimental Brain Research, 177*(1), 21-30. doi:10.1007/s00221-006-0650-0

Strömmer, J. M., Tarkka, I. M., & Astikainen, P. (2014). Somatosensory mismatch response in young and elderly adults. *Frontiers in Aging Neuroscience, 6*, 293. doi:10.3389/fnagi.2014.00293 [doi]

Talati, A., & Hirsch, J. (2005). Functional specialization within the medial frontal gyrus for perceptual go/no-go decisions based on "what," "when," and "where" related information: An fMRI study. *Journal of Cognitive Neuroscience, 17*(7), 981-993. doi:10.1162/0898929054475226 [doi]

Tarkka, I. M., Könönen, M., Pitkänen, K., Sivenius, J., & Mervaala, E. (2008). Alterations in cortical excitability in chronic stroke after constraint-induced movement therapy. *Neurological Research, 30*(5), 504-510.

Tarkka, I. M., Savic, A., Pekkola, E., Rottensteiner, M., Leskinen, T., Kaprio, J., & Kujala, U. M. (2016). Long-term physical activity modulates brain processing of somatosensory

stimuli: Evidence from young male twins. *Biological Psychology,* doi:S0301-0511(16)30029-1 [pii]

Tarkka, I. M., & Treede, R. D. (1993). Equivalent electrical source analysis of pain-related somatosensory evoked potentials elicited by a CO2 laser. *Journal of Clinical Neurophysiology : Official Publication of the American Electroencephalographic Society, 10*(4), 513-519.

Tesarz, J., Gerhardt, A., Schommer, K., Treede, R. D., & Eich, W. (2013). Alterations in endogenous pain modulation in endurance athletes: An experimental study using quantitative sensory testing and the cold-pressor task. *Pain, 154*(7), 1022-1029. doi:10.1016/j.pain.2013.03.014 [doi]

Waller, K., Kaprio, J., & Kujala, U. M. (2008). Associations between long-term physical activity, waist circumference and weight gain: A 30-year longitudinal twin study. *International Journal of Obesity (2005), 32*(2), 353-361. doi:0803692 [pii]

Figure Legends

Fig. 1. SMMR grand average wave forms of deviant stimuli in inactive (A) and active (B) co-twins. All 128 channels are superimposed, average reference is used and topographic voltage distribution maps are shown as 10 ms mean values at selected time points (86-96ms, 148-158ms, 252-262 ms and 280-290 ms), where later equivalent dipole source analysis indicated significant differences between co-twins. 0 is the onset of stimulation.

Fig. 2. Seven-dipole source model generated from grand average deviant waveform and presented in average MR image in sagittal (A) and verticofrontal (B) planes. Six dipoles are visible in these depicted planes, one dipole accounting for eye movement activity is not visible here. SD1=red, SD2=light purple, SD3=green, SD4=magenta, SD5=brown, SD6=blue. See Table 2 for three-dimensional source location coordinates.

Fig. 3. Source moments (not ERPs) of the developed source model explaining deviant data sets and detected significant differences between groups are shown: Source SD2 for deviant (first from left, light purple in Fig. 2), difference during 280-290 ms from stimulus onset, Source SD3 for deviant (second from left, green in Fig. 2), difference during 148-158 ms from stimulus onset, Source SD4 for deviant (third from left, magenta in Fig. 2), differences during 86-96 and 252-262 after stimulus onset. Standard stimuli data were also modeled and source SD6 (fourth from left, light blue in Fig. 2) shows standard stimulus data sets where difference during 252-262 ms after stimulus onset was found. Significant differences are indicated with gray bars and zero time-point is the stimulus onset.

Fig. 4. The WFU Atlas regions of interest (ROIs), which were initially suggested by the spatio-temporal source model, were used in analysing possible structural differences in

individual MR images between inactive and active co-twins. ROIs have been rendered on cortical surface in such a way that the stronger colours indicate more superficial locations, whereas weaker colours indicate more deeper regions.

Fig. 5. Structural MR images of co-twins differed in GM voxel count in right anterior cingulate ROI. Only the above ROI shown in green gave higher GM voxel count in inactive co-twins.

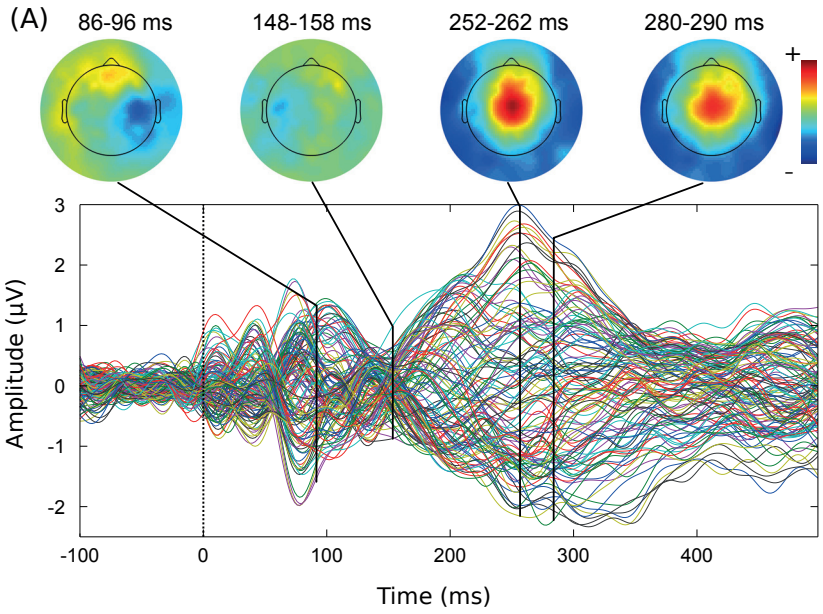
(A)
86-96 ms
148-158 ms
252-262 ms
280-290 ms
+
-
Amplitude (μV)
3
2
1
0
-1
-2
-100
0
100
200
300
400
Time (ms)

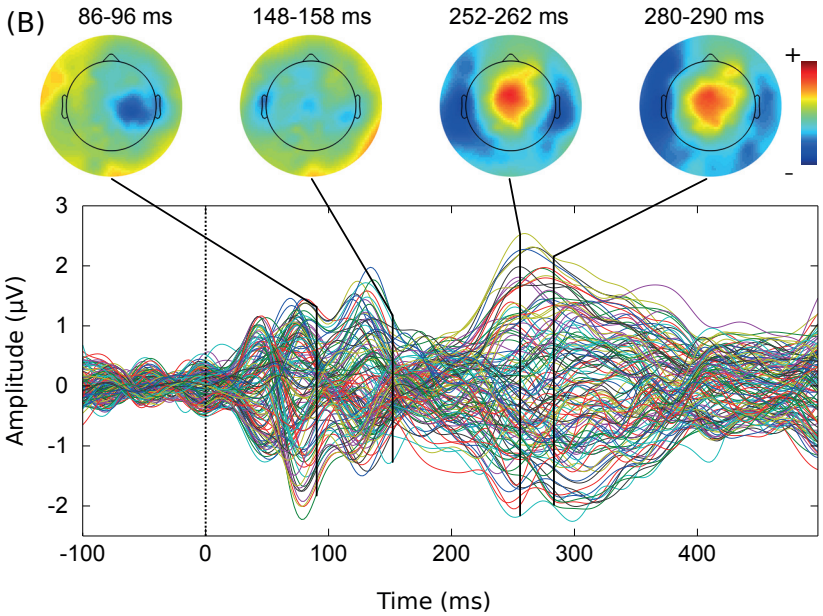
(B)
86-96 ms
148-158 ms
252-262 ms
280-290 ms
+
-
Amplitude (μV)
3
2
1
0
-1
-2
-100
0
100
200
300
400
Time (ms)

Figure 2

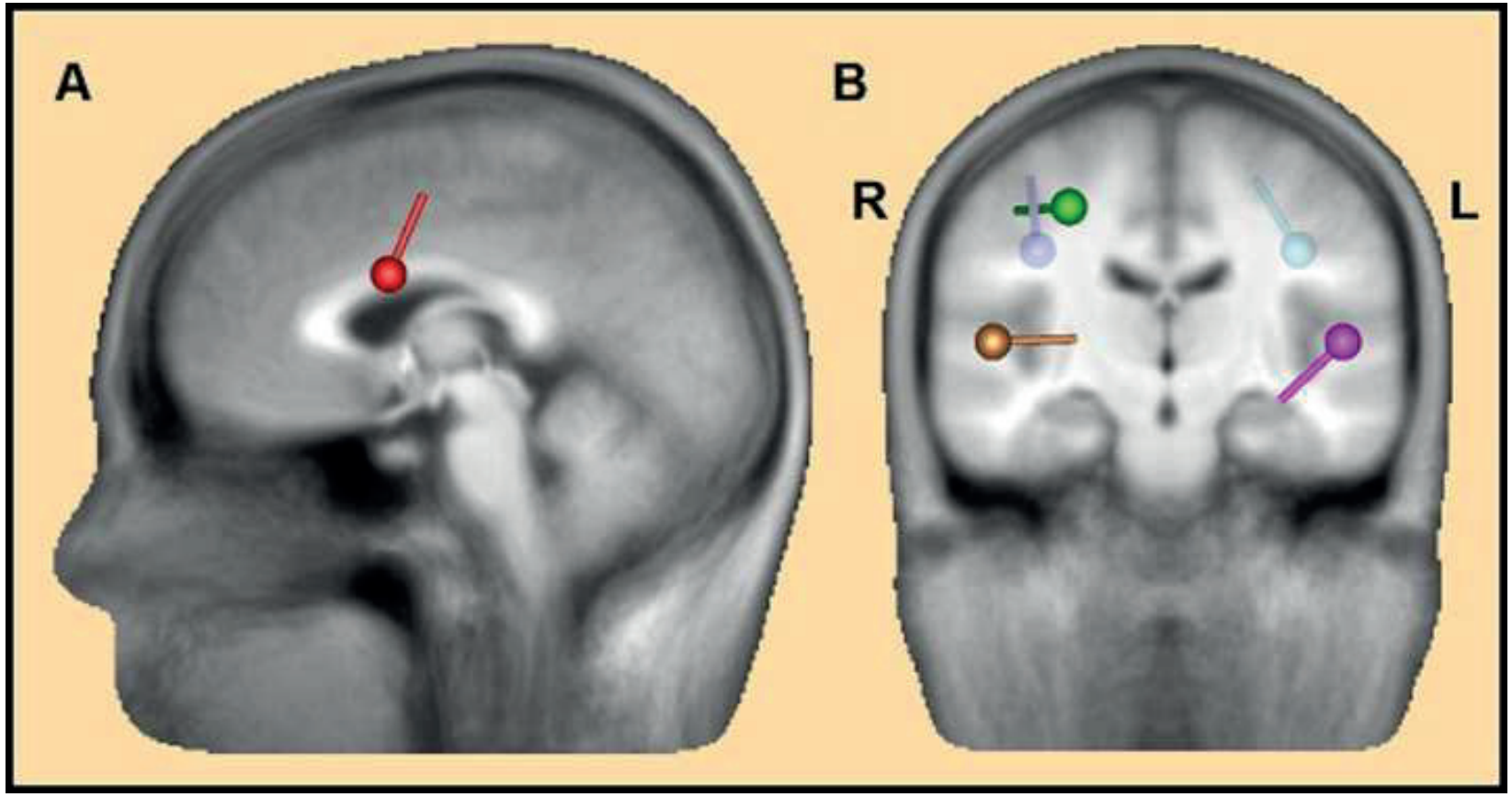

Figure 3

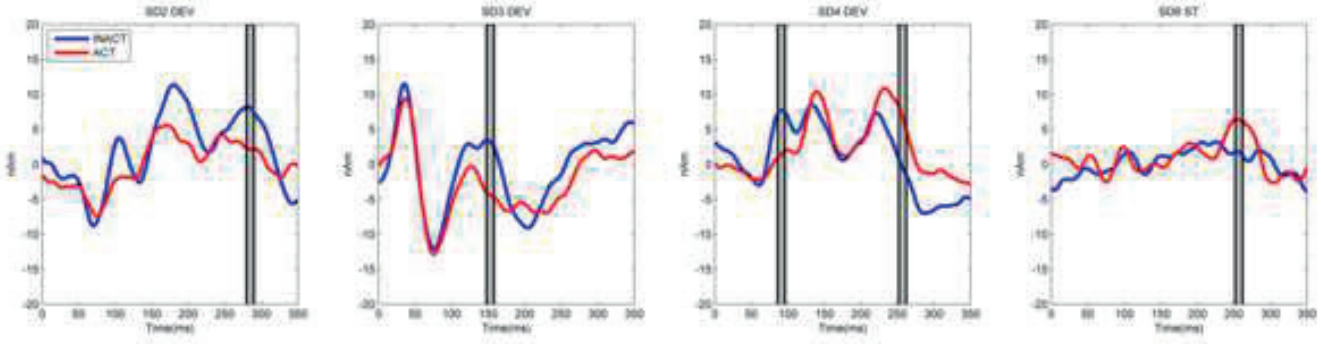

Figure 4

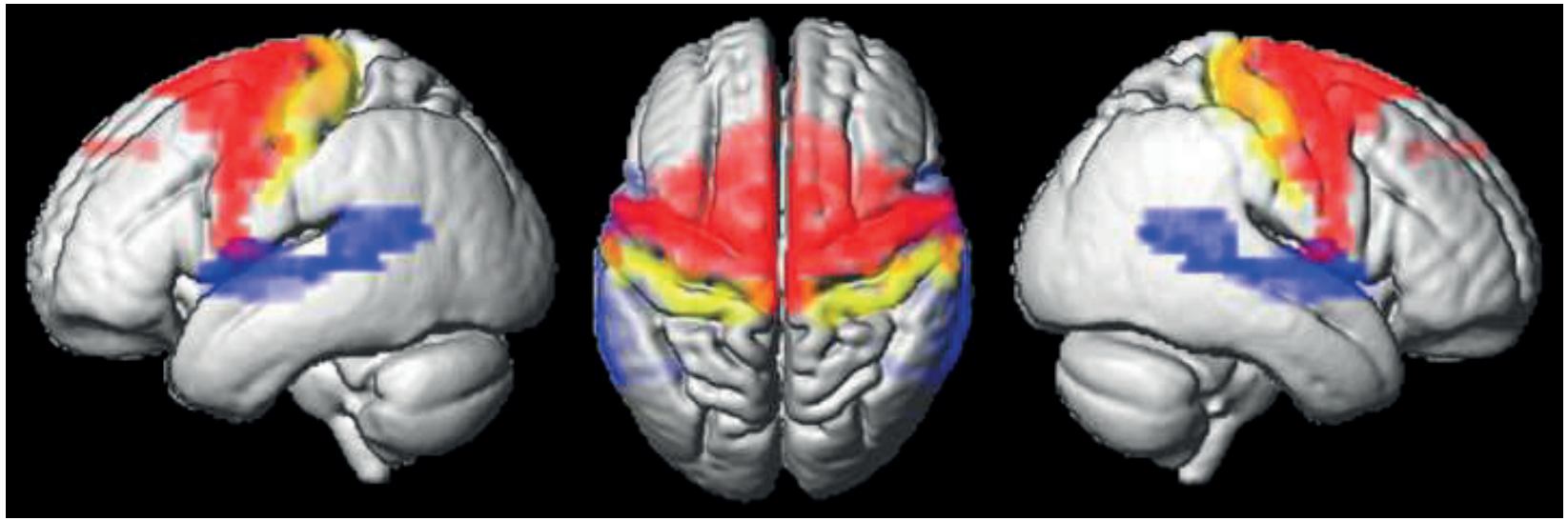

Figure 5

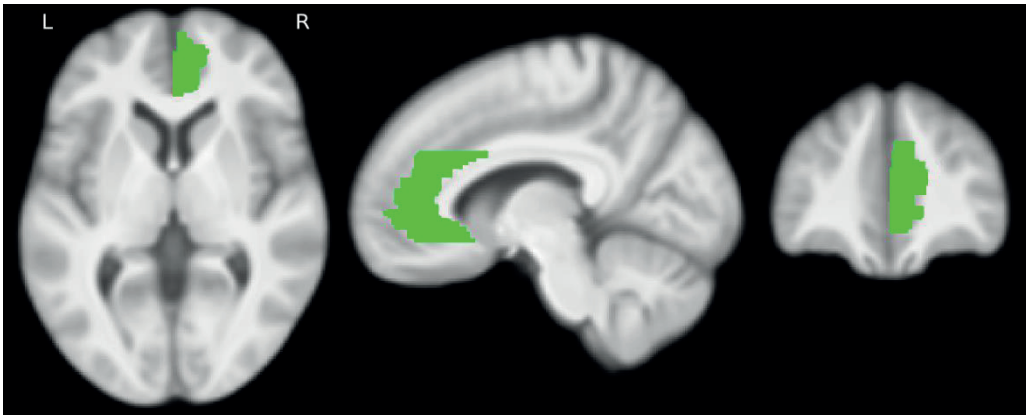

Table 1

Table 1. Participant characteristics, 18 individuals (9 monozygotic male twin pairs), means and (±SD).

	Inactive co-twin	**Active co-twin**	**p-value[#]**
Age, y	34.3 (1.4)	34.1 (1.5)	0.686
Height, cm	178.5 (5.3)	179.7 (5.7)	0.012*
Weight, kg	78.0 (13)	75.9 (9)	0.424
BMI	24.3 (3)	23.4 (2)	0.269
Fat%	23.8 (5)	20.3 (4)	0.040*
Waist circ., cm	88.7 (9)	85.2 (7)	0.123
VO_2max, ml/kg/min	37.2 (3.5)	43.1 (4)	0.008**
3-yr-MET	1.4 (1.0)	4.5 (2.1)	0.003***
SMMR standards, n	92 (7)	90 (10)	
SMMR deviants, n	91 (6)	90 (8)	
GM volume, ml	668.3 (31)	675.3 (38)	0.815
WM volume, ml	685.0 (49)	696.1 (41)	0.606
CSF volume, ml	229.0 (36)	227.6 (39)	0.963
Ant. cingulate, voxel	544 (9)	536 (12)	0.046*[≀]

[#] Mann-Whitney U-test. *p<.05 **p<.01 ***p<.005

[≀] Wilcoxon Signed Rank -test

Table 2

Table 2. Source location coordinates of the source model generated for the grand average deviant wave form of the active twins. Six equivalent electrical source dipoles (SD) localized in the brain and seventh dipole modeled the remaining eye movements (after eye movement correction). Approximate brain regions are given in Talairach labels and Brodmann areas are in parenthesis.

Fitting window Component	**Source location (x, y, z)**	**Brain region, Talairach (Brodmann Area)**
SD 1	2.9, 24.6, 54.5	Ventral anterior cingulate (R) (BA 24)
SD 2	32.7, -6.5, 65.5	Postcentral gyrus (R) (BA 3)
SD 3	24.8, 9.9, 74.6	Frontal medial gyrus (R) (BA 6)
SD 4	-43.8, 3.7, 38.6	Superior temporal gyrus (L) (BA 22)
SD 5	43.8, 3.7, 38.6	Superior temporal gyrus (R) (BA 22)
SD 6	-32.7, -6.5, 65.5	Postcentral gyrus (L) (BA 3)
SD 7	30.1, 66.5, 6.2	-

Table 3

Table 3. Four regions of interest (ROI) in each hemisphere were selected and compared from whole brain structural MR images of the brains of co-twins. The gray matter voxel counts in ROIs were compared between inactive and active individuals within each twin pair using Wilcoxon Signed Rank Test. For the ROIs Brodmann areas are given in parenthesis after Talairach labels. Note, that only right anterior cingulate shows a difference.

Brain region Talairach, right	p-value	Brain region Talairach, left	p-value
Anterior cingulate (BA24)	0.046*	Anterior cingulate (BA24)	0.612
Postcentral gyrus (BA3)	0.204	Postcentral gyrus (BA3)	0.401
Frontal medial gyrus (BA6)	0.270	Frontal medial gyrus (BA6)	0.574
Superior temporal gyrus (BA22)	0.262	Superior temporal gyrus (BA22)	0.575

*$p<0.05$

II

DETECTING DIFFERENCES WITH MAGNETOENCEPHALOGRAPHY OF SOMATOSENSORY PROCESSING AFTER TACTILE AND ELECTRICAL STIMULI

by

Hautasaari, P., Kujala, U. M. & Tarkka, I. M. 2019.

Journal of Neuroscience Methods 311, 331-337

Journal of Neuroscience Methods 311 (2019) 331–337

Contents lists available at ScienceDirect

Journal of Neuroscience Methods

journal homepage: www.elsevier.com/locate/jneumeth

Detecting differences with magnetoencephalography of somatosensory processing after tactile and electrical stimuli

Pekka Hautasaari[a,b,*], Urho M. Kujala[a], Ina M. Tarkka[a,b]

[a] Health Sciences, Faculty of Sport and Health Sciences, University of Jyväskylä, Jyväskylä, Finland
[b] Jyväskylä Centre for Interdisciplinary Brain Research, University of Jyväskylä, Jyväskylä, Finland

ARTICLE INFO

Keywords:
Functional brain imaging
Human sensory cortex
Mismatch response
Cutaneous nerve stimulation
Tactile stimulation

ABSTRACT

Background: Deviant stimuli within a standard, frequent stimulus train induce a cortical somatosensory mismatch response (SMMR). The SMMR reflects the brain's automatic mechanism for the detection of change in a somatosensory domain. It is usually elicited by electrical stimulation, which activates nerve fibers and receptors in superficial and deep skin layers, whereas tactile stimulation is closer to natural stimulation and activates uniform fiber types. We recorded SMMRs after electrical and tactile stimuli.

Method: 306-channel magnetoencephalography recordings were made with 16 healthy adults under two conditions: electrical (eSMMR) and tactile (tSMMR) stimulations. The SMMR protocol consisted of 1000 stimuli with 10% deviants to fingers.

Results: Sensor-level analysis revealed stronger activation after deviant stimulation in bilateral channel locations approximately corresponding to parietal cortical areas within both stimulation conditions. Between conditions, deviant tSMMR showed stronger activation in the ipsilateral channels. Based on sensor-level results, two components, M50 and SMMR (40–58 and 110–185 ms), were compared at the source-level. Deviant stimulation elicited stronger contralateral SI activation during M50 component in both conditions. SMMR was observed with both conditions, activating contralateral SII after deviant stimulation. However, only tSMMR showed long latency activation in bilateral SI cortices. This suggests that there is an integration of both body sides during the automatic stages of tactile processing in SI cortices.

Conclusions: This study indicates that tactile stimulation (tSMMR) is a feasible method for investigating the brain's mechanism for detecting somatosensory changes; this may extend the clinical utility of tSMMR for assessing disorders involving altered somatosensory processing.

1. Introduction

Mismatch negativity (MMN) reflects the activation of a cortical automatic mechanism capable of detecting small changes in the sensory environment (Näätänen, 1992). Furthermore, within the predictive coding theory, it has been interpreted as reflecting early sensory information processing from the environment (Garrido et al., 2009). MMN has been most extensively studied in the auditory domain (Näätänen et al., 2007) and to some extent in the visual domain (Pazo-Alvarez et al., 2003) with an oddball stimulus paradigm such that, within a frequent standard stimulus train, an infrequent stimulus elicits the MMN response. Corresponding to the extensively studied MMN in the auditory domain, deviant somatosensory stimuli (e.g. electrical or tactile) within a standard, frequent stimulus train induces a cortical somatosensory mismatch response (SMMR) in adults (Akatsuka et al., 2005, 2007a; Kekoni et al., 1997; Shinozaki et al., 1998) and also in children (Restuccia et al., 2009). In older adults, the characteristics of the SMMR have been investigated; they are reported to display an attenuated amplitude with a prolonged latency (Strömmer et al., 2014) indicative of age-related changes in the somatosensory change detection mechanism. Here, we will use the term somatosensory mismatch response (SMMR), instead of mismatch negativity, as it encompasses the mismatch phenomenon regardless of the measurement method (e.g. EEG or MEG).

In the somatosensory domain, the SMMR is frequently reported to occur about 100–200 ms after stimulus onset, with the deviant stimulus evoking stronger brain activation than a standard stimulus (Akatsuka et al., 2005; Kekoni et al., 1997; Shinozaki et al., 1998). An earlier component within the 30–70 ms time window has also been reported to exhibit stronger activation after deviant stimulation (Akatsuka et al.,

* Corresponding author at: Faculty of Sport and Health Sciences, University of Jyväskylä, P.O. Box 35, FI-40014, Finland.
E-mail address: pekka.t.hautasaari@student.jyu.fi (P. Hautasaari).

https://doi.org/10.1016/j.jneumeth.2018.09.014
Received 11 June 2018; Received in revised form 10 September 2018; Accepted 10 September 2018
Available online 12 September 2018

2007a, b; Shinozaki et al., 1998). Akatsuka et al. (2005) speculated that this earlier component may be enhanced during tasks that subjects can clearly discriminate with the long latency enhanced component becoming generated during tasks which require fine discrimination between the sensory stimuli. The generation of somatosensory mismatch responses has been observed in the primary (SI) and secondary (SII) somatosensory cortices in studies using magnetoencephalography (MEG) (Akatsuka et al., 2007b; Naeije et al., 2018).

Previous studies investigating mismatch response processing among different domains in the brain (Downar et al., 2000; Zhao et al., 2015) have detected domain-specific processing in the primary and secondary cortices in a given sensory domain (e.g. auditory, visual or somatosensory) however, any stimulus comparison within a domain is uncommon. SMMR has been mostly elicited using electrical stimulation and instead studies with different types of somatosensory stimuli are limited, although a few investigators have applied mechanical vibratory stimuli (Kekoni et al., 1997; Spackman et al., 2007) and more recently pneumatic tactile stimuli (Naeije et al., 2018, 2016; Shen et al., 2017) revealing that SMMR can be elicited within the somatosensory domain with different types of stimuli.

Electrical stimulation activates large numbers of receptors and nerve fibers with varying conduction velocities in both the superficial and deep layers of the skin (Forss et al., 1994; Gandevia et al., 1982; Kimura, 2001) and this may produce discomfort in some subjects. However, subjects are more likely to tolerate tactile stimuli and these may be closer to the natural stimuli capable of activating more uniform fiber types (Pratt et al., 1979). An additional and important advantage of mechanical tactile stimulation is its compatibility with registration methods which have a low tolerance of electromagnetic fields e.g. fMRI or MEG (Kawohl et al., 2007). Our aim was to study the feasibility of applying tactile stimulation in order to reliably detect SMMR cortical processing. Furthermore, we wanted to investigate the features of the mechanism involved in the automatic change detection in the human brain to somatosensory stimulations by comparing electrical and tactile stimuli. A better understanding of somatosensory processing, electrical or tactile, may reveal new ways to clarify the underlying mechanisms in those disorders in which sensory processing is severely disturbed.

2. Materials and methods

2.1. Subjects

The study was approved by the Local Ethics Committee (3.12.2015) and conducted in accordance with the Declaration of Helsinki. All subjects gave written informed consent prior to participation. Sixteen healthy volunteers (see Table 1 for the characteristics of the participants) were recruited into the study. All subjects were right-handed and they had no history of neurological or psychiatric diseases or alcoholic or narcotic addictions. All subjects filled the RBDI mood questionnaire (Raitasalo, 2007), a depression scale developed for use in Finland based on the short version of the Beck Depression Inventory (Beck et al., 1961) to exclude any depressive and/or anxiety symptoms. Before the magnetoencephalographic (MEG) recording, a short recording was conducted with each subject to ensure that no magnetic objects were present in the head or upper body which could generate artifacts or contaminate the MEG recording.

Table 1
Participant characteristics, 16 individuals (10 men, 6 women) means, (± SD) and range.

	Mean	SD	Range
Age, year	28.7	4.7	18–36
Body Mass Index, BMI	23.4	3.2	19.9–30.7
Stimulus intensity in electrical stimulation, 2nd finger, mA	4.9	1.0	3–7
Stimulus intensity in electrical stimulation, 5th finger, mA	4.1	0.9	3–6
Analysed standard electrical stimulations, n	86	13.0	52–99
Analysed deviant electrical stimulations, n	86	12.2	58–99
Analysed standard tactile stimulations, n	82	13.5	49–99
Analysed deviant tactile stimulations, n	81	15.3	39–99

2.2. Experimental design

2.2.1. Electrical stimulation

The somatosensory mismatch response (SMMR), an automatic location deviance detection, was elicited under two conditions. In condition I (eSMMR), electrical stimuli were delivered (DeMeTec SCG30, DeMeTec GmbH, Langgöns, Germany) to the right index and little fingers through flexible non-magnetic metal ring electrodes (Technomed Europe Ltd., Maastricht, the Netherlands), placed above the distal and proximal phalanges in each finger. The stimulus was a monophasic square-wave current pulse of 0.2 ms duration. The intensity was set separately for each finger in collaboration with the participant to a level where a clear but comfortable sensation was perceived in both fingers, nevertheless the intensity was always set to a minimum of 120% of the sensory threshold (see Table 1 for mean electrical stimulation intensities). A stimulus delay of 3 ms was detected from the stimulus artefact and this was taken into account in the data analysis.

2.2.2. Tactile stimulation

In condition II (tSMMR), tactile stimuli were applied to the distal phalanges of the right index and little fingers. The stimulus locations were as close as possible to those used to elicit eSMMR. Tactile stimuli were generated with an air-pressure stimulator built in-house producing a 0.4 bar pressure pulse delivered through a plastic tube of 5 mm diameter. Air pressure inflated plastic membranes (surface area 2.0 cm^2) at the end of the tubes producing a clear tactile sensation on the fingertip. The stimulus delay was measured to be 21 ms from the trigger to the contact with fingers and this was taken into account in data analysis.

2.2.3. Experimental protocol

The same protocol was followed in both conditions. The somatosensory stimulations were applied in two halves subsequently: in the first half, standard stimuli were presented to the index finger and deviant stimuli to the little finger, and in the second half, the stimulus locations were reversed thus producing a mismatch in location independently from the individual finger activated during the stimulation flow. A total of 1000 stimuli were delivered, of which 10% were pseudo-randomly delivered deviants. The inter-stimulus interval was 500 ms. Participants were asked not to pay attention to the stimuli and instead to focus their gaze on a neutral mark about 1 m in front of them. Table 1 lists the mean number of analyzed stimuli with both conditions.

2.3. MEG recording

The recordings were carried out while the participants were seated in a magnetically shielded room (Vacuumschmelze, GmbH, Hanau, Germany). Eye movements and blinks were recorded with electrooculogram (EOG) with a bandpass filter of 0.1–330 Hz and the gain set to 2000. The participants were instructed to avoid blinking, voluntary eye movements and other unnecessary movements during recording. Five head position indicators (HPI) were placed on the scalp. The HPI coil locations in relation to three anatomical landmarks (nasion and bilateral preauricular points) were registered with a 3-D digitizer (Fastrak®, Polhemus, Vermont, USA) with additional points from the scalp, forehead and nose crest for more accurate representation of the individual head shape prior to the MEG recording. MEG was recorded with the helmet-shaped 306-channel device (Elekta Neuromag®, Triux™, Stockholm, Sweden). MEG signals were recorded using a bandpass filter of 0.1–330 Hz and digitized with sampling frequency of

1000 Hz. MEG and EOG signals were stored for later offline processing and analysis.

2.4. Data analysis

First, Maxfilter software (Elekta Neuromag®, Stockholm, Sweden) was applied using signal space separation (SSS) (Taulu and Simola, 2006; Taulu et al., 2004) in order to detect bad channels automatically as well as reducing artifacts and correcting for head position across participants. Further data preprocessing and analysis was conducted with Statistical Parametric Mapping 12 (SPM12) software (Litvak et al., 2011) available in http://www.fil.ion.ucl.ac.uk/spm running under Matlab 2015a (The Mathworks Inc. Natick, MA, USA).

Next, MEG raw data was converted into SPM12 format. Correction was made for a stimulus delay of 3 ms in electrical stimulation and a delay of 21 ms in tactile stimulation. The total numbers of standard stimulations were 900 in both conditions and from these, 100 stimulations were picked as trials to match the amount of deviant stimuli. In both conditions, all 100 deviant stimulations and 100 standard stimulations preceding each deviant stimulation were selected for further analysis as trials. 100 trials provided an acceptable signal-to-noise ratio. Data was epoched in relation to stimulus triggers including the time window of interest (-100 to 350 ms) with 400 ms buffers to avoid distortions caused by filtering. Data was high-pass filtered at 0.1 Hz, low-pass filtered at 60 Hz and the baseline was corrected using data from -100 to 0 ms in relation to the stimulus triggers. Next, the trials were cropped for the time window of interest from -100 to 350 ms for analysis. EOG artefacts were identified from all trials and those trials with EOG amplitude exceeding 70μV were excluded from further analysis. After preprocessing, the number of trials between standard and deviant stimulations in both conditions did not differ by more than 10 stimulations within each subject. Table 1 provides details of the average trial counts from all subjects. For sensor-level analysis, planar gradiometer channel pairs were combined into one value by taking root mean square (RMS) of the two gradiometers in each sensor location and all surviving trials were averaged. For source analysis, all surviving trials were averaged with 102 magnetometer and 204 planar gradiometer channels.

With preprocessed combined gradiometer data, we proceeded to the sensor-level analysis. In SPM12, scalp-time images were created from each individual average, using a time-window from 0 to 300 ms. Scalp-time images were created in SPM12 by projecting the sensor locations in 2D space and interpolating them, with time serving as the third dimension. These images were used to compare standard and deviant waveforms within each of the conditions and then they were used to compare the deviant waveforms between the two conditions. Differences detected in sensor-level analysis were used for determining the time-windows for comparing standard and deviant stimulations within each of the conditions and deviant stimulations between the conditions at the source-level.

Source models were generated from each subject's averaged trials using all planar gradiometers and magnetometers in both conditions. Source modelling was done with SPM12 group inversion. Since no individual MR images were available, an anatomy template (MNI brain) provided by SPM12 was used for head model with a cortical mesh size of 8196 vertices. According to MEG guideline recommendations (Gross et al., 2013), an accurate digitization of the individual head shape is an appropriate method for further source location analysis of electromagnetic activity. This shape can be used, instead of the individual MRI, to approximately align the subject's head to a template head (Holliday et al., 2003) to allow for averaging across subjects. Anatomy templates were aligned for each subject with the HPI data collected before the MEG recording (Darvas et al., 2006). The forward model was computed as a single sphere and inverse reconstruction was performed with SPM12 multiple sparse priors (MSP) method for the whole trial time window from -100 to 350 ms. The obtained source models explained 97.42 and 97.29 percent of variances in electrical and tactile responses, respectively. Lastly, source modelling results from each individual and from both conditions were transformed into cortical mesh/surface (GIfTI) images for statistical analysis summarizing average activity from two time windows: 40–58 ms and 110–185 ms. These time windows were established already in the sensor level analysis.

2.5. Statistical analysis

Statistical analysis was performed with SPM12 software as a regional field strength analysis. All group analysis of the MEG data was performed first at the sensor-level and subsequently in source space. Group level differences within and between conditions were detected by statistical analysis in SPM12 using paired samples t-test. The height threshold was set to $p < 0.001$ (uncorrected for multiple comparisons). Clusters surviving the primary threshold were regarded as significant when falling below FWE-corrected cluster-level threshold of 0.05. No minimum cluster size was determined.

3. Results

Sensor-level analysis of the whole time window from 0 to 300 ms

Table 2
Statistical results from sensor-level analysis.

	Cluster-level p-value[d] FWE-corr.	voxels per cluster	Peak-level p-value[d] FWE-corr.	T	Z	Peak coordinates and cluster peak time in scalp-time images (mm, mm, ms)[e]
Electrical	< 0.001	704	0.038	8.21	4.98	−26, 8, 45
deviant > standard [a,b,c,g]	< 0.001	2630	0.317	6.34	4.36	−21, 2, 126
	0.002	403	0.523	5.84	4.15	43, -3, 167
Tactile	< 0.001	5065	0.009	9.40	5.31	55, 24, 165
deviant > standard [a,b,c,g]			0.023[f]	8.53	5.08	47, 40, 162
	< 0.001	6633	0.032	8.23	4.99	−34, 24, 166
	0.145	160	0.047	7.90	4.89	−17, 13, 48
Tactile deviant > Electrical deviant [a,b,c,g]	< 0.001	2230	0.091	6.72	4.50	38, 2, 147

[a] Degrees of freedom = 15, Voxel size 4.3 mm 5.4 mm 1.0 ms.
[b] Volume 239,596 voxels.
[c] Height threshold T = 3.73, p = 0.001 (unc.).
[d] p-values adjusted for search volume.
[e] Coordinates projected to 2D plane with time as the third dimension.
[f] Two separate statistically significant peaks within cluster.
[g] > indicates direction of stronger activation.

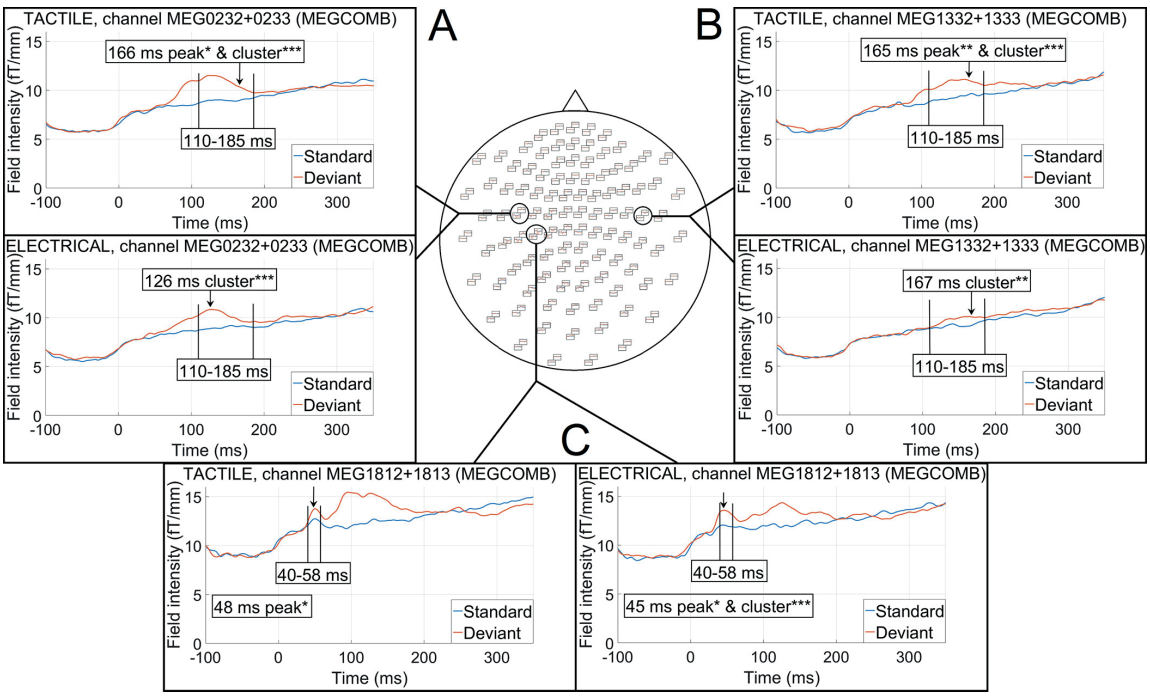

Fig. 1. Grand average RMS combined gradiometer waveforms from representative channels for both conditions illustrating differences between deviant and standard stimulations. The locations of the representative channels approximately correspond to contra- and ipsi-lateral parietal cortical areas. Arrows indicate cluster and/or peak-level time points of statistical differences. Vertical lines illustrate the time windows, determined for source-level analysis, enclosing early latency contralateral (C) and long-latency bilateral (A & B) waveform components. (*$p < 0.05$, **$p < 0.01$ & ***$p < 0.001$).

revealed differences within both conditions between standard and deviant stimulations (Table 2). Our analysis method indicated peak cluster time points showing differences within major waveform components. Fig. 1 shows grand average RMS gradiometer waveforms from representative channels illustrating these differences within conditions between deviant and standard stimulations. Electrical stimulation revealed three clusters in channel locations approximately corresponding to the parietal cortical area whereas deviant stimulation showed stronger activation than standard stimulation in contralateral channels around the 45 ms and 126 ms peak cluster time points, and in the ipsilateral channels at around the 167 ms time point. At the 45 ms time point, also a peak-level difference in the contralateral channels was detected. Tactile stimulation revealed two clusters also in channel locations approximately corresponding to the parietal cortical area where deviant stimulation showed stronger activation than standard stimulation in the bilateral channels. Ipsilateral channels revealed two peak-level differences at 162 ms and 165 ms and on the contralateral side at 166 ms. The contralateral channels revealed a peak-level difference at the 48 ms time point however, the corresponding cluster did not reach a difference that was statistically significant. Further comparisons between the conditions detected differences after deviant stimulation, where tactile stimulation revealed one cluster with stronger activation in the ipsilateral channels around the 147 ms time point.

Based on the sensor-level differences, the time windows enclosing the two main waveform components were determined from 40 ms to 58 ms and from 110 ms to 185 ms (Fig. 1) for source-level analysis. Source-level analysis revealed within and between condition differences, which are summarized in Table 3. During the 40–58 ms time window, deviant stimulation showed one cluster with stronger activation than in standard stimulation in the contralateral SI cortex in both conditions. However, there were no differences between the conditions in this time window. The long-latency time window 110–185 ms showed within condition differences when comparing the deviant and standard stimulations. Electrical stimulation revealed one cluster with a stronger activation after the deviant stimulation in the contralateral SII cortex. Tactile stimulation showed three clusters with stronger activation after the deviant stimulation in the contralateral SII cortex and bilateral SI cortices. In the comparison of deviant stimulations between the conditions, tactile stimulation showed two clusters with stronger activation than was observed with the electrical stimulation in bilateral SI cortices. Fig. 2 illustrates the differences in brain activity during the time windows 40–58 ms and 110–185 ms within and between conditions.

4. Discussion

In the present study, we investigated the features of automatic somatosensory change detection system after two different stimulus types. Our study demonstrates the feasibility of using tactile stimulation in reliably detecting SMMR, with differences in the source level activation when compared to electrical stimulation. Both tactile and electrical deviant stimulation elicited the early latency component (M50) within the 40–58 ms time window in the contralateral SI cortex and the somatosensory mismatch response component (SMMR) within the 110–185 ms time window in the SI and SII cortices. The difference between stimulation types emerged after deviant stimulation, where the SI cortex was active bilaterally during the SMMR component after tactile stimulation.

In the present study, while differing in the type of stimulus being delivered, both conditions elicited somatosensory mismatch responses. As compared to the early M50 component observed in the present study, there are previous reports of a similarly enhanced early

Table 3
Statistical results from source-level analysis.

	Cluster-level p-value[d] FWE-corr.	vertices per cluster	Peak-level p-value[d] FWE-corr.	T	Z	Peak MNI coordinates within cluster
Electrical deviant > standard 40–58 ms [a,b,c,e]	0.005	46	0.353	4.21	3.37	−48, −38, 45
Tactile deviant > standard 40–58 ms [a,b,c,e]	0.003	55	0.243	4.45	3.50	−38, −39, 39
Electrical deviant > standard 110–185 ms [a,b,c,e]	0.025	34	0.080	5.23	3.89	−60, −44, 27
Tactile deviant > standard 110–185 ms [a,b,c,e]	0.019	37	0.174	4.69	3.62	−62, −44, 29
	0.034	31	0.348	4.17	3.35	−43, −23, 38
	0.034	31	0.371	4.12	3.32	44, −23, 39
Tactile deviant > Electrical deviant 110–185 ms [a,b,c,e]	0.049	30	0.190	4.54	3.54	−43, −23, 38
	0.045	31	0.202	4.49	3.52	44, −23, 39

[a] Degrees of freedom = 15.
[b] Volume 8196 vertices.
[c] Height threshold T = 3.73, p = 0.001 (unc.).
[d] p-values adjusted for search volume.
[e] > indicates direction of stronger activation.

component occurring after deviant stimulus either regarding latency (Akatsuka et al., 2005, 2007a; Shinozaki et al., 1998) or source location in the contralateral SI cortex (Akatsuka et al., 2007b). The SMMR component latencies in both conditions in the present study were similar and corresponded well with previous reports (Akatsuka et al., 2005; Kekoni et al., 1997; Shinozaki et al., 1998; Strömmer et al., 2014) occurring within the 110–185 ms time window. The source analysis revealed an active source location for the SMMR component in both conditions in the contralateral SII cortex and this finding is consistent with previous studies (Akatsuka et al., 2007b; Naeije et al., 2018). Interestingly, in addition to the contralateral SII activation, tactile stimulation elicited bilateral SI cortex activation during the SMMR component. It is well known that the SI cortex receives stimuli from the contralateral side of the body but previous research has suggested that also the ipsilateral SI cortex is involved in bilateral integration of tactile stimuli (Tamè et al., 2016). The recent review of Tamè et al. (2016) emphasized the importance of the concept that there is already an early bilateral involvement of the SI cortex in tactile processing.

Similarly to our results, Akatsuka et al. (2007a; 2007b) also reported contralateral SI activation, in addition to contralateral SII, occurring during the late component within the 150–250 ms time window. Although they used a single dipole model and only the strongest generator was selected as the source in either SI or in SII in individual subjects, they concluded that two or more sources may generate the late component (Akatsuka et al., 2007a). Late SI activation around or later than the 100 ms post-stimulus has also been observed previously, e.g. in Otsuru et al. (2011) after the intensity change in electrical pulse trains as well as in Allison et al. (1989), where intracortical SEP recording revealed long-latency contra- and ipsi-lateral SI activations. Korvenoja et al. (1995) observed ipsilateral late sensorimotor cortex activation after electrical median nerve stimulation and after mechanical tactile stimulation as reported by Hadoush et al. (2010). In particular, the ipsilateral SI cortex activation has been elusive to record after somatosensory stimulation possibly either due to interindividual variability or due to weaker responses generated at the ipsilateral SI that might be masked by larger amplitude responses from

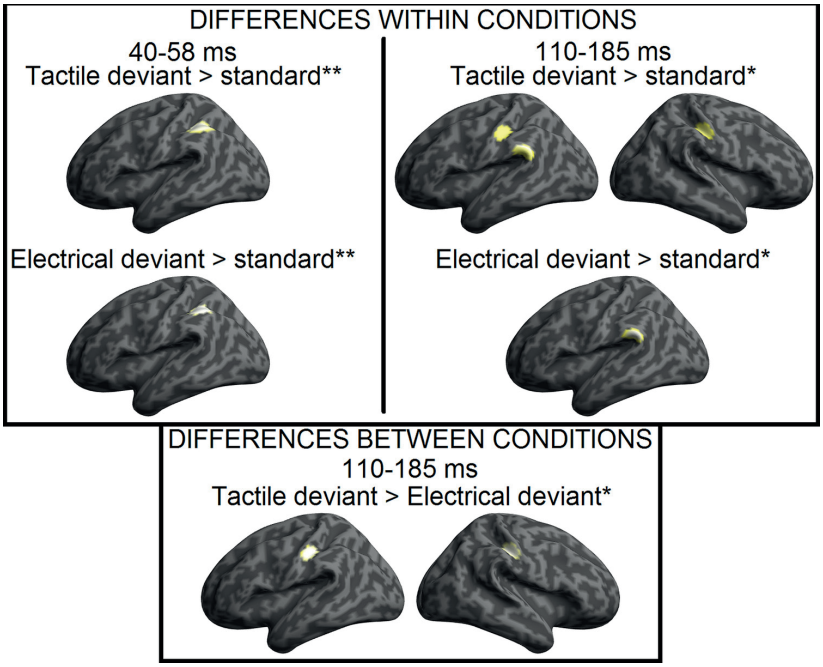

Fig. 2. Differences in brain activation within conditions showing significantly different activation in the contralateral SI cortex during the 40–58 ms time window after tactile and electrical deviant stimulations, respectively, compared to standard stimulation. During the 110–185 ms time window as compared to standard stimulation, tactile deviant stimulation evoked significantly different brain activations in bilateral SI and contralateral SII cortex while electrical deviant stimulation showed significantly different activation in the contralateral SII cortex. Differences between conditions, as shown in the lower part of the figure, revealed the significantly different activation in the bilateral SI cortices during the 110–185 ms time window after tactile deviant stimulation when comparing deviant stimulations between conditions. (> in figure indicates the direction of the stronger activation. *p < 0.05, **p < 0.01 & ***p < 0.001).

the ipsilateral SII (Allison et al., 1989; Korvenoja et al., 1995). Hadoush et al. (2010) reported similar results as found here with differences in the activated brain areas between mechanical tactile and electrical stimulation and they hypothesized that the ipsilateral SI activation could be recorded more consistently after mechanical tactile stimulation in contrast with electrical stimulation due to the more selective tactile sensory input. Whereas tactile stimuli activate more uniform fiber types (Pratt et al., 1979), electrical stimulation activates a large number of fiber types with different conduction velocities (Forss et al., 1994; Gandevia et al., 1982; Kimura, 2001).

Our results indicate that tactile stimulation is a feasible method for investigating the somatosensory change detection system. In addition to basic research conducted with healthy individuals, the exploitation of tactile stimulation could be beneficial in the investigation of disorders manifesting with sensory deficits, e.g. reduced tactile acuity in chronic neck pain (Harvie et al., 2018), sensory processing deficits in multiple sclerosis (Arpin et al., 2017) and impaired tactile processing in the autism spectrum disorder (Puts et al., 2014; Tavassoli et al., 2016). Although mismatch negativity studies have reported changes in the automatic change detection system usually manifesting as an attenuated auditory MMN amplitude in diverse disorders (e.g. in dyslexia, autism and Parkinson's disease), the possibilities of applying somatosensory MMR in clinical studies have been under-utilized (Näätänen, 2009). However, Restuccia et al. (2007) have identified abnormal SMMRs in patients with cerebellar damage. Furthermore, Chen et al. (2018) recently demonstrated abnormal somatosensory mismatch negativity in cervical dystonia patients while their auditory mismatch negativity was normal as compared to healthy controls. This finding reinforces the value of using domain specific experimental tools e.g. the somatosensory experimental paradigm in disorders presenting with somatosensory domain pathologies. The practical advantages of tactile stimulation are its compatibility with imaging methods that have a low tolerance to electromagnetic fields, such as fMRI and MEG, the lack of stimulus-related artifacts; it may also be more tolerable e.g. to small children as well as being more reminiscent of natural stimuli (Kawohl et al., 2007).

Somatosensory mismatch responses are influenced by many different parameters in somatosensory stimulation paradigm. Our stimulation paradigm, involving temporal, location and probability parameters, ensured that the two stimulation points could be automatically discriminated. Akatsuka et al. (2005) applied their paired pulse stimulation paradigm and speculated that a sufficient temporal difference, during which the two stimuli could be clearly discriminated, was needed to elicit the enhanced N60 component. In their subsequent studies, Akatsuka et al. (2007b) state that with respect to stimulus location, the somatosensory mismatch response did not depend on the distance between the two stimulus points as long as the two points could be automatically discriminated and furthermore, the deviant stimulus probability at 10% induced larger components at 30–70 ms and 150–250 ms as compared to a more frequent probability at 30% or 50% (Akatsuka et al., 2007a). However, it would be advantageous to conduct further research with a wider variety of stimulus parameters e.g. stimulus frequency or intensity and to utilize more sophisticated analysis methods. For example, it could be beneficial to investigate connectivity between active brain areas as this could clarify the reasons for the differences between processing of different stimulus types. The lack of individual structural MR images in our data limits the accuracy of the source localization at the level of cytoarchitectonic areas however, according to MEG recording and reporting guidelines (Gross et al., 2013, see Materials and Methods section 2.4) digitization of individual head shapes can be used with MRI templates to allow the localization of the distinct source activity.

In conclusion, our data shows that tactile stimulation is a feasible method for reliably detecting SMMR and further for elucidating the somatosensory change detection system while producing somewhat similar brain activations as the more often used electrical stimulation. Tactile stimulation elicited a larger number of active brain areas during the SMMR component than electrical stimulation as it elicited bilateral SI activation, in addition to contralateral SII activation, possibly due to more selective sensory input by tactile stimulation. Increasing our understanding of the somatosensory processing may help to reveal the mechanisms underlying the altered sensory processing present in several disorders. Tactile stimulation could be a beneficial method for studying patient groups with altered sensory processing since, as compared to electrical stimulation, it may be more tolerable and patient-friendly as well as being closer to natural tactile stimulation.

Declarations of interest

None of the authors have potential conflicts of interest to be disclosed.

Acknowledgements

We wish to thank the Jyväskylä Centre for Interdisciplinary Brain Research, University of Jyväskylä, Jyväskylä, Finland, for providing the MEG facilities. This work was supported by the Juho Vainio Foundation, Helsinki, Finland (201410296), Ministry of Education and Culture, Helsinki, Finland (OKM/56/626/2013) and Jenny & Antti Wihuri Foundation, Helsinki, Finland (00170073).

References

Akatsuka, K., Wasaka, T., Nakata, H., Inui, K., Hoshiyama, M., Kakigi, R., 2005. Mismatch responses related to temporal discrimination of somatosensory stimulation. Clin. Neurophysiol. 116 (8), 1930–1937. https://doi.org/10.1016/j.clinph.2005.04.021.

Akatsuka, K., Wasaka, T., Nakata, H., Kida, T., Kakigi, R., 2007a. The effect of stimulus probability on the somatosensory mismatch field. Exp. Brain Res. 181 (4), 607–614. https://doi.org/10.1007/s00221-007-0958-4.

Akatsuka, K., Wasaka, T., Nakata, H., Kida, T., Hoshiyama, M., Tamura, Y., Kakigi, R., 2007b. Objective examination for two-point stimulation using a somatosensory oddball paradigm: an MEG study. Clin. Neurophysiol. 118 (2), 403–411. https://doi.org/10.1016/j.clinph.2006.09.030.

Allison, T., McCarthy, G., Wood, C.C., Williamson, P.D., Spencer, D.D., 1989. Human cortical potentials evoked by stimulation of the median nerve. II. Cytoarchitectonic areas generating long-latency activity. J. Neurophysiol. 62 (3), 711–722. https://doi.org/10.1152/jn.1989.62.3.711.

Arpin, D.J., Gehringer, J.E., Wilson, T.W., Kurz, M.J., 2017. A reduced somatosensory gating response in individuals with multiple sclerosis is related to walking impairment. J. Neurophysiol. 118, 2052–2058. https://doi.org/10.1152/jn.00260.2017.

Beck, A.T., Ward, C.H., Mendelson, M.M., Mock, J.J., Erbaugh, J.J., 1961. An inventory for measuring depression. Arch. Gen. Psychiatry 4 (6), 561–571. https://doi.org/10.1001/archpsyc.1961.01710120031004.

Chen, J.-C., Macerollo, A., Sadnicka, A., Lu, M.-K., Tsai, C.-H., Korlipara, P., Bhatia, K., Rothwell, J.C., Edwards, M.J., 2018. Cervical dystonia: Normal auditory mismatch negativity and abnormal somatosensory mismatch negativity. Clin. Neurophysiol. 129 (9), 1947–1954. https://doi.org/10.1016/j.clinph.2018.05.028.

Darvas, F., Ermer, J.J., Mosher, J.C., Leahy, R.M., 2006. Generic head models for atlas-based EEG source analysis. Hum. Brain Mapp. 27 (2), 129–143. https://doi.org/10.1002/hbm.20171.

Downar, J., Crawley, A.P., Mikulis, D.J., Davis, K.D., 2000. A multimodal cortical network for the detection of changes in the sensory environment. Nat. Neurosci. 3 (3), 277–283. https://doi.org/10.1038/72991.

Forss, N., Salmelin, R., Hari, R., 1994. Comparison of somatosensory evoked fields to airpuff and electric stimuli. Electroencephalogr. Clin. Neurophysiol. 92 (6), 510–517.

Gandevia, S., Burke, D., McKeon, B., 1982. The relationship between the size of a muscle afferent volley and the cerebral potential it produces. J. Neurology, Neurosurg., Psychiatry 45 (8), 705–710. https://doi.org/10.1136/jnnp.45.8.705.

Garrido, M.I., Kilner, J.M., Stephan, K.E., Friston, K.J., 2009. The mismatch negativity: a review of underlying mechanisms. Clin. Neurophysiol. 120 (3), 453–463. https://doi.org/10.1016/j.clinph.2008.11.029.

Gross, J., Baillet, S., Barnes, G.R., Henson, R.N., Hillebrand, A., Jensen, O., Jervi, K., Litvak, V., Maess, B., Oostenveld, R., Parkkonen, L., Taylor, J.R., van Wassenhove, V., Wibral, M., Schoffelen, J., 2013. Good practice for conducting and reporting MEG research. NeuroImage 65, 349–363. https://doi.org/10.1016/j.neuroimage.2012.10.001.

Hadoush, H., Inoue, K., Nakanishi, K., Kurumadani, H., Sunagawa, T., Ochi, M., 2010. Ipsilateral primary sensorimotor cortical response to mechanical tactile stimuli. NeuroReport 21 (2), 108–113. https://doi.org/10.1097/WNR.0b013e3283349a17.

Harvie, D.S., Edmond-Hank, G., Smith, A.D., 2018. Tactile acuity is reduced in people with chronic neck pain. Musculoskelet. Science Practise 33, 61–66. https://doi.org/10.1016/j.msksp.2017.11.009.

Holliday, I.E., Barnes, G.R., Hillebrand, A., Singh, K.D., 2003. Accuracy and applications

of group MEG studies using cortical source locations estimated from participants' scalp surfaces. Hum. Brain Mapp. 20 (3), 142–147. https://doi.org/10.1002/hbm.10133.

Kawohl, W., Waberski, T.D., Darvas, F., Norra, C., Gobbelé, R., Buchner, H., 2007. Comparative source localization of electrically and pressure-stimulated multichannel somatosensory evoked potentials. J. Clin. Neurophysiol. 24 (3), 257–262. https://doi.org/10.1097/WNP.0b013e3180555e49.

Kekoni, J., Hämäläinen, H., Saarinen, M., Gröhn, J., Reinikainen, K., Lehtokoski, A., Näätänen, R., 1997. Rate effect and mismatch responses in the somatosensory system: ERP-recordings in humans. Biol. Psychol. 46 (2), 125–142. https://doi.org/10.1016/S0301-0511(97)05249-6.

Kimura, J., 2001. Electrodiagnosis in Diseases of Nerve and Muscle: Principles and Practice, 3rd. ed. Oxford University Press, New York.

Korvenoja, A., Wikström, H., Huttunen, J., Virtanan, J., Laine, P., Aronen, H., Seppäläinen, A.-M., Ilmoniemi, R., 1995. Activation of ipsilateral primary sensorimotor cortex by median nerve stimulation. NeuroReport 6 (18), 2589–2593. https://doi.org/10.1097/00001756-199512150-00033.

Litvak, V., Mattout, J., Kiebel, S., Phillips, C., Henson, R., Kilner, J., Barnes, G., Oostenveld, R., Daunizeau, J., Flandin, G., Penny, W., Friston, K., 2011. EEG and MEG data analysis in SPM8. Comput. Intell. Neurosci. 2011, 852961. https://doi.org/10.1155/2011/852961.

Näätänen, R., 1992. Attention and Brain Function. Erlbaum, Hillsdale (N.J.).

Näätänen, R., 2009. Somatosensory mismatch negativity: a new clinical tool for developmental neurological research? Dev. Med. Child. Neurol. 51 (12), 930–931. https://doi.org/10.1111/j.1469-8749.2009.03386.x.

Näätänen, R., Paavilainen, P., Rinne, T., Alho, K., 2007. The mismatch negativity (MMN) in basic research of central auditory processing: a review. Clin. Neurophysiol. 118 (12), 2544–2590. https://doi.org/10.1016/j.clinph.2007.04.026.

Naeije, G., Vaulet, T., Wens, V., Marty, B., Goldman, S., De Tiège, X., 2016. Multilevel cortical processing of somatosensory novelty: a magnetoencephalography study. Front. Hum. Neurosci. 10, 259. https://doi.org/10.3389/fnhum.2016.00259.

Naeije, G., Vaulet, T., Wens, V., Marty, B., Goldman, S., De Tiège, X., 2018. Neural basis of early somatosensory change detection: a magnetoencephalography study. Brain Topogr. 31 (2), 242–256. https://doi.org/10.1007/s10548-017-0591-x.

Otsuru, N., Inui, K., Yamashiro, K., Urakawa, T., Keceli, S., Kakigi, R., 2011. Effects of prior sustained tactile stimulation on the somatosensory response to the sudden change of intensity in humans: an magnetoencephalography study. Neuroscience 182, 115–124. https://doi.org/10.1016/j.neuroscience.2011.03.019.

Pazo-Alvarez, P., Cadaveira, F., Amenedo, E., 2003. MMN in the visual modality: a review. Biol. Psychol. 63 (3), 199–236. https://doi.org/10.1016/S0301-0511(03)00049-8.

Pratt, H., Starr, A., Amlie, R.N., Politoske, D., 1979. Mechanically and electrically evoked somatosensory potentials in normal humans. Neurology 29 (9), 1236–1244. https://doi.org/10.1212/WNL.29.9_Part_1.1236.

Puts, N.A.J., Wodka, E.L., Tommerdahl, M., Mostofsky, S.H., Edden, R.A.E., 2014. Impaired tactile processing in children with autism spectrum disorder. J. Neurophysiol. 111 (9), 1803–1811. https://doi.org/10.1152/jn.00890.2013.

Raitasalo, R., 2007. Mielialakysely : Suomen Oloihin Beckin Lyhyen Depressiokyselyn Pohjalta Kehitetty Masennusoireilun Ja Itsetunnon Kysely. Kelan tutkimusosasto., Helsinki.

Restuccia, D., Della Marca, G., Valeriani, M., Leggio, M.G., Molinari, M., 2007. Cerebellar damage impairs detection of somatosensory input changes. A somatosensory mismatch-negativity study. Brain 130, 276–287. https://doi.org/10.1093/brain/awl236.

Restuccia, D., Zanini, S., Cazzagon, M., Del Piero, I., Martucci, L., Della Marca, G., 2009. Somatosensory mismatch negativity in healthy children. Dev. Med. Child Neurol. 51 (12), 991–998. https://doi.org/10.1111/j.1469-8749.2009.03367.x.

Shen, G., Smyk, N.J., Meltzoff, A.N., Marshall, P.J., 2017. Using somatosensory mismatch responses as a window into somatotopic processing of tactile stimulation. Psychophysiology 2017, 1–14. https://doi.org/10.1111/psyp.13030.

Shinozaki, N., Yabe, H., Sutoh, T., Hiruma, T., Kaneko, S., 1998. Somatosensory automatic responses to deviant stimuli. Cognitive Brain Res. 7 (2), 165–171. https://doi.org/10.1016/S0926-6410(98)00020-2.

Spackman, L.A., Boyd, S.G., Towell, A., 2007. Effects of stimulus frequency and duration on somatosensory discrimination responses. Exp. Brain Res. 177 (1), 21–30. https://doi.org/10.1007/s00221-006-0650-0.

Strömmer, J.M., Tarkka, I.M., Astikainen, P., 2014. Somatosensory mismatch response in young and elderly adults. Front. Aging Neurosci. 6, 293. https://doi.org/10.3389/fnagi.2014.00293.

Tamè, L., Braun, C., Holmes, N.P., Farnè, A., Pavani, F., 2016. Bilateral representations of touch in the primary somatosensory cortex. Cognitive Neuropsychol. 33 (1-2), 48–66. https://doi.org/10.1080/02643294.2016.1159547.

Taulu, S., Simola, J., 2006. Spatiotemporal signal space separation method for rejecting nearby interference in MEG measurements. Phys. Med. Biol. 51 (7), 1759–1768. https://doi.org/10.1088/0031-9155/51/7/008.

Taulu, S., Kajola, M., Simola, J., 2004. Suppression of interference and artifacts by the signal space separation method. Brain Topogr. 16 (4), 269–275 doi:BRAT.0000032864.93890.f9.

Tavassoli, T., Bellesheim, K., Tommerdahl, M., Holden, J.M., Kolevzon, A., Buxbaum, J.D., 2016. Altered tactile processing in children with autism spectrum disorder. Autism Res. 9 (6), 616–620. https://doi.org/10.1002/aur.1563.

Zhao, C., Valentini, E., Hu, L., 2015. Functional features of crossmodal mismatch responses. Exp. Brain Res. 233 (2), 617–629. https://doi.org/10.1007/s00221-014-4141-4.

III

BILATERAL ACTIVATIONS IN OPERCULO-INSULAR AREA SHOW TEMPORAL DISSOCIATION AFTER PERIPHERAL ELECTRICAL STIMULATION IN HEALTHY ADULTS

by

Hautasaari, P., Saloranta, H., Savić, A. M., Korniloff, K., Kujala, U. M. & Tarkka, I. M. 2018.

European Journal of Neuroscience (Epub ahead of print).

Bilateral activations in operculo-insular area show temporal dissociation after peripheral electrical stimulation in healthy adults

Pekka Hautasaari,[1,2] Harri Saloranta,[1] Andrej M. Savić,[3,4] Katariina Korniloff,[1] Urho M. Kujala,[1] and Ina M. Tarkka[1,2]

[1]Health Sciences, Faculty of Sport and Health Sciences, University of Jyväskylä, Jyväskylä, Finland, [2]Jyväskylä Centre for Interdisciplinary Brain Research, University of Jyväskylä, Jyväskylä, Finland, [3]School of Electrical Engineering, University of Belgrade, Belgrade, Serbia, [4]Tecnalia Serbia Ltd., Belgrade, Serbia

Keywords: magnetoencephalography; sensory cortex; nociception; median nerve; radial nerve

Address for correspondence:

Pekka Hautasaari, MSc
Faculty of Sport and Health Sciences
University of Jyväskylä
P.O. Box 35, FI-40014 Finland
pekka.t.hautasaari@student.jyu.fi

ORCIDs:
Pekka Hautasaari: 0000-0002-0403-9602
Harri Saloranta
Andrej M. Savic: 0000-0003-4510-210X
Katariina Korniloff: 0000-0002-0753-1483
Urho M. Kujala: 0000-0002-9263-1992
Ina M. Tarkka: 0000-0002-7552-5819

ABSTRACT

Interhemispheric transfer is necessary for sensory integration and coordination of body sides. We studied how somatosensory input from one body side may reach both body sides. First, we investigated with 17 healthy adults which uni- and bilateral brain areas were involved in consecutive stages of automatic sensory processing of non-nociceptive peripheral stimulation. Somatosensory evoked fields (SEFs) to electrical stimulation were recorded with 306-channel magnetoencephalography in two conditions. First, SEFs were registered following sensory radial nerve (RN) stimulation to dorsal surface of the right hand and second, following median nerve (MN) stimulation at the right wrist. Cortical activations were located in contralateral postcentral gyrus after MN and RN stimulations and in bilateral operculo-insular area after RN stimulation. First component occurred earlier after MN than RN stimulation. Middle latency components had similar latencies with stronger activation in contralateral postcentral gyrus after MN than RN stimulation. Interestingly, long latency components located in bilateral operculo-insular area after RN stimulation showed latency difference between hemispheres, i.e. activation peaked earlier in contralateral than in ipsilateral side. Additional experiments comparing novel intracutaneous nociceptive, RN and MN electrical stimuli confirmed bilateral long latency activation elicited by each stimulus type and highlighted latency differences between hemispheres. Variations in activation of bilateral operculo-insular areas may corroborate their role in pain network and in multisensory integration. Our findings imply that these areas present a relay station in multisensory stimulus detection.

INTRODUCTION

Long held key conception in cortical sensory physiology is that primary somatosensory cortex (SI) responds exclusively or mainly to tactile and other somatosensory stimulation from contralateral side of the body. This is evidenced in textbooks and noninvasive studies (Kakigi et al., 2000a; Noback et al., 2005; Penfield & Rasmussen, 1950) and yet interhemispheric transfer is necessary for sensory integration and coordination of both sides of the body. The most prominent structure responsible for interhemispheric transfer is corpus callosum (CC), which may have, depending on task requirements, inhibitory or excitatory function (Fling et al., 2013; van der Knaap & van der Ham, 2011). To date, the exact nature of this transfer is not known however, for example, the importance in limiting spreading of excitatory function via CC in severe epileptic seizure prevention with corpus callosotomy has been well established for decades (Englot et al., 2017). Neuropsychological literature has presented evidence in brain-damaged patients of e.g. simultaneous bilateral tactile sensations produced by unilateral peripheral stimuli suggesting that the normally occurring inhibitory mechanism limiting the sensation to contralateral side is damaged in such a patient (Medina & Rapp, 2008). In order to understand the effects of specific brain damages it may be necessary to acknowledge, in addition to the dominant neurophysiological viewpoint of contralateral representation of somatosensory input in SI, more context-dependent integration of somatosensory inputs from both body sides. The secondary somatosensory cortex (SII) has been shown to contain bilateral functions and, furthermore, solid functional interaction between SI and SII has been well demonstrated (Forss et al., 2001; Hagiwara et al., 2014; Kakigi et al., 2000a; Karhu & Tesche, 1999; Raij et al., 2008; Wasaka et al., 2007). For instance, Hagiwara et al. (2014) elegantly demonstrated synchrony between two areas in specific time points in bilateral SIIs following unilateral somatosensory stimulation utilizing functional connectivity analysis, applying a method called weighted phase-lag index for

cortico-cortical synchrony, and showed increased amount of local functional coupling in elderly participants compared to young participants. As the cortical processing of somatosensory stimuli appears to be modulated by task, lesion or age, then also the perception of intensity of stimulation needs to be considered. The transition from sensory electrical stimulus to nociceptive electrical stimulus may be small current-wise (Omori et al., 2013) but considering cortical processing it may be substantial as distinctly painful stimuli activates cortical pain network (Apkarian et al., 2005). Pain processing network includes primary somatotopic representation of painful stimuli in primary somatosensory cortex (Omori et al., 2013) and a matrix of cortical areas in humans including secondary somatosensory cortices, insula, anterior cingulate cortex, thalamus, prefrontal cortex and posterior parietal cortex (Apkarian et al., 2005; Kakigi et al., 2000b; Tarkka & Treede, 1993). Especially intriguing region in this pain network is the insula, which has been implicated in a large number of mainly sensory functions, including pain perception, but even social emotions and other cognitive processes have been placed in insula. As insula receives afferents from some of the sensory thalamic nuclei, amygdala and limbic and association cortical areas, it is plausible that it has a role in tactile recognition (Augustine, 1996) and it may also be essential in formation of multimodal sensory integration (Nieuwenhuys, 2012). For multimodal sensory integration and further associative processes it would be necessary to integrate functions in both hemispheres.

Our aim was to investigate which uni- and bilateral brain areas are involved in consecutive stages of automatic sensory processing of non-nociceptive peripheral electrical stimulation in healthy adults. The data was recorded with whole head magnetoencephalography (MEG) and the somatosensory evoked fields (SEF) from sensory radial nerve (RN) stimulation were compared with those of median nerve (MN) stimulation. Additional experiments were

performed to elucidate the differences in bilateral brain activation first observed in comparing RN and MN stimulations. Cortical fields elicited by novel intracutaneous stimuli were compared with those of RN and MN stimuli in a strict fashion. Noninvasively detected sources of SEFs after sensory and mixed nerve stimulations were evaluated in this setting where non-nociceptive and nociceptive stimuli were delivered in the same body region activating same peripheral pathways but resulting in differences in activated brain network.

MATERIALS AND METHODS

Participants

Seventeen healthy adults participated in the study (for participant characteristics see table 1). Participants had no history of neurological or psychiatric diseases or alcoholic or narcotic addictions. RBDI mood questionnaire (Raitasalo, 2007), a depression scale developed for use in Finland based on the short version of the Beck Depression Inventory (Beck et al., 1961), was used to determine that none of the participants had any depressive and/or anxiety symptoms. All participants were right-handed. Before recording, participants were seated in the MEG device and a short recording was done to ensure that e.g. no metal objects in the head or upper body were present to generate artifacts or contaminate MEG recording. Additional experiments were performed with 5 subjects (see table 2). The research plan for original study and additional experiments was approved by the Ethics Committee of the University of Jyväskylä and the tenets of Helsinki Declaration were followed. All participants gave written informed consent prior to participation.

(Tables 1 and 2 about here)

Experiment

The study was conducted under two conditions. In condition I, somatosensory evoked fields (SEFs) were registered from sensory radial nerve (RN) stimulation to the dorsal surface of the right hand prior to a motor task of the same hand. A weak electric shock (Digitimer Ltd., model DS7A, Welvyn Garden City, UK) was applied 80 times to the dorsal surface of the right hand randomly with 4-6 s interstimulus intervals (ISI). A motor task was instructed as reaction-time movement where the electric stimuli served as a go-stimulus and the participant was asked to react with index finger abduction to each stimulus while keeping the forearm and hand as relaxed as possible. The requested task occupied subject's attention during RN stimulation. Previous research has reported that spatial attention towards stimulated hand does not modulate the source strengths of early SEF components (Mauguière et al., 1997a). The stimulating electrodes (diameter 1 cm) were placed on the proximal end of the first metacarpal (anode) and on the distal head of the ulna (cathode). The stimulus intensity was set to twice individual sensory threshold (mean 7.7 ±2.2 mA) and stimulus was a monophasic square-wave current pulse of 0.2 ms duration. The stimulus did not induce any reported pain. The randomization of the stimulus intervals was generated by pre-programmed computer script. In condition II, SEFs were registered following median nerve (MN) stimulation at right wrist. Weak electric shocks were applied to the wrist above median nerve. Stimulus intensity was set to individual motor threshold (mean 5.8 ±1.4 mA) producing weak thumb movement and the stimulus was a monophasic square-wave current pulse of 0.2 ms duration, applied with ISI of 5 Hz for a total of 300 stimuli. The whole hand and forearm were relaxed throughout MN stimulation period. Even though RN condition included a voluntary movement, only the early stages of cortical stimulation processing, well before the onset of voluntary movement, were compared between RN and MN.

For additional experiments RN, MN and a novel intracutaneous electrical stimuli (modified from Kochs et al., 1996) were applied, all with similar randomized ISI (4-6 s) and same number of repetitions (80) without attentional task. Nociceptive intracutaneous stimuli (NOCI) were delivered to the tip of right middle finger. The superficial epidermal layers of the glabrous skin were removed with a small stainless steel drill with a diameter of 1.5 mm. A non-magnetic copper tip electrode, diameter 1 mm, height 2 mm, was placed to the small skin hole and attached with surgical tape. A non-magnetic metal ring return electrode was placed in the metacarpophalangeal joint of the middle finger. The delivered current pulse of 0.2 ms duration activated palmar digital branch of the median nerve and likely activated superficial nociceptive nerve terminals. The perception of this stimulus was described as a stinging pain. The individual pain threshold was tested and for data collection stimulus intensity (mean 4.6 ±2.2 mA) was set to produce 6 in visual-analog pain scale (VAS 0-10).

Recordings were carried out while the participants were seated in the magnetically shielded room (Vacuumschmelze, GmbH, Hanau, Germany). Eye movements and blinks were recorded with electro-oculogram (EOG) with a bandpass filter of 0.1-330 Hz and a gain set to 2000. The participants were instructed to avoid blinking, voluntary eye movements and other unnecessary movements during recording. Five head position indicators (HPI) were placed on the scalp. The HPI coil locations in relation to three anatomical landmarks (nasion and bilateral preauricular points) were measured with a 3-D digitizer (Fastrak®, Polhemus, Vermont, USA) with additional points from scalp, forehead and nose crest for more accurate representation of the individual head shape. MEG was recorded with the helmet-shaped 306-channel device (Elekta Neuromag®, Triux™, Stockholm, Sweden). MEG signals were recorded using a bandpass filter of 0.1-330 Hz. MEG and EOG signals were stored for later offline processing and analysis.

Data analysis

First, MEG data was filtered with MaxFilter software (Elekta Neuromag®, Stockholm, Sweden) using signal space separation (SSS) in order to reduce artifact components that are not caused by brain activity while preserving signals originating from the brain (Taulu & Simola, 2006; Taulu et al., 2004). Further data preprocessing and analysis was conducted with Brainstorm software (version released 15 Feb 2017) (Tadel et al., 2011) and Statistical Parametric Mapping v. 12 (SPM12) software (Litvak et al., 2011) available in http://www.fil.ion.ucl.ac.uk/spm running under Matlab 2015a (The Mathworks Inc. Natick, MA, USA). Since no individual magnetic resonance images (MRI) were available, an anatomy template (ICBM152) provided by Brainstorm was used. According to MEG guidelines recommendation (Gross et al., 2013), an accurate digitization of the individual head shape is an appropriate method for further source location analysis of electromagnetic activity. This shape can be used, instead of the individual MRI, to approximately align the subject's head to a template head (Holliday et al., 2003) to allow for averaging across subjects. Anatomy templates were aligned and warped for each subject with HPI data collected before MEG recording (Darvas et al., 2006). Event markers for the electrical stimulation were recorded simultaneously with MEG registration in all recordings. Artifacts from eye movements and blinks were identified and cleaned using signal-space projection (SSP) method (Uusitalo & Ilmoniemi, 1997) available in Brainstorm. After artifact removal, the data was segmented to epochs according to the stimulus onset. The complete time window of a single epoch was from -10 ms to +180 ms, with zero marking the stimulus onset. Segmentation process was the same for original RN and MN data as well as additional experiments. First 10 ms (-10 to -1 ms) of the time window was used as a baseline. Separate averages of all conditions were computed for each participant, including additional

experiments, from all artifact-free epochs and in the original experiment grand averages were formed.

Source modeling was done utilizing Brainstorm with distributed models. The forward model was computed with overlapping spheres where one local sphere was assigned to each sensor. Source models were generated from each participant's averaged epochs using minimum norm estimate in dynamic statistical parametric mapping (dSPM). Orientations of source dipoles were constrained normally to cortical surface and all gradiometer sensors of MEG recording were included.

The identified regions of interest (ROI), indicated by dSPM, were analyzed using Brainstorm's scout function for temporal analysis and SPM12 software for regional and source strength analysis. In Brainstorm, the scouts were applied for each participant's averaged source maps. The specific locations of the scouts were determined in the source maps by singular maximum amplitudes within four separate time periods indicated by averaged gradiometer waveform components: 15 - 25 ms, 25 - 35 ms, 60 - 80 ms and 100 - 140 ms. Each scout was set to cover 20 vertices, corresponding to 2.97 cm^2 on average on the cortical surface. One scout represented mean activity in each source location and the scout waveforms were used to compare brain activities between conditions in temporal domain using time points of peak source field strengths and mean amplitudes over 10 ms time windows after source activation onsets.

Source strengths, regional, and hemispheric differences in ROIs were compared between conditions in SPM12 utilizing extension toolbox WFU PickAtlas (version 3.05) (Maldjian et al., 2003). Volumetric statistical parametric maps of the t-statistics were computed from each

individual's average source map for 5 ms (short latency components) or 10 ms (middle and long latency components) time windows. These time windows were picked according to mean peak source strengths identified from the scout waveforms. Atlas-based ROI masks (Lancaster et al., 1997; Lancaster et al., 2000) including bilateral postcentral gyrus and bilateral insula were used for voxel-based statistical comparison.

Statistical analysis

Statistical analysis was performed with IBM SPSS 24 (IBM, Armonk, NY, USA) for temporal analysis and with SPM12 software for regional field strength analysis. Temporal variables were compared with paired samples t-test, with the significance threshold set at $p < 0.05$. All group analysis of MEG data was done in source space. Group level differences between identified brain regions were detected by voxel-level statistical analysis in SPM12 with two-sample t-test. Primary threshold was set to $p < 0.001$ or $p < 0.005$ (uncorrected for multiple comparisons) and corrected for multiple comparisons by the false discovery rate (FDR) method. Clusters were regarded as significant when falling below FDR-corrected cluster-level threshold of 0.05. No minimum cluster size was determined.

RESULTS

Main brain activations were identified from gradiometer waveforms and dSPM activation maps. First component after stimulus onset in RN condition had mean peak amplitude at 32 (±4.9) ms and in MN condition at 20 (±2.0) ms, both locating in postcentral gyrus. In both conditions, middle latency component was identified in postcentral gyrus with the mean peak amplitude at 67 (±4.8) ms in RN condition and 65 (±7.0) ms in MN condition. In RN condition, long latency bilateral posterior operculo-insular area activation was identified with the mean peak amplitude at 112 (±11.6) ms in contralateral side to stimulation and at 130

(±21.7) ms in ipsilateral side. It is noteworthy that MN stimulation did not show corresponding long latency activations when ISI was 5 Hz. RN (purely sensory) condition (7.7 ±2.2 mA) had slightly but statistically significantly stronger stimulus intensity than MN (mixed sensory and motor) condition (5.8 ±1.4 mA) ($p = 0.001$, $t = 5.44$, $df = 16$). For data visualization, the grand average MEG waveforms of RN SEF and MN SEF from gradiometers covering left parietal area are shown in figure 1 with whole head topographies at mean peak component time points, middle latency component illustrated at 66 ms for both conditions (maximal values: MN 65 ms and RN 67 ms). Mean reaction time in motor task after RN stimulation was 221 (±51) ms indicating that no on-going motor activity was present during the analyzed time window of -10 to 180 ms.

(Figure 1 about here)

Mean MNI coordinates and spatial differences for peak activations identified with scouts for each component are shown in table 3. Spatial distances for short- and middle latency coordinates in contralateral postcentral gyrus were calculated and revealed 4.5 mm distance between MN SEF 20 ms and RN SEF 32 ms components and 1.8 mm distance within MN condition between SEF 20 ms and SEF 65 ms components. Moreover, 6.8 mm distance was detected within RN condition between SEF 32 ms and SEF 67 ms components and finally 9.3 mm distance was detected between MN SEF 65 ms and RN SEF 67 ms components.

(Table 3 about here)

Temporal analysis showed differences between conditions in first components after stimulation. Mean peak activation of the first component in MN SEF occurred earlier, at 20

(±2.0) ms, than in RN SEF, at 32 (±4.9) ms ($p = 0.001$, $t = 9.63$, $df = 16$). Mean time points of peak activities of the middle latency components showed no statistically significant differences between components of MN SEF at 65 (±7.0) ms and RN SEF at 67 (±4.8) ms ($p = 0.40$, $t = 0.87$, $df = 16$). Long latency activation in the posterior operculo-insular area following RN SEF showed hemispheric temporal difference where contralateral peak activation, in relation to the stimulated hand, occurred earlier (112 ±11.6 ms) than in the ipsilateral side (130 ±21.7 ms) ($p = 0.001$, $t = -4.45$, $df = 16$). This difference was also present in the initiation of bilateral posterior operculo-insular area activations as the contralateral activation started significantly earlier ($p = 0.003$, $t = 3.51$, $df = 16$). Figure 2 shows activation maps at mean peak time points and corresponding time courses of these sources.

(Figure 2 about here)

ROI analysis in SPM12 with extension tool WFU PickAtlas indicated highest active clusters, i.e. highest source strengths, when comparing activations between conditions. MN condition showed stronger activation in short latency component when comparing MN SEF 20 ms and RN SEF 32 ms within 5 ms analysis window around the mean peak time points and showed highest active clusters in contralateral postcentral gyrus and secondary somatosensory area (SII). MN condition showed also stronger activation in middle latency component when comparing MN SEF 65 ms and RN SEF 67 ms within 10 ms analysis window around mean peak time points with highest active cluster in contralateral postcentral gyrus. RN condition showed stronger activation in long latency bilateral components when comparing contralateral (RN SEF 112 ms and MN SEF 112 ms) and ipsilateral (RN SEF 130 ms and MN SEF 130 ms) activations within corresponding 10 ms time windows around mean peak

time points, which were identified in RN condition with highest active clusters in bilateral posterior operculo-insular area. See table 4 and figure 3 for significantly different clusters and mean peak coordinates within clusters.

(Table 4 and figure 3 about here)

Additional experiments with 5 subjects first replicated short latency SEF results in MN and RN stimulation, with short latency component peaking earlier after MN (20 ±2.2 ms) than RN (26.6 ±5.6 ms) stimulation ($p = 0.05$, $t=-2.8$, $df = 4$). Also, NOCI short latency component at 25.2 (±2.6) ms occurred later than that of MN ($p = 0.039$, $t = -3.03$, $df = 4$). Furthermore, additional experiments produced evidence that long latency components can be obtained with MN stimulation, when ISI is longer. This can be observed in source activations in figure 4 B and C. NOCI stimulation produced similar brain activations than RN stimulation with corresponding short latency component (NOCI 26.6 ±5.6, RN 25.2 ±2.6 ms, $p = 0.544$, $t = -0.66$, $df = 4$). Interestingly, nociceptive stimulation produced long latency bilateral activations, which resembled those elicited by RN in contra- and ipsilateral hemispheres both in original and additional experiments. Those responses in ipsilateral hemisphere after NOCI stimulation in additional experiments differed from MN in timing, NOCI 118.4 ±14.4 ms and MN 103.6 ±12.6 ms ($p = 0.01$, $t = -4.6$, $df = 4$). ROI analysis with 5 subjects among additional experiments did not reveal differences in source strengths between conditions. Additionally, we compared long latency source strengths of 5 subjects from original study with the data of additional experiments. This comparison revealed stronger cluster-level activation in contralateral operculo-insular area after long ISI MN stimulation (height threshold $p = 0.001$ (unc.), FDR-corr. $p = 0.021$, voxels per cluster = 10, $t = 6.74$, $df = 8$, peak coordinate within cluster = -46, -20, 16) compared to short ISI MN

stimulation. Furthermore, NOCI stimulation revealed stronger activation in contra- (height threshold $p = 0.005$ (unc.), FDR-corr. $p = 0.006$, voxels per cluster = 39, $t = 6.64$, $df = 8$, peak coordinate within cluster = -38, -24, 20) and in ipsilateral (height threshold $p = 0.005$ (unc.), FDR-corr. $p = 0.002$, voxels per cluster = 44, $t = 6.07$, $df = 8$, peak coordinate within cluster = 32, -24, 20) operculo-insular areas compared to short ISI MN stimulation.

(Figure 4 about here)

DISCUSSION

Our results show that peripheral stimulation to only slightly diverging hand areas produces spatial and temporal dissociation in brain activations. We demonstrated that first SEF activation occurred earlier in postcentral gyrus after MN stimulation than after RN stimulation, even though middle latency SEF occurred at similar time points, also in postcentral gyrus. Interestingly, RN stimulation activated posterior operculo-insular area bilaterally with temporal differences at onset times and at mean peak activation times between contra- and ipsilateral hemispheres while MN stimulation with shorter ISI did not elicit long latency activations. However, this discrepancy corresponds well with previous research showing that long-latency responses in SII areas decrease with shorter ISI (Wikström et al., 1996). With additional experiment using similar ISI we were able to replicate the short latency SEF results and confirm that with longer ISI long-latency responses are obtained after MN stimulation.

First SEF components in our experiments corresponded well with previous research, especially in case of median nerve stimulation where the first component peaked at 20 ms (Hari et al., 1993; Kakigi, 1994; Tiihonen et al., 1989) and the first component after radial

nerve stimulation peaked at 32 ms (Inui et al., 2003). Nociceptive stimulation in our additional experiments produced short latency response corresponding to RN response. Furthermore, obtained source locations of the early SEF components corresponded well with previous research (Kakigi et al., 2000a; Mauguière et al., 1997b) locating in the contralateral postcentral gyrus. Previous research has provided evidence for short latency bilateral activation in postcentral gyrus indicating possible transcallosal interhemispheric transfer between contra- and ipsilateral primary somatosensory cortices (Schnitzler et al., 1995). However, this was not seen in the present study probably due to different stimulus paradigms. In addition to contralateral activation in postcentral gyrus, regional analysis showed also contralateral SII activation during short latency component, the finding corresponding with Karhu and Tesche (1999), who also observed contralateral SII area activation 20-30 ms after MN stimulation. Using radial nerve stimulation for eliciting somatosensory evoked fields is rather less common, however, the possible advantage in studying sensory systems could be that the radial nerve area on the dorsum of the hand only activates sensory afferents (Kimura, 2001), when median nerve at the wrist is a mixed nerve and its stimulation thus activates also motor fibers (Kimura, 2001). Previous invasive (Barba et al., 2008) and non-invasive (Srisa-an et al., 1996) research has, similarly to our present results, located the generator of middle latency components at around 60 ms in the postcentral gyrus. It is interesting to note, although first components differed in latency between MN and RN conditions (12 ms later for RN stimulation), the middle latency components occurred at similar latencies.

We found long-latency bilateral SEF sources after radial nerve stimulation and proposed that these activations originate in posterior insular area based on latencies (Inui et al., 2003; Liberati et al., 2016) and MNI location coordinates. The present data indicated mean MNI coordinates for long-latency activation at 112 ms in the contralateral (left) hemisphere in (-

44.4, -22.8, 15.7) and at 130 ms in the ipsilateral (right) hemisphere in (47.0, -17.6, 13.5) according to scouts. These peak MNI coordinates within clusters located in left hemisphere in (-44, -19, 15) and in right hemisphere in (44, -19, -15) according to SPM analysis (see tables 3 and 4). These coordinates correspond rather well to the center of gravity coordinates in posterior insula cytoarchitectonic areas Ig1 (left: -34, -28, 14 and right: 35, -27, 11) or Ig2 (left: -38, -22, 11 and right: 38, -21, 10) defined by Kurth et al. (2010), compared to operculum 1 area (OP1) where center of gravity mean coordinates were in the left hemisphere in (-52.0, -26.5, 26.8) and in right hemisphere in (52.7, -26.0, 25.6) (Eickhoff et al., 2006a). The aforementioned OP1 location Eickhoff et al. (2006a) proposed to indicate most likely SII area in humans.

Still, overlapping posterior insular and secondary somatosensory cortex (SII) activation is possible (Inui et al., 2003), although we were not able to distinguish separate brain areas contributing to these bilateral activations. One reason may be the close proximity of locations and activations reported by Inui et al. (2003) in SII and posterior insula. In the present study, activated areas were localized in the general area often labeled as parietal operculum and usually considered as the SII region (zu Eulenburg et al., 2013). Eickhoff et al. (2006a; 2006b) were able to dissociate the parietal operculum to four different cytoarchitectonic areas and they raised the question if SII region is an appropriate term for this brain area while it seems that it includes a number of anatomically and physiologically distinct areas. Furthermore, previous research has shown that posterior insular area is connected reciprocally to the neighboring SII area and receives projections also from the SI cortex (Augustine, 1985; Friedman et al., 1986) highlighting the complexity of this brain area involved in somatosensory processing.

In our present study, we found 15-18 ms latency difference between contra- and ipsilateral peak activations both in RN and in NOCI in the posterior operculo-insular areas where contralateral side peaked earlier. This result corresponds well with previous studies reporting similar latency differences between hemispheres in posterior insular area, in e.g. Inui et al. (2003) using non-nociceptive transcutaneous electrical stimulation to radial nerve area and in Liberati et al. (2016) using vibrotactile stimulation with intracerebral recording and, furthermore, in SII e.g. in Karhu and Tesche (1999) using electrical median nerve stimulation. This interhemispheric delay has been attributed to callosal transmission between contra- and ipsilateral SII areas (Frot & Mauguiere, 1999; Karhu & Tesche, 1999) but also direct thalamo-cortical connection to ipsilateral hemisphere has been suggested (Forss et al., 1999). Somatosensory cortices seem to process information in parallel (Liang et al., 2011) or serial (Khosnejad et al., 2014) manner between brain areas. However, this is still under debate and recent combined fMRI and MEG study demonstrated that early neural activity, first 100 ms after somatosensory stimulus, is best explained by parallel and subsequent activity by serial processing route (Klingner et al., 2016). It is suggested that insula shares connections with dorsal thalamus (Augustine, 1996; Dum et al., 2009; Friedman & Murray, 1986) but rather little is known about connections to and from insula. Previous evidence suggests that insula plays a role in multisensory integration processing multimodal stimuli (Kurth et al., 2010; Liberati et al., 2016; zu Eulenburg et al., 2013). This multimodal activation in posterior insular cortex may encompass convergence of afferent somatosensory information in this area (zu Eulenburg et al., 2013) and maybe posterior insula was activated due to pure sensory input in the present experiment.

Our original study included differences in stimulus parameters, which limited our interpretation. The differences in interstimulus intervals (shorter in MN stimulation)

contributed to differences in long latency components (Mauguière et al., 1997a; Wikström et al., 1996). Additional experiments with fully comparable interstimulus intervals and pain-specific electrical stimulation to fingertip provided support for bilateral long latency activations elicited by all electrical stimuli and RN and NOCI dissociation from MN in long latency activation. We recognize the lack of individual MRIs in our data. This may render some inaccuracy in specific locations however, digitization of individual head shapes can be utilized with MRI template for localization of distinct activity according to MEG recording and reporting guidelines by Gross et al. (2013, see Materials and Methods section). Furthermore, we cannot completely rule out possible effects from preparation phase to motor task before RN stimulation, although no active movement was observed during our analysis window.

CONCLUSION

Spatial and temporal dissociation was observed in brain activations following slightly diverging hand stimulation areas. Early and middle latency activations located in contralateral postcentral gyrus showing differences in source strengths however, only early component peak latencies of RN and NOCI stimulations differed from MN stimulation while middle latency components occurred at similar latencies. Interestingly, RN stimulation showed long latency activation in bilateral operculo-insular areas. Insular area is implicated to process multimodal sensory information and function as a multisensory integration node. It is also known to participate in pain network and part of the activity after RN stimulation may be owed to possible discomfort experienced from stimulus. This suggestion is supported by the similarity of source activations we obtained in additional experiments with novel nociceptive stimulation. We showed that specific peripheral stimulation activates, in addition

to primary sensory areas in contralateral postcentral gyrus, bilateral operculo-insular areas with distinct latency difference between contra- and ipsilateral hemispheres.

ACKNOWLEDGMENTS

We want to thank the Jyväskylä Centre for Interdisciplinary Brain Research, University of Jyväskylä, Jyväskylä, Finland, for providing the MEG facilities. The study was funded by Juho Vainio Foundation, Helsinki, Finland grant (201410296) and Ministry of Education and Culture, Helsinki, Finland (OKM/56/626/2013). All procedures performed in the present study involving human participants were in accordance with the ethical standards of the institutional (University of Jyväskylä) research and ethics committee and with the Declaration of Helsinki. All participants gave written informed consent prior to participation.

CONFLICT OF INTEREST

Authors have nothing to report.

AUTHOR CONTRIBUTIONS

Study concept and design: PH, HS, IMT

Data collection and analysis or revision of manuscript: All authors

Interpretation of data and writing of manuscript: PH, IMT

DATA ACCESSIBILITY

Data of this paper is available upon request via corresponding author from University of Jyväskylä servers.

ABBREVIATIONS

CC, corpus callosum; dSPM, dynamic statistical parametric mapping; EOG, electro-oculogram; FDR, false discovery rate; HPI, head position indicator; ISI, interstimulus interval; MEG, magnetoencephalography; MN, median nerve; MRI, magnetic resonance image; NOCI, intracutaneous nociceptive stimuli; OP1, operculum 1 area; RN, radial nerve; ROI, region of interest; SEF, somatosensory evoked field; SI, primary somatosensory cortex; SII, secondary somatosensory cortex; SPM12, statistical parametric mapping v. 12; SSP, signal-space separation; SSS, signal space separation; VAS, visual analog pain scale

References

Apkarian, A. V., Bushnell, M. C., Treede, R. D. & Zubieta, J. K. (2005) Human brain mechanisms of pain perception and regulation in health and disease. *Eur. J. Pain.,* **9**, 463-484.

Augustine, J. R. (1985) The insular lobe in primates including humans. *Neurol. Res.,* **7**, 2-10.

Augustine, J. R. (1996) Circuitry and functional aspects of the insular lobe in primates including humans. *Brain. Res. Rev.*, **22**, 229-244.

Barba, C., Valeriani, M., Colicchio, G. & Mauguière, F. (2008) New depth short-latency somatosensory evoked potential (SEP) component recorded in human SI area. *Neurosci. Lett.*, **432**, 179-183.

Beck, A. T., Ward, C. H., Mendelson, M. M., Mock, J. J. & Erbaugh J. J. (1961) An inventory for measuring depression. *Arch. Gen. Psychiatry.*, **4**, 561-571.

Darvas, F., Ermer, J. J., Mosher, J. C. & Leahy, R. M. (2006) Generic head models for atlas-based EEG source analysis. *Hum. Brain. Mapp.*, **27**, 129-143.

Dum, R. P., Levinthal, D. J. & Strick, P. L. (2009) The Spinothalamic System Targets Motor and Sensory Areas in the Cerebral Cortex of Monkeys. *J. Neurosci.*, **29**, 14223-14235.

Eickhoff, S. B., Amunts, K., Mohlberg, H. & Zilles, K. (2006a) The Human Parietal Operculum. II. Stereotaxic Maps and Correlation with Functional Imaging Results. *Cerebral Cortex*, **16**, 268-279.

Eickhoff, S. B., Schleicher, A., Zilles, K. & Amunts, K. (2006b) The Human Parietal Operculum. I. Cytoarchitectonic Mapping of Subdivisions. *Cerebral Cortex*, **16**, 254-267.

Englot, D. J., Birk, H. & Chang, E. F. (2017) Seizure outcomes in nonresective epilepsy surgery: an update. *Neurosurg. Rev.*, **40**, 181-194.

Fling, B. W., Benson, B. L. & Seidler, R. D. (2013) Transcallosal sensorimotor fiber tract structure-function relationships. *Hum. Brain. Mapp.*, **34**, 384-395.

Forss, N., Narici, L. & Hari, R. (2001) Sustained activation of the human SII cortices by stimulus trains. *Neuroimage*, **13**, 497-501.

Forss, N., Hietanen, M., Salonen, O. & Hari, R. (1999) Modified activation of somatosensory cortical network in patients with right-hemisphere stroke. *Brain*, **122**, 1889-1899.

Friedman, D. P. & Murray, E. A. (1986) Thalamic connectivity of the second somatosensory area and neighboring somatosensory fields of the lateral sulcus of the macaque. *J. Comp. Neurol.*, **252**, 348-373.

Friedman, D. P., Murray, E. A., O'Neill, J. B. & Mishkin, M. (1986) Cortical connections of the somatosensory fields of the lateral sulcus of macaques: Evidence for a corticolimbic pathway for touch. *J. Comp. Neurol.*, **252**, 323-347.

Frot, M. & Mauguière, F. (1999) Timing and Spatial Distribution of Somatosensory Responses Recorded in the Upper Bank of the Sylvian Fissure (SII Area) in Humans. *Cerebral Cortex*, **9**, 854-863.

Gross, J., Baillet, S., Barnes, G. R., Henson, R. N., Hillebrand, A., Jensen, O., Jerbi, K., Litvak, V., Maess, B., Oostenveld, R., Parkkonen, L., Taylor, J. R., van Wassenhove, V., Wibral, M. & Schoffelen, J. (2013) Good practice for conducting and reporting MEG research. *Neuroimage*, **65**, 349-363.

Hagiwara, K., Ogata, K., Okamoto, T., Uehara, T., Hironaga, N., Shigeto, H., Kira, J. & Tobimatsu, S. (2014) Age-related changes across the primary and secondary somatosensory areas: an analysis of neuromagnetic oscillatory activities. *Clin. Neurophysiol.*, **125**, 1021-1029.

Hari, R., Karhu, J., Hämäläinen, M., Knuutila, J., Salonen, O., Sams, M. & Vilkman, V. (1993) Functional Organization of the Human First and Second Somatosensory Cortices: a Neuromagnetic Study. *Eur. J. Neurosci.*, **5**, 724-734.

Holliday, I. E., Barnes, G. R., Hillebrand, A. & Singh, K. D. (2003) Accuracy and applications of group MEG studies using cortical source locations estimated from participants' scalp surfaces. *Hum. Brain. Mapp.*, **20**, 142-147.

Inui, K., Tran, T. D., Qiu, Y., Wang, X., Hoshiyama, M. & Kakigi, R. (2003) A comparative magnetoencephalographic study of cortical activations evoked by noxious and innocuous somatosensory stimulations. *Neuroscience*, **120**, 235-248.

Kakigi, R. (1994) Somatosensory evoked magnetic fields following median nerve stimulation. *Neurosci. Res.*, **20**, 165-174.

Kakigi, R., Hoshiyama, M., Shimojo, M., Naka, D., Yamasaki, H., Watanabe, S., Xiang, J., Maeda, K., Lam, K., Itomi, K. & Nakamura, A. (2000a) The somatosensory evoked magnetic fields. *Prog. Neurobiol.*, **61**, 495-523.

Kakigi, R., Watanabe, S. & Yamasaki, H. (2000b) Pain-Related Somatosensory Evoked Potentials. *J. Clin. Neurophysiol.*, **17**, 295-308.

Karhu, J. & Tesche, C. D. (1999) Simultaneous early processing of sensory input in human primary (SI) and secondary (SII) somatosensory cortices. *J. Neurophysiol.*, **81**, 2017-2025.

Khoshnejad, M., Piché, M., Saleh, S., Duncan, G. & Rainville, P. (2014) Serial processing in primary and secondary somatosensory cortex: A DCM analysis of human fMRI data in response to innocuous and noxious electrical stimulation. *Neurosci. Lett.*, **577**, 83-88.

Kimura, J. (2001) Electrodiagnosis in diseases of nerve and muscle: principles and practice. New York: Oxford University Press. 991 p.

Klingner, C. M., Brodoehl, S., Huonker, R. & Witte, O. W. (2016) The Processing of Somatosensory Information Shifts from an Early Parallel into a Serial Processing Mode: A Combined fMRI/MEG Study. *Front. Syst. Neurosci.*, **10**, 103.

Kochs, E., Scharein, E., Mollenberg, O. & Bromm, B. (1996) Analgesic efficacy of low-dose ketamine. Somatosensory-evoked responses in relation to subjective pain ratings. *Anesthesiology*, **85**, 304-14.

Kurth, F., Eickhoff, S. B., Schleicher, A., Hoemke, L., Zilles, K. & Amunts, K. (2010) Cytoarchitecture and Probabilistic Maps of the Human Posterior Insular Cortex. *Cerebral Cortex*, **20**, 1448-1461.

Lancaster, J. L., Rainey, L. H., Summerlin, J. L., Freitas, C. S., Fox, P. T., Evans, A. C., Toga, A. W. & Mazziotta, J. C. (1997) Automated labeling of the human brain: A

preliminary report on the development and evaluation of a forward-transform method. *Hum. Brain. Mapp.*, **5**, 238-242.

Lancaster, J. L., Woldorff, M. G., Parsons, L. M., Liotti, M., Freitas, C. S., Rainey, L., Kochunov, P. V., Nickerson, D., Mikiten, S. A. & Fox, P. T. (2000): Automated Talairach Atlas labels for functional brain mapping. *Hum. Brain. Mapp.*, **10**, 120-131.

Liang, M., Mouraux, A. & Iannetti, G. D. (2011) Parallel Processing of Nociceptive and Non-nociceptive Somatosensory Information in the Human Primary and Secondary Somatosensory Cortices: Evidence from Dynamic Causal Modeling of Functional Magnetic Resonance Imaging Data. *J. Neurosci.*, **31**, 8976-8985.

Liberati, G., Klöcker, A., Safronova, M. M., Ferrão Santos, S., Ribeiro Vaz, J., Raftopoulos, C. & Mouraux, A. (2016) Nociceptive Local Field Potentials Recorded from the Human Insula Are Not Specific for Nociception. *PLoS Biol.*, **14**, e1002345.

Litvak, V., Mattout, J., Kiebel, S., Phillips, C., Henson, R., Kilner, J., Barnes, G., Oostenveld, R., Daunizeau, J., Flandin, G., Penny, W. & Friston, K. (2011) EEG and MEG data analysis in SPM8. *Comput. Intell. Neurosci.*, **2011**, 852961.

Maldjian, J. A., Laurienti, P. J., Kraft, R. A. & Burdette, J. H. (2003) An automated method for neuroanatomic and cytoarchitectonic atlas-based interrogation of fMRI data sets. *Neuroimage*, **19**, 1233-1239.

Mauguière, F., Merlet, I., Forss, N., Vanni, S., Jousmäki, V., Adeleine, P. & Hari, R. (1997a) Activation of a distributed somatosensory cortical network in the human brain: a dipole modelling study of magnetic fields evoked by median nerve stimulation. Part II: effects of stimulus rate, attention and stimulus detection. *Electroencephalogr. Clin. Neurophysiol.*, **104**, 290-295.

Mauguière, F., Merlet, I., Forss, N., Vanni, S., Jousmäki, V., Adeleine, P. & Hari, R. (1997b) Activation of a distributed somatosensory cortical network in the human brain. A dipole modelling study of magnetic fields evoked by median nerve stimulation. Part I: location and activation timing of SEF sources. *Electroencephalogr. Clin. Neurophysiol.*, **104**, 281-289.

Medina, J. & Rapp, B. (2008) Phantom tactile sensations modulated by body position. *Curr. Biol.*, **18**, 1937-1942.

Nieuwenhuys, R. (2012) The insular cortex: A review. *Prog. Brain. Res.*, **195**, 123-163.

Noback, C. R., Strominger, N. L., Demarest, R. J. & Ruggiero, D. A. (2005) The Human Nervous System, Structure and Function. Totowa, New Jersey, USA: Humana Press. 416 p.

Omori, S., Isose, S., Otsuru, N., Nishihara, M., Kuwabara, S., Inui, K. & Kakigi, R. (2013) Somatotopic representation of pain in the primary somatosensory cortex (S1) in humans. *Clin. Neurophysiol.*, **124**, 1422-1430.

Penfield, W. & Rasmussen, T. (1950) The cerebral cortex of man : a clinical study of localization of function. New York: Macmillan. 248 p.

Raij, T., Karhu, J., Kicic, D., Lioumis, P., Julkunen, P., Lin, F. H., Ahveninen, J., Ilmoniemi, R. J., Mäkelä, J. P., Hämäläinen, M., Rosen, B. R. & Belliveau, J. W. (2008) Parallel input makes the brain run faster. *Neuroimage*, **40**, 1792-1797.

Raitasalo, R. (2007) Mielialakysely : Suomen oloihin Beckin lyhyen depressiokyselyn pohjalta kehitetty masennusoireilun ja itsetunnon kysely. Helsinki: Kelan tutkimusosasto. 87 p. English summary (in Finnish).

Schnitzler, A., Salmelin, R., Salenius, S., Jousmäki, V. & Hari, R. (1995) Tactile information from the human hand reaches the ipsilateral primary somatosensory cortex. *Neurosci. Lett.*, **200**, 25-28.

Srisa-an, P., Lei, L. & Tarkka, I. M. (1996) Middle latency somatosensory evoked potentials: noninvasive source analysis. *J. Clin. Neurophysiol.*, **13**, 156-163.

Tadel, F., Baillet, S., Mosher, J. C., Pantazis, D. & Leahy, R. M. (2011) Brainstorm: a user-friendly application for MEG/EEG analysis. *Comput. Intell. Neurosci.*, **2011**, 879716.

Tarkka, I. M. & Treede, R. (1993) Equivalent Electrical Source Analysis of Pain-Related Somatosensory Evoked Potentials Elicited by a CO2 Laser. *J. Clin. Neurophysiol.*, **10**, 513-519.

Taulu, S. & Simola, J. (2006) Spatiotemporal signal space separation method for rejecting nearby interference in MEG measurements. *Phys. Med. Biol.*, **51**, 1759-1768.

Taulu, S., Kajola, M. & Simola, J. (2004) Suppression of Interference and Artifacts by the Signal Space Separation Method. *Brain. Topogr.*, **16**, 269-275.

Tiihonen, J., Hari, R. & Hämäläinen, M. (1989) Early deflections of cerebral magnetic responses to median nerve stimulation. *Electroencephalogr. Clin. Neurophysiol.*, **74**, 290-296.

Uusitalo, M. A. & Ilmoniemi, R. J. (1997) Signal-space projection method for separating MEG or EEG into components. *Med. Biol. Eng. Comput.*, **35**, 135-140.

van der Knaap, L. J. & van der Ham, I. J. (2011) How does the corpus callosum mediate interhemispheric transfer? A review. *Behav. Brain. Res.*, **223**, 211-221.

Wasaka, T., Kida, T., Nakata, H., Akatsuka, K. & Kakigi, R. (2007) Characteristics of sensori-motor interaction in the primary and secondary somatosensory cortices in humans: a magnetoencephalography study. *Neuroscience*, **149**, 446-456.

Wikström, H., Huttunen, J., Korvenoja, A., Virtanen, J., Salonen, O., Aronen, H. & Ilmoniemi, R. J. (1996) Effects of interstimulus interval on somatosensory evoked magnetic

fields (SEFs): a hypothesis concerning SEF generation at the primary sensorimotor cortex. *Electroencephalogr. Clin. Neurophysiol.*, **100**, 479-487.

zu Eulenburg, P., Baumgärtner, U., Treede, R. & Dieterich, M. (2013) Interoceptive and multimodal functions of the operculo-insular cortex: Tactile, nociceptive and vestibular representations. *Neuroimage*, **83**, 75-86.

FIGURE CAPTIONS

Figure 1. Grand average waveforms of (A) radial SEF and (B) median SEF from gradiometer channels covering left parietal area from the original experiments with 17 subjects. Zero denotes onset of stimulation. Whole head topographies at designated time points are illustrated. Note different topographic mapping scales for 20 and 32 ms and for 66, 112 and 130 ms.

Figure 2. Initial components 20 ms (MN) and 32 ms (RN), following components at 65 ms (MN) and 67 ms (RN) (A) and bilateral components at 112 ms and 130 ms (B) are shown for median and radial nerve stimulations from the original experiments. dSPM maps illustrate the activations at mean peak time points in contralateral postcentral gyrus (A) and bilateral operculo-insular areas (B). Temporal differences in source activities between MN SEF (cyan) and RN SEF (green) are illustrated in the middle (A) corresponding to postcentral gyrus and (B) to bilateral operculo-insular area activation time courses. Contralateral side to stimulated hand is shown in solid circle superimposed on activation on dSPM maps and the corresponding time course with solid line (A and B) and ipsilateral side is similarly shown with dashed circles and lines (B).

Figure 3. Activation maps (SPM) showing voxel-based cluster-level differences from the original experiments between (A) MN SEF at 20 (± 2) ms time window and RN SEF at 32 (± 2) ms time window. (B) shows differences between MN SEF and RN SEF at 66 (± 5) ms time window and (C) between RN SEF and MN SEF at 112 (±5) ms time window. Lastly (D) shows differences between RN SEF and MN SEF at 130 (± 5) ms time window. MNI coordinates with corresponding red arrow for peak activation within a cluster are shown

above activation maps (A-D). Short latency comparison (A) showed also a more caudal secondary cluster with peak MNI coordinates within cluster in (-54, -19, 19). Atlas based ROI masks were used to include bilateral postcentral gyrus (A and B) and bilateral insula (C and D). Examples of ROI masks are shown in three different horizontal planes (Z-coordinates given above figures).

Figure 4. Short- and long-latency components from MN, RN and NOCI stimulations are illustrated in one representative subject from the additional experiments. dSPM maps illustrate the activations at mean peak time points (MN in cyan, RN in green and NOCI in blue) in contralateral postcentral gyrus (A) and contra- (B) and ipsilateral (C) operculo-insular areas. Temporal differences in source activities between MN SEF (cyan), RN SEF (green) and NOCI SEF (blue) are illustrated with superimposed waveforms corresponding to postcentral gyrus (A) and to bilateral operculo-insular area (B and C) activation time courses.

TABLE 1. Participant characteristics, 17 individuals (10 men, 7 women) means, (±SD) and range.

	Mean	SD	Range
Age, year	30.7	6.2	18-41
Height, cm	177	11.2	159-203
Weight, kg	74	13.1	59-95
BMI	23.6	3.0	20.3-30.7
Stimulus intensity on median nerve, mA	5.8	1.4	3.5-9.0
Stimulus intensity on radial nerve, mA	7.7	2.2	5.0-12.0
Reaction time, ms	221	51	146-326
Radial nerve (RN) stimulations, n	77	3.3	68-80
Median nerve (MN) stimulations, n	299	3.5	286-300
Scout size on cortical surface, cm^2	2.97	0.42	1.77-3.77

TABLE 2 Additional experiment: 5 individuals (3 men, 2 women) means, (±SD) and range.

	Mean	SD	Range
Age, year	34.4	4.4	28-39
Height, cm	171	11.8	158-183
Weight, kg	68	14.4	49-86
BMI	23.2	2.5	19.6-25.7
Stimulus intensity on median nerve, mA	5.8	1.0	4.5-7.0
Stimulus intensity on radial nerve, mA	6.6	1.6	5.0-8.5
Stimulus intensity on intracutaneous, mA	4.6	2.2	2.0-7.5
Median nerve (MN) stimulations, n	79	1.2	77-80
Radial nerve (RN) stimulations, n	80	0.4	79-80
Intracutaneous (NOCI) stimulations, n	79	1.3	77-80

TABLE 3. MNI location coordinates of component mean peak activations identified with scouts and spatial differences between early and middle latency components.

	MNI coordinates			Spatial difference between coordinates	
	X	Y	Z		
MN 20 ms	-38.4	-21.0	51.2	MN 20 ms – RN 32 ms	4.5 mm
RN 32 ms	-35.1	-23.1	53.4	MN 20 ms – MN 65 ms	1.8 mm
MN 65 ms	-37.9	-22.5	50.3	MN 65 ms – RN 67 ms	9.3 mm
RN 67 ms	-31.7	-28.9	52.8	RN 32 ms – RN 67 ms	6.8 mm
RN 112 ms	-44.4	-22.8	15.7		
RN 130 ms	47.0	-17.6	13.5		

TABLE 4. Cluster-level statistical differences and peak MNI coordinates within clusters.

		Cluster-level p-value[d]		Peak-level p-value[d]			Peak MNI coordinates within cluster
	Height threshold	FDR-corr.	voxels per cluster	FDR-corr.	T	Z	
MN 20 ms - RN 32 ms [a,b]	T = 3.37, p = 0.001 (unc.)	< 0.001	66	0.128	5.06	4.30	-44, -25, 43
		0.017	14	0.099	5.45	4.55	-54, -19, 19
MN 66 ms - RN 66 ms [a,b]	T = 3.37, p = 0.001 (unc.)	< 0.001	53	0.050	5.41	4.53	-48, -25, 41
RN 112 ms - MN 112 ms [a,c]	T = 3.37, p = 0.001 (unc.)	0.007	24	0.224	4.76	4.11	-44, -19, 15
RN 130 ms - MN 130 ms [a,c]	T = 2.74, p = 0.005 (unc.)	0.002	59	0.309	4.47	3.91	-44, -19, 15
		0.021	28	0.555	3.46	3.16	44, -19, 15

[a] Degrees of freedom = 32, Voxel size 2.0 x 2.0 x 2.0 mm
[b] Volume 6046 voxels
[c] Volume 3861 voxels
[d] p-values adjusted for search volume

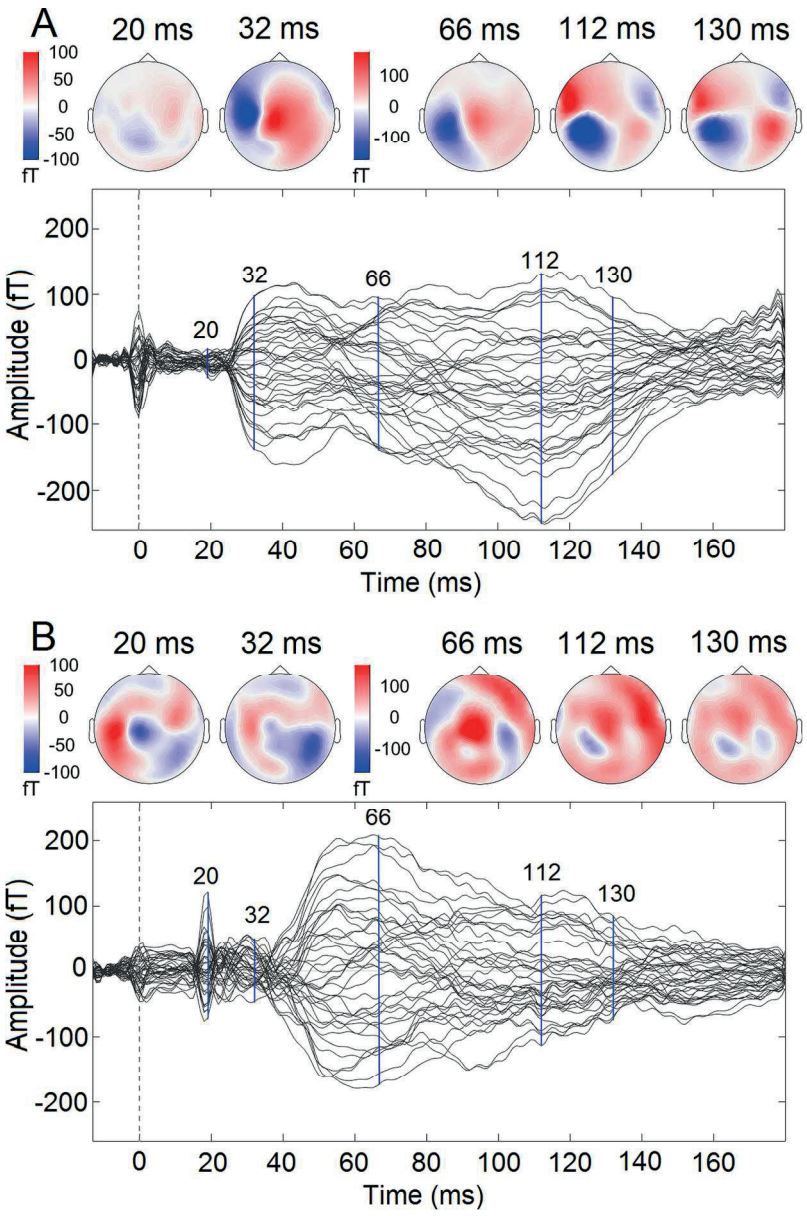

Figure 1

132x199mm (300 x 300 DPI)

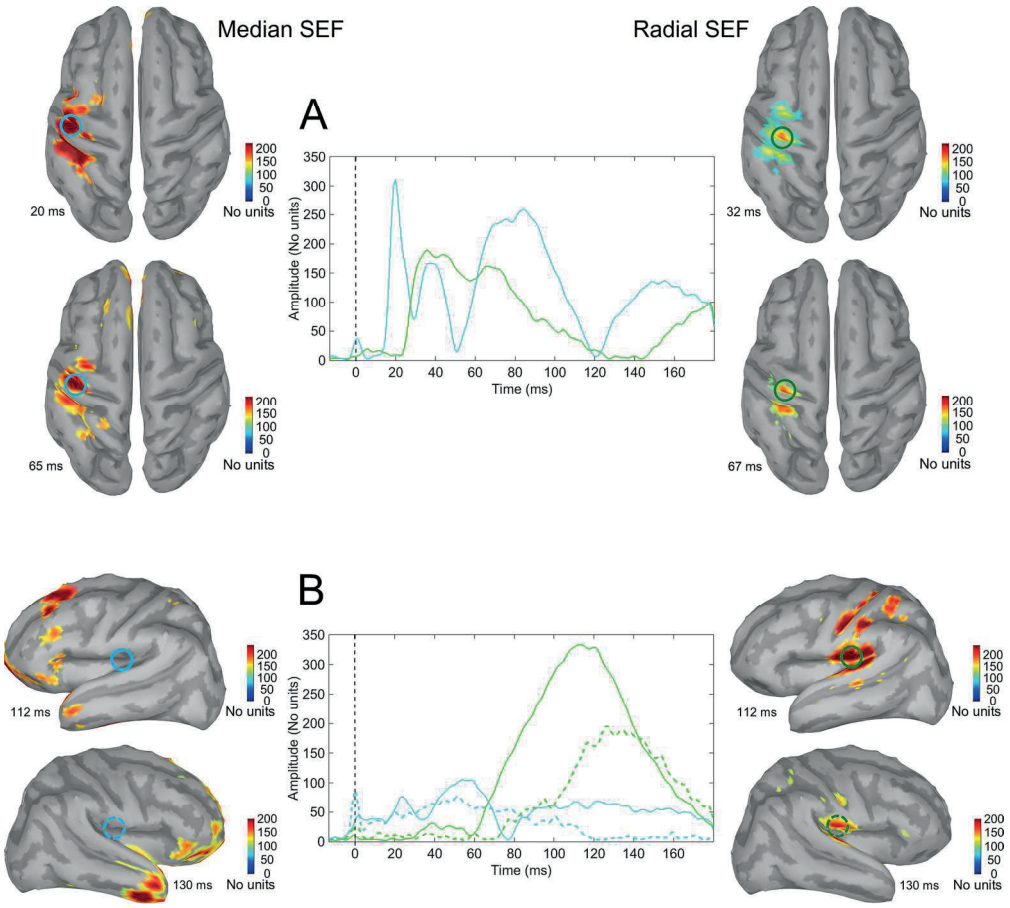

Figure 2

164x147mm (300 x 300 DPI)

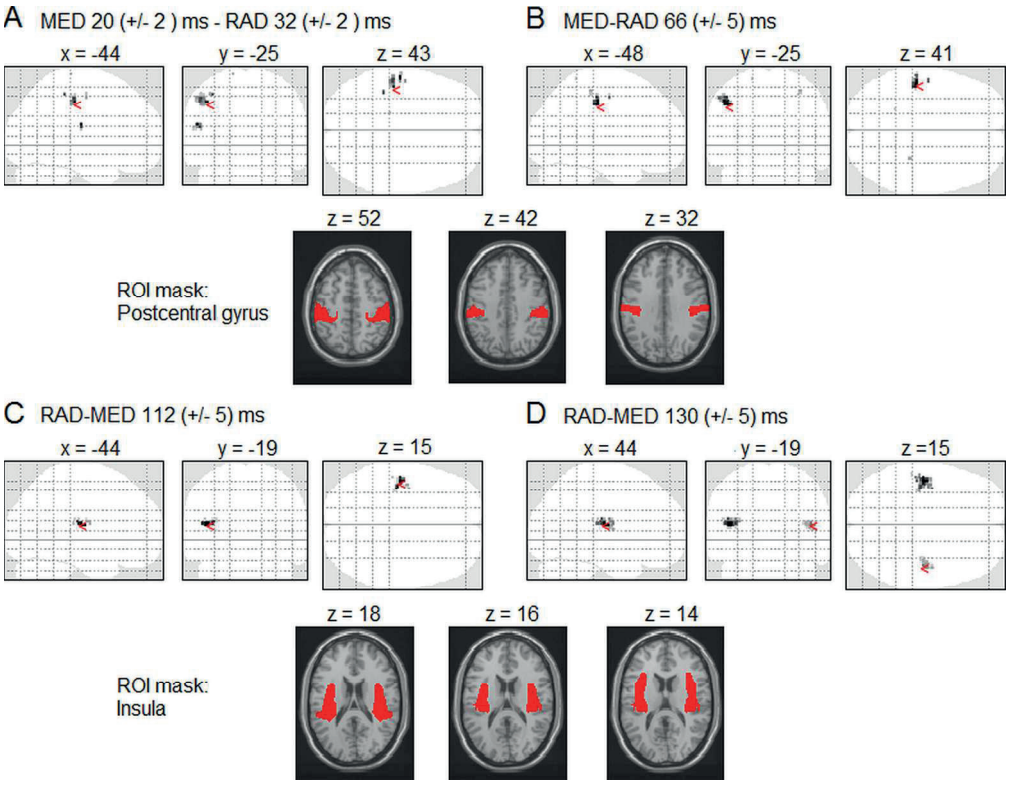

Figure 3

142x109mm (300 x 300 DPI)

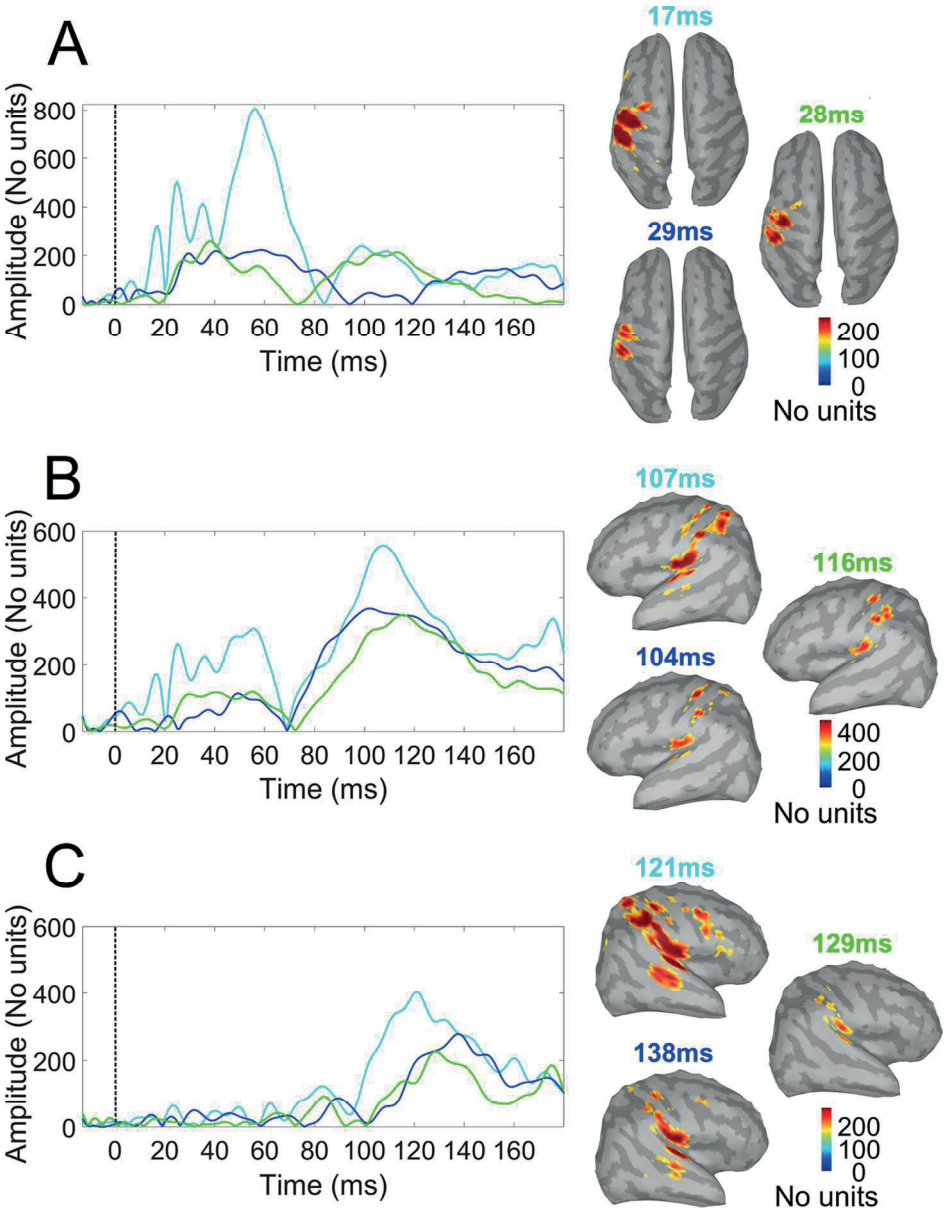

Figure 4

112x144mm (300 x 300 DPI)

Hautasaari et al.

Graphical abstract text

Sensory integration and coordination of body sides requires interhemispheric transfer in the human brain. We studied somatosensory processing after innocuous electrical stimulation of median and radial nerves and after intracutaneous nociceptive stimulation. Our results show that pure sensory peripheral stimulation activates, in addition to primary sensory areas in contralateral postcentral gyrus, bilateral operculo-insular areas with distinct latency difference between hemispheres.

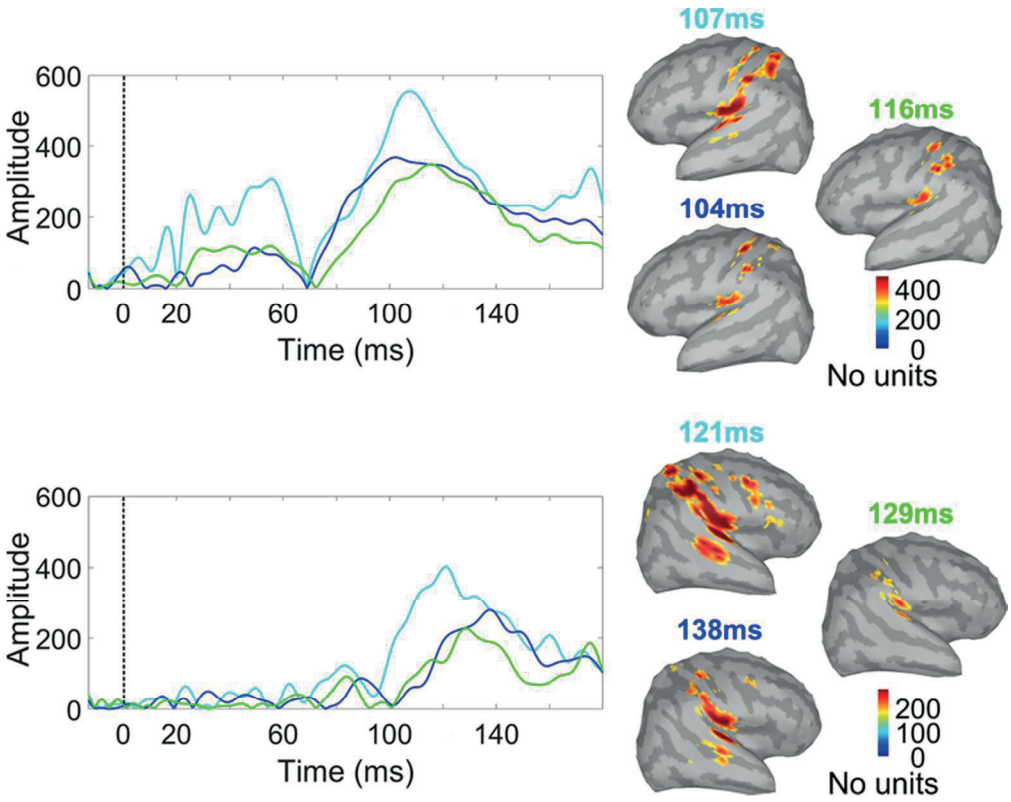

Graphical abstract figure

69x54mm (300 x 300 DPI)

IV

ACUTE EXERCISE MODULATES PAIN-INDUCED RESPONSE ON SENSORIMOTOR CORTEX ~20 HZ OSCILLATION

by

Hautasaari, P., McLellan, S., Koskio, M., Pesonen, H. & Tarkka, I. M.

Submitted manuscript.

Request a copy from the author.